ANNEX VIII | 2008 | 8DHC-08-02




IEA DHC|CHP

International Energy Agency
IEA Implementing Agreement on District Heating and Cooling,
including the integration of CHP

IMPROVED COGENERATION AND HEAT UTILIZATION IN DH NETWORKS

General Preface Annex VIII

Introduction

The International Energy Agency (IEA) was established in 1974 in order to strengthen the co-operation between member countries and reduce the dependency on oil and other fossil fuels. Thirty years later, the IEA again drew attention to serious concerns about energy security, investment, the environment and energy poverty. The global situation is resulting in soaring oil and gas prices, the increasing vulnerability of energy supply routes and ever-increasing emissions of climate-destabilising carbon dioxide.

At the 2005 Gleneagles G8 an important role was given to the IEA in advising on alternative energy scenarios and strategies aimed at a clean, clever and competitive energy future. Two years later, at the Heiligendamm G8, it was agreed that "instruments and measures will be adopted to significantly increase the share of combined heat and power (CHP) in the generation of electricity". District Heating and Cooling is an integral part of the successful growth of CHP: heat networks distribute what would otherwise be waste heat to serve local communities.

The IEA is active in promoting and developing knowledge of District Heating and Cooling: while the DHC programme (below) itself is the major global R&D programme, the IEA Secretariat has also initiated the International DHC/CHP Collaborative the kick-off event of which took place in March 2, 2007 with a 2-year Work Plan aiming to raise the profile of DHC/CHP among policymakers and industry. More information on the Collaborative is to be found on IEA's website `www.IEA-org`.

The major international R&D programme for DHC/CHP

DHC is an integrative technology that can make significant contributions to reducing emissions of carbon dioxide and air pollution and to increasing energy security.

The fundamental idea of DHC is simple but powerful: connect multiple thermal energy users through a piping network to environmentally optimum energy sources, such as combined heat and power (CHP), industrial waste heat and renewable energy sources such as biomass, geothermal and natural sources of heating and cooling.

The ability to assemble and connect thermal loads enables these environmentally optimum sources to be used in a cost-effective way, and also offers ongoing fuel flexibility. By integrating district cooling carbon-intensive electrically-based air-conditioning, rapidly growing in many countries, can be displaced.

As one of the IEA's 'Implementing Agreements', the District Heating & Cooling programme is the major international research programme for this technology. Active now for more than 25 years, the full name of this Implementing Agreement is 'District Heating and Cooling including the integration of Combined Heat and Power'. Participant countries undertake co-operative actions in energy research, development and demonstration.

Annex VIII

In May 2005 Annex VIII started, with the participation from Canada, Denmark, Finland, the Netherlands, Norway, South Korea, Sweden, United Kingdom, United States of America. Below you will find the Annex VIII research projects undertaken by the Implementing Agreement

Project title	Company	
New Materials and Constructions for Improving the Quality and Lifetime of District Heating Pipes including Joints – Thermal, Mechanical and Environmental Performance	Chalmers University of Technology Project Leader: Ulf Jarfelt	8DHC-08-01
Improved Cogeneration and Heat Utilization in DH Networks	Helsinki University of Technology Project Leader: Carl-Johan Fogelholm	8DHC-08-02
District Heating Distribution in Areas with Low Heat Demand Density	ZW Energiteknik Project leader: Heimo Zinko	8DHC-08-03
Assessing the Actual Energy Efficiency of Building Scale Cooling Systems	International District Energy Association Project leader: Robert P. Thornton	8DHC-08-04
Cost Benefits and Long Term Behaviour of a new all Plastic Piping System	NUON Project leader: Hans Korsman	8DHC-08-05

Benefits of membership

Membership of this implementing agreement fosters sharing of knowledge and current best practice from many countries including those where:

- DHC is already a mature industry
- DHC is well established but refurbishment is a key issue
- DHC is not well established

Membership proves invaluable in enhancing the quality of support given under national programmes. Participant countries benefit through the active participation in the programme of their own consultants and research organisations. Each of the projects is supported by a team of experts, one from each participant country. As well as the final research reports, other benefits include sharing knowledge and ideas and opportunities for further collaboration.
New member countries are very welcome – please simply contact us (see below) to discuss.

Information

General information about the IEA Programme District Heating and Cooling, including the integration of CHP can be obtained from our website www.iea-dhc.org or from:

The Operating Agent	IEA Secretariat
SenterNovem	Energy Technology Policy Division
Ms. Inge Kraft	Mr Jeppe Bjerg
P.O. Box 17	9, Rue de la Federation
NL-6130 AA SITTARD	F-75739 Paris, Cedex 15
The Netherlands	France
Telephone: +31-46-4202299	Telephone: +33-1-405 766 77
Fax: +31-46-4528260	Fax: +33-1-405 767 59
E-mail: i.kraft@senternovem.nl	E-mail: jeppe.bjerg@iea.org

Improved cogeneration and heat utilization in DH networks

Carl-Johan Fogelholm[1], Alemayehu Gebremedhin[2], Sangsu Kim[3], Linda Pedersen[4], Tuula Savola[1], Jacob Stang[4], Tor-Martin Tveit[1] and Heimo Zinko[2]

1) Helsinki University of Technolgy
   Energy Engineering and Environmental Protection
   PL 4400, FI-02015 TKK
   Finland

2) Linköping University / IKP / Division of Energy Systems
   SE-58 183 Linköping,
   Sweden

3) Korea District Heating Corporation
   186, Bundang-dong, Bundang-gu,
   Seongnam-si, Gyeonggi-do, 463-908
   Korea

4) SINTEF Energy Research
   NO-7465 Trondheim
   Norway

Contents

1 Introduction

A cogeneration plant supplying a single building or connected to a small DH network is usually heavily dependent on the heat demand. Long-term heat storaging can make it possible to produce more electricity in the cogeneration plant, to use biofuels or other renewable fuels instead of fossil fuels and to connect new areas to the network. The investigation of these issues requires knowledge on the heat load profiles of the network and the electricity production of the cogeneration plant. In addition to thermal storage, the cogeneration can be improved by using CHP process configurations which have high power production efficiencies at partial heat loads.

The objective of this project has been to evaluate and develop approaches that will improve the economic feasibility and the thermal efficiency of cogeneration through better utilisation of the produced heat and higher power generation in the CHP plant. The results can be applied both in cogeneration plants producing electricity, heat and cooling for a single building and in a district heating network system situated in or near areas with low heat densities. The economic feasibility of cogeneration in small DH networks is currently low and should be increased for future expansion of district heating.

The objective has been achieved by generating load models for heat and electricity, analysing and evaluating long-term storage technologies and by developing an optimisation model of DH systems. The optimisation model is then applied to an existing DH network. The work as been divided into the following three sub-tasks:

- Sub-task 1
  - A: Load model for heat and electricity – development
  - B: Load model for heat and electricity – demonstration
  - C: Load model demonstration for a larger CHP plant
- Sub-task 2
  - A: Improvement of CHP applications with long-term storage
  - B: Analysis of suitable long-term storage technologies and their cost/volume
  - C: Construct an economic model for optimizing the combined use of cogeneration plants, heat storage and DH network (transport pipe as well as local net).
  - D: Evaluate the improved economy of combined use of cogeneration plants and long-term storage in district heating systems for some selected cases representing situations in the countries from the working group.

- Sub-task 3
    - A: Increasing the power production of CHP plants integrated in DH networks
    - B: Improving the DH network with efficient combining of CHP plants and thermal storages
    - C: Increasing the CHP production and combining long-term thermal storages – Transferring the methods into existing DH network

In Section 2 the load model for estimating load profiles for simultaneous heat and electricity loads in actual systems is presented (sub-task 1). The background for the load model has been hourly load measurements of various buildings in Trondheim and Bergen, Norway. A case study is performed in order to test the model and the case study is also applied in Section 3 (described in detail in Section 3.2.2). Section 3 presents an analysis of suitable long-term storage technologies and their cost/volume relations, together with an economic model for optimizing the combined use of cogeneration plants, heat storage and DH network. An evaluation of the improved economy of combined use of cogeneration plants and long-term storage in district heating systems for some selected cases is also presented in the section (sub-task 2). In Sections 4 through 6 various changes to CHP plants to increase the efficiency together with a multi-period MINLP model for optimising the structural changes and the operation of CHP plants in DH networks with long-term thermal storages are presented (sub-task 3). The final conclusions are presented in Section 7.

The lead institute of the project has been *Helsinki University of Technology*, Finland, while *Linköping University*, Sweden, *Sintef Energy Research, Norway* and *Korea Distric heating Corporation*, Korea, have been participant institutes.

2 Load modeling of heat and electricity demand

Load modeling of heat and electricity demand is a very important part of planning for mixed energy distribution systems or combined heat and power (CHP) production. The maximum heat and electricity load demand, as well as load duration profiles and annual heat and electricity demand are important input parameters when planning for mixed energy distribution systems for a specified area.

2.1 Introduction

A load model for estimation of simultaneous heat and electricity demand in buildings for a specified planning area is developed for the purpose of planning for mixed energy distribution systems. The building design load and the actual load may differ a great deal. As a consequence, a model based on statistical analyses of actual data is preferred. The model is based on statistical analyses of hourly measured district heat and electricity consumption in various buildings.

The load model for simultaneous heat and electricity demand in buildings is presented in this chapter along with the load aggregation method. A case study is performed in order to test the model and the case study is also applied in Section 3 for the purpose of simulating long-term storage of heat for optimization of a CHP plant.

2.2 Background

The background for the load model has been hourly load measurements of various buildings in Trondheim and Bergen, Norway. The buildings represented the building categories corresponding to the division of building categories in the Energy Performance of Buildings Directive [1]; Single family Houses (SH) and Apartment Blocks (AB), Educational Buildings (EB), Office Buildings (OB), Hospital Buildings (HB) and Hotels with Restaurants (HR). The measurement period varied from nine months for single family houses and apartment blocks, and two to four and a half years for the other building categories.

The hourly district heat measurements comprised the end-uses space heating, ventilation heating and heating of tap water, whereas the hourly electricity measurements comprised the end-uses lighting, pumps, fans and electrical appliances. Cooling has not been analyzed due to the lack of measurements for this end-use in the building sample. However, the model can incorporate cooling when such measurements are available, i.e. when cooling loads are included in the electricity measurements.

A lot of background information concerning the measured buildings was collected in order to subdivide the building categories. This included both physical determinants and control regime parameters such as available area, building year, insulation standard, indoor temperature, operation of the ventilation system, and more. Hourly and daily mean temperatures were also collected from the two locales, as well as yearly representation of the normal climate known as the design reference year (DRY) [7] or a reference year.

2.3 The heat load model

The heat load model is based on piece-wise linear regression analyses for every hour of the day and day type. The day types are divided into weekdays (Mondays through Fridays) and weekends/holidays (Saturdays and Sundays) based on significantly different load profiles for the various day types. A scatter plot of daily mean temperature vs. hourly district heat consumption for an office building, OB2, in Trondheim is shown in Figure 1 for weekdays hour 12.

Figure 1 illustrates the difference between temperature-dependent and temperature-independent district heat consumption; hence, the different parts have to be analyzed separately. First of all, the change-point temperature have to be found, i.e. the daily mean temperature separating the temperature-dependent and temperature-independent district heat consumption.

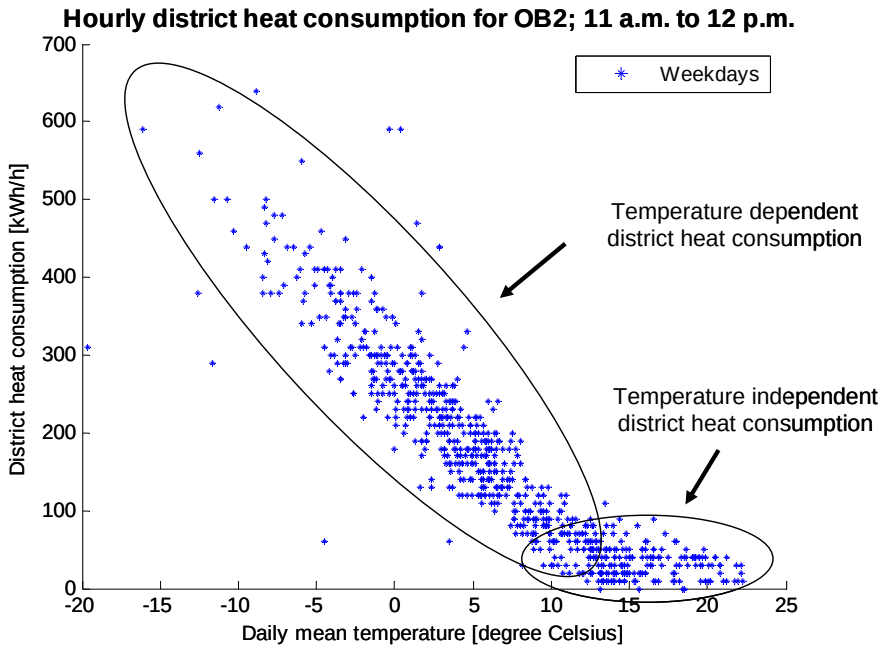

Figure 1: Scatter plot of daily mean temperature vs. hourly district heat consumption for OB2 in Trondheim for weekdays hour 12, i.e. district heat consumption from 11 a.m. to 12 p.m. for nearly five years (January 2002 – October 2006) ***Error! Reference source not found.****].*

A linear regression equation may be expressed as:

$$Y_i = \alpha + \beta \cdot x_i + e_i$$

x_i is the independent regressor variable and Y_i is the dependent random variable. e_i is called the residual and describes the error in the fit of the model [17].

The change-point temperature is found by assuming a linear correlation between hourly district heat consumption and daily mean temperature. The regression coefficients α and β are calculated for temperature steps of 0.1°C, starting at a daily mean temperature of 17°C and stepping down to 0°C. The change-point temperature is found in the range where the β-values fluctuated least, i.e. an approximately constant β-value indicates that the influence of the temperature-independent heat consumption is neglectable.

The mathematical procedure developed to find the change-point temperature for a given building at a given hour is based on α- and β-values in the following way [8]:
Calculate the temperature range of Δθ = 5°C in which the total sum of squares of the α-values is smallest. The α-values are calculated in advance for change-point temperatures from 17°C and down to 0°C with a temperature step of 0.1°C.
Calculate the temperature band of Δθ = 1°C where the minimum total sum of squares of the β-values occur within the temperature range of Δθ = 5°C found in number 1. The temperature band slide from the highest temperature in the temperature range to the lowest with a temperature step of 0.1°C.
The temperature-dependent season is then found within the temperature band given in number 2. The change-point temperature is defined as the average temperature within the temperature band.

For more information concerning the mathematical procedure and the verification of the heat load model, see Pedersen [8].

2.3.1 Temperature-dependent heat load model

Linear regression analysis is performed on every hour of the day for each day type for the temperature-dependent district heat consumption, i.e. on the hourly district heat measurements below the change-point temperature. The regression coefficients α and β are found based on the least square method [6] for both day types. The heat load demand for a given hour *j* and day type *d* is shown:

$$\Phi_{HL,j,d} = \alpha_{j,d} + \beta_{j,d} \cdot \theta + e_{j,d}$$

$e_{j,d}$	Residuals for a given hour *j* and day type *d*.
$\alpha_{j,d}$	The specific regression coefficient for a given hour *j* and day type *d*.
$\beta_{j,d}$	The specific regression coefficient for a given hour *j* and day type *d*.
$\Phi_{HL,j,d}$	Heat load demand for a given hour *j* and day type *d*.
θ	Daily mean temperature.
d	Day type; weekday (WD) or weekend/holiday (WE).
j	1, 2, 3, …, 24 where 1 = 12 a.m. to 1 a.m., , …, 24 = 11 p.m. to 12 a.m.

The design heat load profiles for weekdays and weekends/holidays are found by inserting the design temperature into the equation for every hour and day type. The design temperature, θ_{dt}, is defined as the average outdoor temperature during the three coldest successive days in a 30-year period: from 1961 to 1990.

2.3.2 Temperature-independent heat load model

The temperature-independent heat load model is based on the hourly district heat consumption during the temperature-independent season, which mainly represents hot tap water consumption. The model is based on the assumption that the heat load above the change-point temperature is independent of outdoor temperature. As a result, the temperature-independent heat load model is based on probability distributions, and the expected values and standard deviations for every hour and day type for all buildings analyzed are calculated. The normal distribution and the Student's t distribution showed the best fit, and consequently, are chosen for the analyses of the hot tap water consumption.

2.3.3 Relative values

It is desirable to make the load profiles compatible with a possible grouping, i.e. by building category or archetype. The latter is a division of buildings based on other criteria than building category. Different archetype classifications are technology, market, user behavior, regulations and design, planning and construction processes [12], among others. The main findings of archetype division in relation to heat load profiles are the operation of the ventilation systems and the ages of the buildings.

For the reason of comparison, it is important to produce relative load profiles [5]. The average daily design load, $\overline{\Phi}_{HL,d}$, is chosen accordingly:

$$\overline{\Phi}_{HL,d} = \frac{1}{24}\sum_{j=1}^{24}\Phi_{HL,j,d}(\theta_{dt}) = \frac{DailyConsumption}{24}$$

$\Phi_{M,j}$ Maximum or design load for hour *j* during weekdays, in [kWh/h].

The design conditions for heat load always occurred during weekdays for the buildings analyzed. The maximum or design daily consumption is found by:

$$DailyConsumption = \sum_{j=1}^{24}(\alpha_{j,d} + \beta_{j,d}\cdot\theta_{dt})$$

Relative design heat load profiles for several buildings within a certain building category are derived in order to compare and generalize the heat load profiles. The relative load profiles are found by dividing the design heat load for each hour and day type by the average design load. The relative heat load profiles for the temperature-independent season are also found by dividing the expected values for each hour and day type by the average design load.

Figure 2 shows the relative design heat load profile for an office building, OB7, during weekdays. The standard deviation bounds are also included in the figure. When the heat load profiles are presented in this form, it allows for comparisons despite the difference in design heat load. The y-axis is given in P.U.; meaning per unit or relative to one.

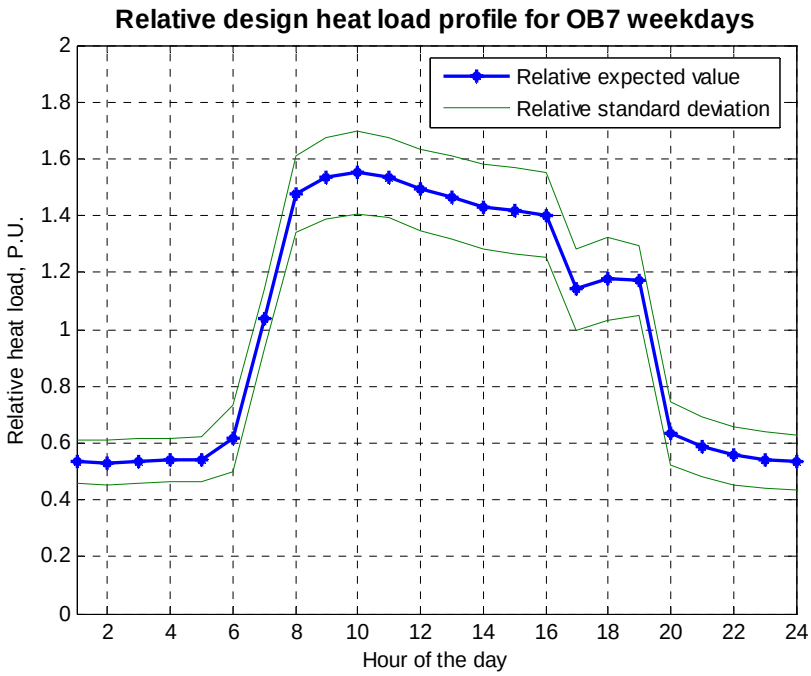

Figure 2: Relative design heat load profile for OB7 in Trondheim for weekdays, including relative standard deviation bounds[8].

2.3.4 Generalization of heat load profiles

In order to generalize the heat load profiles for different building categories, it is very important to sort the buildings into different archetypes regarding building type and regulation regime. When the buildings analyzed have been classified according to archetype, the relative expected value for each archetype is calculated based on each building's relative expected value.

The sample size, N, within each archetype should be larger than 30 in order to use the normal distribution when generalizing the heat load profiles. If X_1, X_2, …, X_n are independent variables from the same probability distribution with mean value, μ, and standard deviation, σ, then the central limit theorem states that [6]:

$$\overline{X} = \frac{1}{n}(X_1 + X_2 + ... + X_n)$$

is approximately Normal($\mu, \sigma/\sqrt{n}$).

The equation implies that the expected relative heat load for every hour *j* and day type *d* for a given archetype can be expressed as:

$$\overline{\Phi}_{HL,j,d} = \frac{1}{n}\sum_{n=1}^{N}\Phi_{HL,j,d,n}$$

n	Number of buildings within the selected archetype.
$\overline{\Phi}_{HL,j,d}$	Relative expected heat load for an archetype hour *j* and day type *d*.

Substitute α and β into the equation for every building within the archetype at a given hour and day type:

$$\overline{\alpha}_{j,d} + \overline{\beta}_{j,d} \cdot \theta = \frac{1}{n}\sum_{n=1}^{N}\alpha_{j,d,n} + \frac{\theta}{n}\sum_{n=1}^{N}\beta_{j,d,n}$$

2.3.5 Examples of heat load profiles

The design heat load profiles are exemplified through the building category Educational Buildings (EB) represented by two archetypes (AT); buildings built before and after 1997 with ventilation systems running on time control. The difference can be explained by changes in the Technical Regulations under the Norwegian Planning and Building Act [10]. More stringent requirements for the coefficient of thermal transmittance for the building envelope was introduced along with more stringent requirements for the ventilation rate in new and retrofitted buildings. Figure 3 and Figure 4 show the generalized design heat load profiles for educational buildings archetype 1 and 2 including standard deviations (STD) for both day types, weekdays (WD) and weekends/holidays (WE).

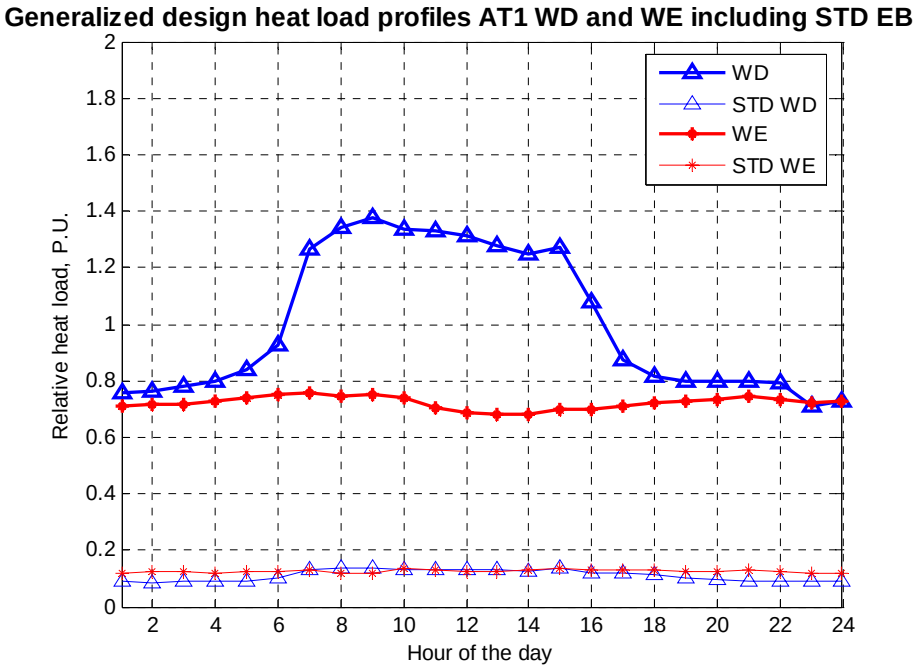

Figure 3: Generalized design heat load profiles for educational buildings (EB), weekdays (WD) and weekends (WE), for archetype 1 (AT1); ventilation systems with time control for buildings built before 1997 ***Error! Reference source not found.***

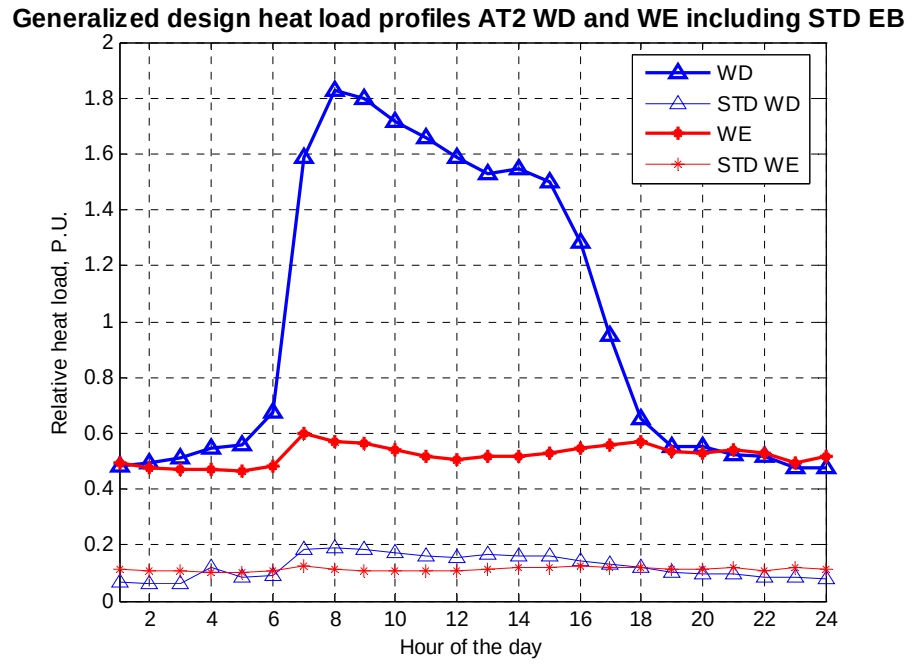

Figure 4: Generalized design heat load profiles for educational buildings (EB), weekdays (WD) and weekends (WE), for archetype 2 (AT2); ventilation systems with time control for buildings built in 1997 and [8].

2.4 The electricity load model

The t-test is applied to the hourly electricity consumption in relationship to outdoor temperature. The test showed a relation between outdoor temperature and hourly electricity consumption for

some hours and no correlation for other hours. The buildings with temperature-dependent electricity consumption are omitted from the analyses based on the criteria of end-use division, i.e. electricity as an energy carrier should only supply lighting, pumps, fans and electrical appliances.

The electricity load model is based on probability distribution analyses for every hour of the day and day type. The electricity load profiles also showed a significant difference between the various day types and are analyzed accordingly.

2.4.1 Probability distributions

Probability distributions are applied in order to analyze the electricity load demand in buildings supplied by a combined heat and power plant, i.e. district heating and electricity as energy carriers. The electricity load model is based on continuous probability distributions. The hourly electricity consumption data for each day type are mainly examined in relation to normal, lognormal and Student's t distributions. See Løvås [6] or Walpole et al. [13] for more information about statistical analyses in general and probability distributions in particular.

Probability plots are used in order to analyze the goodness of fit for the various distributions in order to calculate the expected value and the standard deviation for each hour and day type for every building. Figure 5 shows a probability plot for an office building, OB2. The Student's t distribution (or T scale distribution) gives a good fit, while the normal distribution does not fit as well. The lognormal distribution does not fit for this particular high load hour. For other hours, especially for low load hours, the normal distribution and also the lognormal distribution may give good fit.

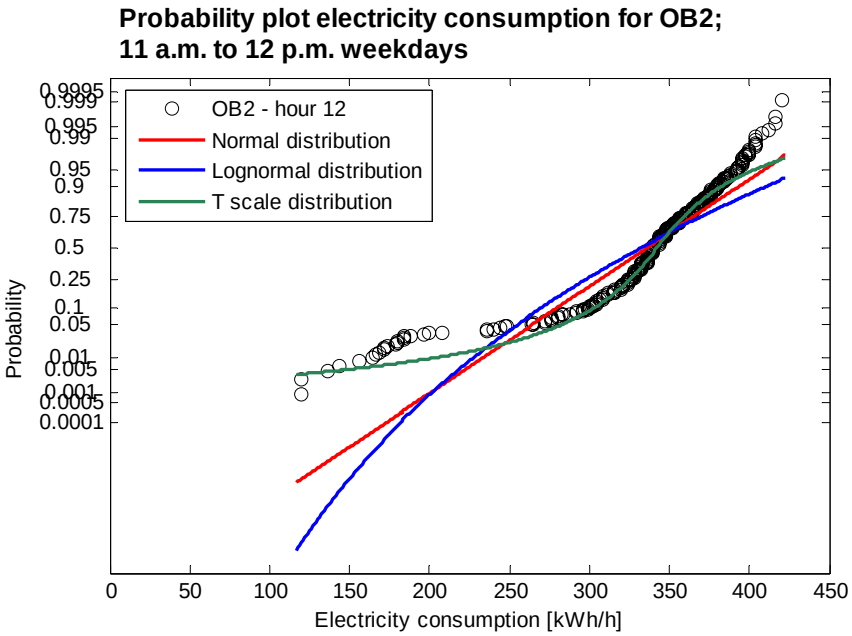

Figure 5: Probability plot of hourly electricity consumption for OB2 weekdays between 11 a.m. and 12 p.m. The goodness of fits are shown for normal, lognormal and Student's t distribution [8].

The analyses of the electricity consumption revealed that there are some seasonal variations which could not be related to outdoor temperature alone. Lighting as an end-use is related to seasonal changes in hours of daylight and sun. Pumps and fans as end-uses are related to space heating and ventilation heating systems. The forward flow temperature in the hydronic space heating systems within a building are mainly controlled by outdoor temperature, resulting in a constant mass flow, and thereby, temperature-independent electricity consumption. The amount of electricity for the pumps is decreased during the temperature-independent season, only circulating hot tap water. The supply air rate in the ventilation system is independent of climatic conditions and strongly related to the building's utilization time. Electrical appliances are related to work-hours and behavioral determinants.

On the basis of this information and t-tests, the electricity consumption is investigated in relation to various seasons, as well as day types and hour of the day. Monthly analyses of the electricity load led to the seasonal division of winter; including December, January and February, summer; including June, July and August, and finally spring/fall; including the remaining months.

2.4.2 Relative values

The electricity load profiles are also derived on relative format for the reason of comparison. The maximum electricity load profiles for the buildings analyzed always occurred during weekdays for the winter season. The average daily design load for electricity, $\overline{\Phi}_{HL,d,s}$, is based on the average expected value for the weekday winter season load profile. The relative electricity load profiles are found by dividing the seasonal load for each hour *j* and day type *d* by the average design load for electricity.

2.4.3 Generalization of electricity load profiles

The same generalization procedure which was applied to the heat load profiles is also applied to the electricity load profiles. Generalized load profiles are calculated for every building category or archetype for each season and day type.

The following equation expresses the expected relative electricity load for every hour *j*, day type *d* and season *s* for a given archetype:

$$\overline{\Phi}_{EL,j,d,s} = \frac{1}{n}\sum_{n=1}^{N}\Phi_{EL,j,d,s,n}$$

$\overline{\Phi}_{EL,j,d,s}$ Relative expected electricity load for an archetype hour *j*, day type *d* and season *s*.

Figure 6 shows the relative electricity load profiles for all office buildings weekdays, including the relative standard deviations for the winter season. The generalized winter electricity load profile for the office building category is plotted along with the accompanying standard deviation, and is shown as black bold lines in the figure.

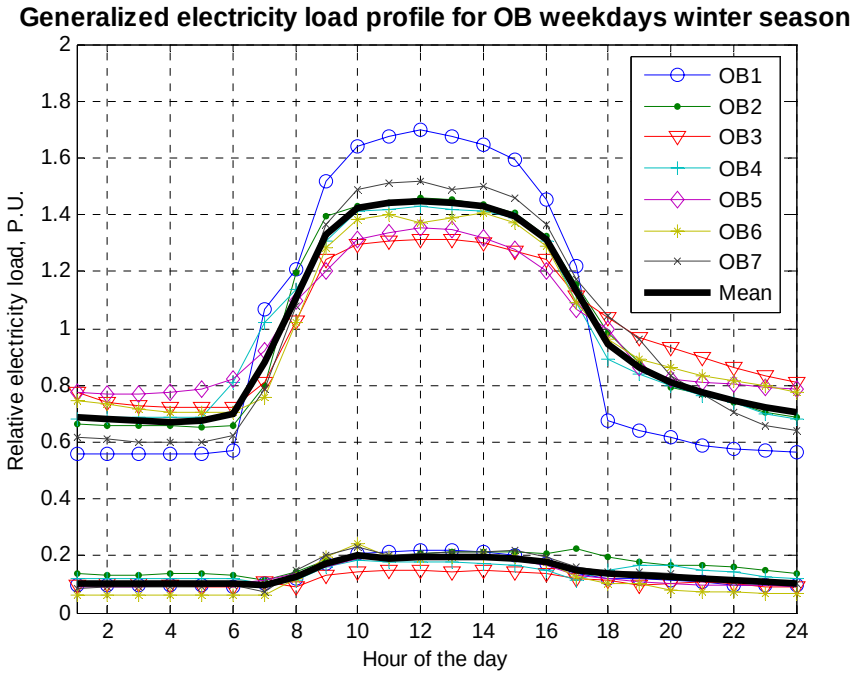

Figure 6: Generalized electricity load profile, including standard deviation for weekdays during the winter season for the office building category [8].

2.4.4 Examples of electricity load profiles

The electricity load profiles for all seasons and day types are exemplified through the building category Single family Houses (SH) and Apartment Blocks (AB). Based on the analyses of single family houses and apartment blocks, it was not found necessary to differentiate between these two building categories. This is mainly due to the fact that most apartment blocks analyzed for this project are only two story wooden buildings with sizes and shapes that are similar to detached houses. The latter buildings are included in the single family house category. Due to large variations within this building category, single family houses and apartment blocks are analyzed in clusters of approximately 10 buildings each. Demographic features within these building categories have not been investigated.

Figure 7 and Figure 8 show the generalized seasonal electricity load profiles for single family houses and apartment blocks including standard deviations (STD) for both day types, weekdays (WD) and weekends/holidays (WE). The seasonal load profiles are very similar during night hours for both day types. However, the differences in daytime electricity load demand for the various seasons are quite evident [8].

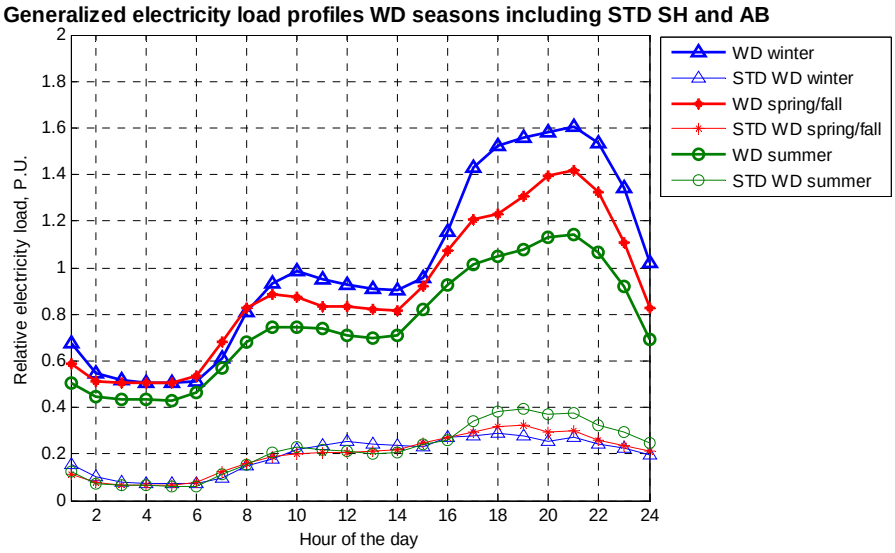

Figure 7: Generalized electricity load profiles, weekdays, for all seasons, including standard deviation for single family houses and apartment blocks [8].

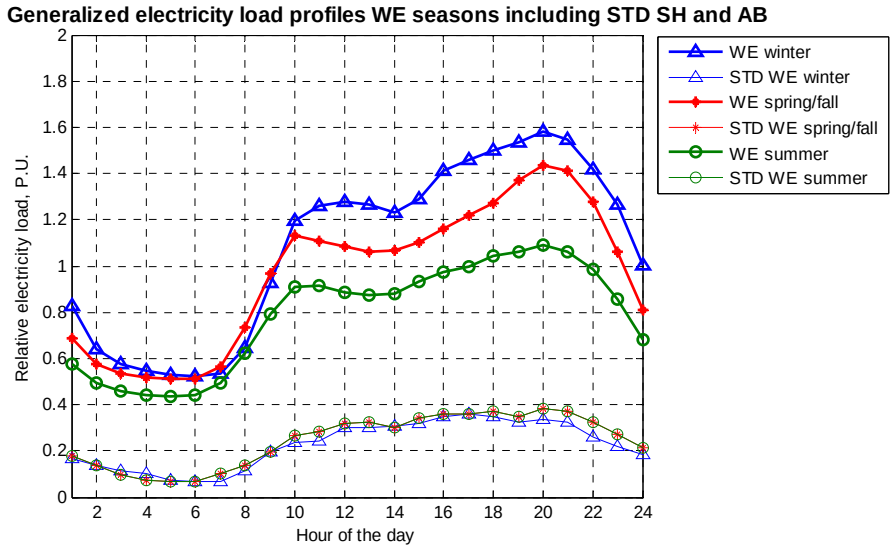

Figure 8: Generalized electricity load profiles, weekends, for all seasons, including standard deviation for single family houses and apartment blocks [8].

2.5 Algorithm for relative and generalized load profiles

The different solution algorithms for producing relative load profiles and generalized load profiles are presented in this chapter, both in writing and in flow charts.

2.5.1 Relative load profile algorithm

The procedure for the solution algorithm for relative load profiles for one building is given in the list below [8] and in Figure 9:

Load specific building file and perform quality assurance on the data.

Calculate the change-point temperature dividing the temperature-dependent and the temperature-independent consumption. Calculate relative design load profile for heat load demand, including

relative regression coefficients, as well as relative temperature-independent heat load profile.

Calculate relative design load profile for electricity load demand as well as seasonal electricity load profiles.

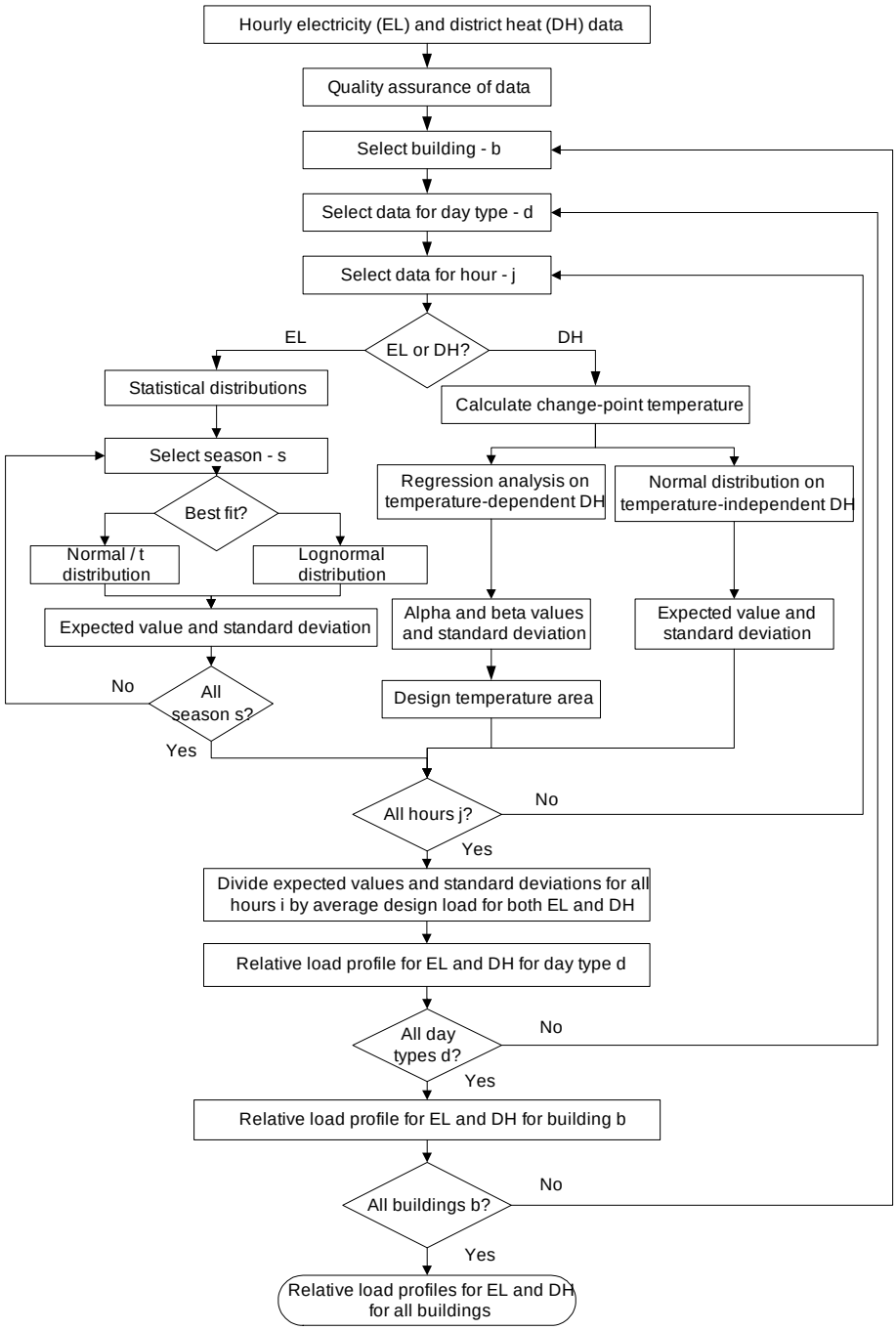

Figure 9: Flow chart showing the method for the estimation of relative heat and electricity load profiles for different buildings[8]

2.5.2 Generalized load profile algorithm

The procedure for the solution algorithm for generalized load profiles for different archetypes/building categories is listed below [8] and in Figure 10:

Load relative heat and electricity load profiles for all buildings analyzed.

Sort load profiles by building category and archetype.

Calculate expected value and standard deviation for all archetypes.

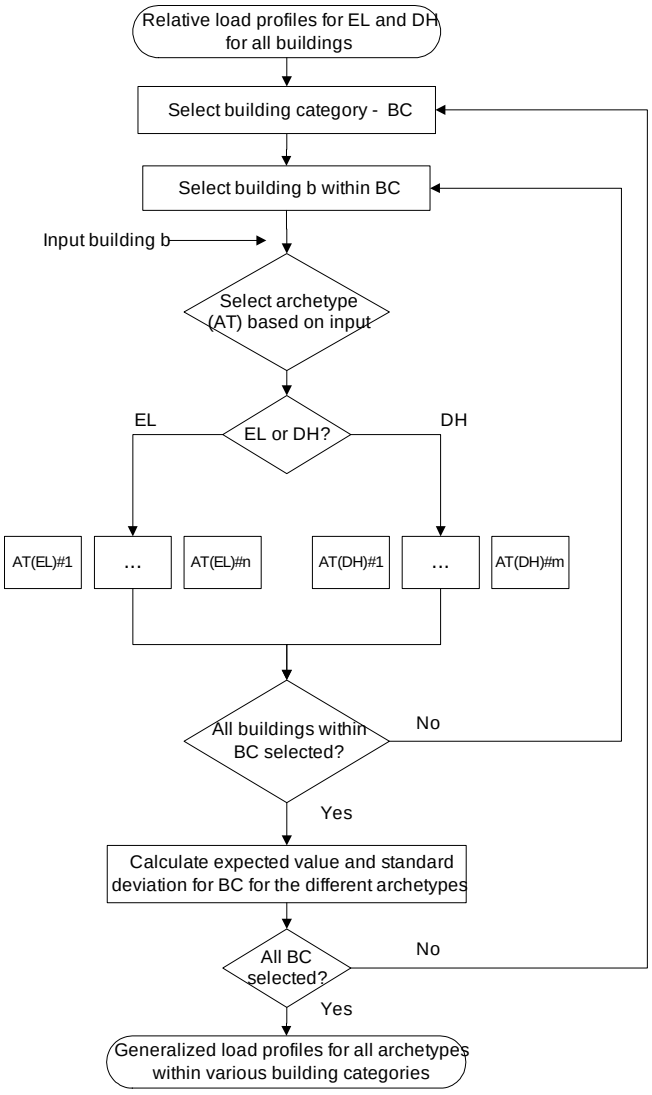

Figure 10: Generalization of relative heat and electricity load profiles for a given building category or archetype [8].

2.6 Load aggregation

The challenge of using the generalized relative load profiles in order to estimate the design load profiles, the maximum loads, the annual energy demands and the load duration profiles for a specified planning area, all divided into heat and electricity, is discussed below.

The energy distribution infrastructure includes both electrical cables/wires and pipelines for district heating. When aggregating the heat and electricity load from the building level to the CHP-plant, the maximum load losses and annual energy losses through the distribution systems must be incorporated. The system boundary is set at the energy production unit, i.e. not including the energy production efficiencies. The coincidence factors for heat and electricity are also explored in relation to aggregated load profiles.

2.6.1 Background

A bottom-up approach is applied for the aggregation of individual building load profiles in order to derive the heat and electricity load profiles for a specified planning area supplied by district heating and electricity from a CHP-plant. The method for aggregating load profiles is based on the sum of normal distributions. It is assumed that the load profiles developed for heat and electricity for different archetypes or building categories are independent and normally distributed [8].

If X_1, X_2, …, X_n are independent variables from the same distribution with means μ_1, μ_2, …, μ_n and variance σ_1^2, σ_2^2, …, σ_n^2 respectively, then the sum of the independent variables can be calculated according to [6]:

$$Y = X_1 + X_2 + ... + X_n$$

The sum of the variables has an approximately normal distribution with Normal($n\mu$, $\sqrt{n}\sigma$).

The variance of Y is the sum of the variance of X:

$$\sigma_Y^2 = \sigma_1^2 + \sigma_2^2 + ... + \sigma_n^2$$

The standard deviation of Y, which is the more interesting variable when incorporating the uncertainty in the analyses, is the positive square root of the variance of Y.

2.6.2 Aggregated design load

The distribution intervals for a normally distributed variable X can be written as follows [6]:

It is a 100(1-α)% certainty that the X value occurs within the interval $\mu \pm (z_{\alpha/2} \cdot \sigma)$
It is a 100(1-α)% certainty that the X value will be less than $\mu + (z_{\alpha} \cdot \sigma)$
It is a 100(1-α)% certainty that the X value will be greater than $\mu - (z_{\alpha} \cdot \sigma)$

The value z_α is called the α-quantile. The latter values are tabulated for various distributions such as the normal and Student's t distribution. The α-values here represent the level of significance and must not be mistaken for the regression coefficient.

The standard deviations are unknown and have to be calculated based on the hourly measured load data. As a consequence, the α-quantiles from the Student's t distribution, t_α, are applied. α-values and the corresponding t_α for the Student's t distribution are tabulated for n-1 degrees of freedom.

The most important distribution interval in relation to maximum heat and electricity load profiles for a specified planning area is expressed in number 2 in the list above. The design conditions for the maximum heat and electricity load profiles are dependent on the accuracy level, but in general terms the maximum load may be expressed as the following equation [8]. This approach has also been applied by Jardini et al.[5] and by Feilberg [2] for all electric buildings.

$$\Phi_{MaxLoad} = \mu_{MaxLoad} + t_\alpha \cdot \sigma_{MaxLoad}$$

$\mu_{MaxLoad}$ $\Phi_{HL,Max}$ or $\Phi_{EL,Max}$ for heat and electricity respectively

A probability of the maximum load occurring below a given value with a 95% likelihood is a good estimate for load modeling of heat and electricity demand for CHP supply. As a result, the 95% α-quantile is chosen for design conditions [8].

2.6.3 Indicators

In order to convert the relative generalized load profiles into real design load profiles and yearly load profiles for a selected building, specific heat and electricity load indicators, in [W/m^2], as well as specific heat and electricity consumption indicators, in [kWh/m^2 yr.], are applied.

Specific heat and electricity loads are calculated for every building category or archetype based on the methods developed for estimating heat and electricity load. The real design heat and electricity loads for each building analyzed within each archetype are calculated, as well as the corresponding standard deviations. The specific loads are used to restore the generalized design load profiles developed for each archetype or building category [8].

The specific loads are calculated for all archetypes/building categories analyzed based on the design temperature in Trondheim of -19°C and the winter season load profile, see Table 1.

Table 1: Specific heat and electricity load for the various archetypes/building categories analyzed based on design temperature of -19°C and winter season load profile.

	Specific load [W/m²]			
Building category/archetype	*DH WD*	*DH WE*	*EL WD*	*EL WE*
Single family houses and apartment blocks	46.0	44.7	10.5	10.3
Office buildings	55.6	44.5	23.8	13.0
Educational buildings – before 1997	61.3	34.0	19.6	6.3
Educational buildings – after 1997	81.3	29.2		
Retirement homes (hospital buildings)	64.0	59.4	23.1	20.2
Hotels with restaurants	42.6	41.1	16.3	15.9

Energy Consumption Indicators (ECI) is a well known term in the field of energy planning, mostly presented based on total energy consumption in buildings. ECIs divided into heat (HCI) and electricity (ELCI) purposes are calculated for every archetype or building category analyzed. The temperature-dependent part of the HCI is normalized using the degree day method, i.e. space heating and ventilation heating are dependent on the climatological year(s) during the measurement period. The HCIs and ELCIs are used to restore the yearly load profiles for heat and electricity purposes respectively[8].

Table 2 shows the specific total, district heat and electricity consumption for the different archetypes/building categories analyzed, all temperature-dependent consumption adjusted to the Trondheim normal climate using degree days.

Table 2: Average specific total, district heat and electricity consumption for the different archetypes/building categories analyzed adjusted to Trondheim normal climate using the degree days ***Error! Reference source not found.****].*

	Specific energy consumption [kWh/m² yr]		
Building category/archetype	*ECI*	*HCI*	*ELCI*
Single family houses and apartment blocks[1]	166	116	49
Office buildings	235	100	135
Educational buildings – before 1997	175	109	69
Educational buildings – after 1997	174	103	69
Retirement homes (hospital buildings)	284	152	132
Hotels with restaurants	233	113	120

The advantages of the ECIs are their ability to incorporate changes in building design and the introduction of new technology. Building design codes may vary from one country to another, and HCIs and ELCIs for various archetypes or building categories should be calculated nationally. The latter indicators have to be adjusted to future development in order to allow for an increase or a decrease in energy consumption in buildings.

[1] The total number does not add up with the numbers from HCI and ELCI due to different buildings analyzed. The same applies for educational buildings because the ELCIs were not divided into the different archetypes.

2.6.4 Coincidence factor

The maximum loads for all customers do not coincide, i.e. the sum of each customer's maximum load is not equal to the maximum load for the specified planning area [8]. This means that [3]:

$$(\Phi_1 + \Phi_2)_{Maximum} < \Phi_{1,Maximum} + \Phi_{2,Maximum}$$

Φ_1, Φ_2 Daily load for each building when design conditions occur

The coincidence factor for *N* buildings has been defined by Fredriksen and Werner [3] among others:

$$CoincidenceFactor = \frac{\Phi_{Maximum(total)}}{\sum_{n=1}^{N} \Phi_{i,Maximum}}$$

The peak load demands for each building analyzed within the archetypes or building categories are not shown in the generalized load profiles because the latter profiles incorporate the coincidence factor for each archetype or building category due to the average expected value. The remaining coincidence factors for heat and electricity loads are given by the shapes of the various load profiles [2].

2.6.5 Distribution losses

Maximum load and annual energy losses in the distribution systems are important parts of estimating heat and electricity demand for CHP. The distribution losses are strongly dependent upon the energy carriers, and electricity and district heating have different characteristics in relation to distribution losses. A brief overview of the latter energy carriers in relation to distribution losses are given in the paragraphs below.

Electricity

The losses in each level of the electricity grid, ΔP_i, may be written as shown below **Error! Reference source not found.**]:

$$\Delta P_i = \frac{R_i}{U_i^2} \cdot (P_i^2 + Q_i^2)$$

$$= \frac{R_i}{U_i^2} \cdot (1 + tg\varphi_i^2) \cdot P_i^2$$

$$= k_i \cdot P_i^2$$

R_i Resistance in grid level *i*, in [Ω].

U_i Voltage level on grid level *i*, in [kV].

P_i Maximum local active power withdrawn on grid level *i*, in [kW].

Q_i Appurtenant reactive power on grid level *i*, in [kvar].

The equations above show that the power or load losses in the grid are dependent on the load level at each time interval. This implies that the losses in the grid are dependent on season, as well as day type and time of day. The annual electricity loss is the sum of the active load losses for every time interval throughout the year [8].

A simplified analysis of the maximum electricity loss and annual electricity losses will be performed in a case study. Actual distribution losses have been collected from electricity distribution companies. The maximum load loss was estimated to approximately 8% based on empirical data, whereas the annual electricity losses in the distribution grid varied between 5 and 6% in the most recent years based on real measurements [9].

District heating

The maximum heat loss and annual heat losses in a district heating distribution system are mainly dependent upon the following criteria [8]:

High or low heat density within the planning area.

Forward flow temperature and flow rates in the primary distribution system.

Insulation standard and design of pipelines.

Temperature efficiencies of the heat exchangers.

The latter criteria are very complex matters and have to be considered for every development project individually. Only a simplified analysis will be performed in a case study, see Chapter 2.8 for demonstration of load modeling.

2.6.6 Algorithm for load aggregation

The procedure for the solution algorithm for aggregation of load profiles for a specified planning area with a given mixture of buildings is listed below [8] and in Figure 11:

Select a specific planning area with a defined mixture of buildings.

Apply generalized heat an electricity load profiles for building b based on the building category.

Use specific load indicators to construct real heat and electricity load profiles as well as standard deviations for design day.

Apply design reference year (DRY) for calculating relative yearly load profiles. Use specific energy indicators to calculate real yearly heat and electricity load profiles.

Add real design heat and electricity load profiles at node connection points as well as standard deviations. Add yearly load profiles at the same node.

Add all design and yearly load profiles at the energy distribution/transformer unit, including a 95% quantile for peak load estimations.

Calculate coincidence factor for heat and electricity for design load profiles.

Choose energy carriers and include distribution losses for maximum load and annual energy accordingly.

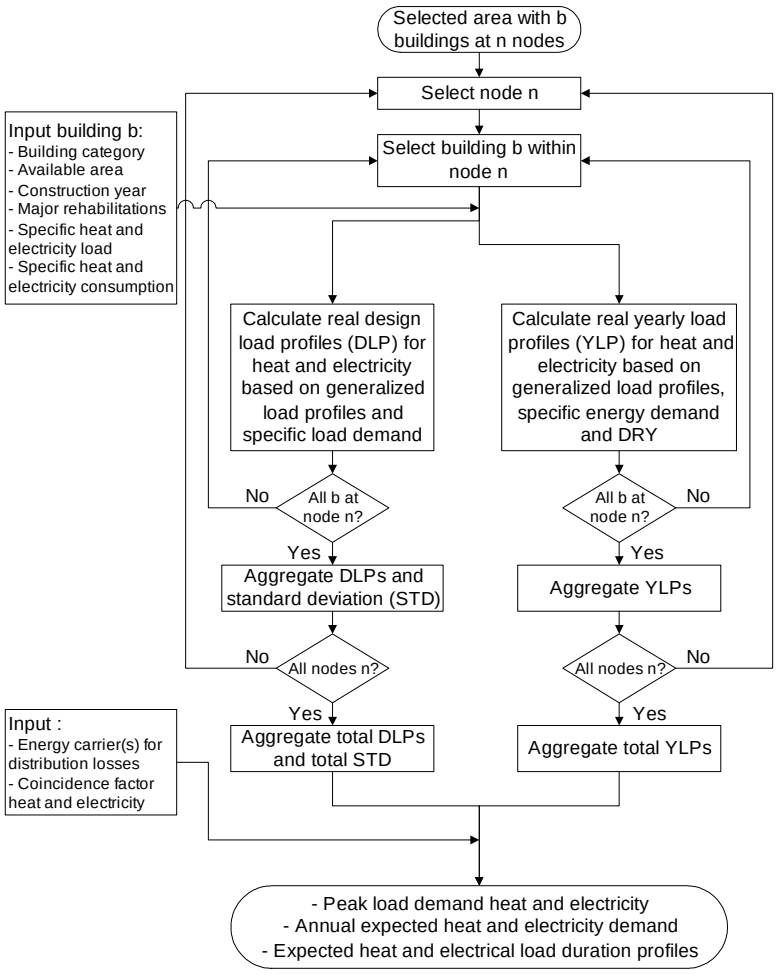

Figure 11: Aggregation of generalized heat and electricity load profiles and energy demand for a specified planning area including distribution load and energy losses [8].

2.7 National adjustments

National adjustment should be made in order to apply the load model for heat and electricity demand. The best approach is to collect national simultaneous hourly measurements of district heat and electricity in buildings to produce national load profiles. It is important incorporate national changes in the building codes which will influence the shape of the load profiles. This is a task that should be performed in the long run when hourly measurements of district heat and electricity become more widespread.

Another approach to national adjustments is to consider the climatic differences between the various countries as well as within the country. It is important to apply the design conditions and the climatic reference year for the locales in question. However, adjustments of the heat consumption indicators are by far the most important. The degree day method should be applied for the temperature-dependent heat consumption.

2.8 Demonstration of load modeling

The demonstration of load modeling is bipartite; the first part is demonstrating the load model for heat and electricity demand presented in the previous chapters and the second part is presenting heat load for a large CHP plant already built (KDHC).

2.8.1 A case study for aggregated load modeling

A case study is performed to show how the generalized load profiles can be applied to a specified planning area in order to estimate the maximum loads, yearly load profiles, load duration profiles and annual energy demands, all divided into heat and electricity purposes. A short description of the planning area along with the solution procedure and results are presented in the paragraphs below.

Description of planning area

It is important to set the system boundaries when estimating the maximum load and annual energy demand for a planning area. Several facts have to be collected in advance in relation to required input variables to the model developed;

Number of buildings within each building category or archetype.

Available area for each building.

Construction year for each building.

Major retrofitting, if any, for each building.

Type of heating within each building: hydronic heating system or electricity distribution system only.

Future development, if any, within the system boundaries.

The case study for this project report is based on a fictitious development area located in Helsinki climate for the purpose of planning for CHP. Table 3 lists the various building categories analyzed and appurtenant number of buildings and average available area. It is assumed that all the buildings within the system boundaries will be built within the planning horizon and that all buildings will have hydronic heating systems.

Table 3: Number of buildings located within the fictitious development area in Helsinki including average available area for every building category.

Building category	*Number*	*Average available area [m^2]*
Single family houses	300	140
Apartment buildings	400	80
Office buildings	18	5000
Educational buildings	4	3000
Nursing homes	4	2500
Hotels with restaurants	4	6000

The specified planning area is located in Helsinki, Finland. The design temperature and a climatic reference year were needed for the purpose of estimating design heat load profiles and yearly load profiles. The design temperature for Helsinki is -26°C and the daily mean temperatures for a Helsinki reference year is shown in Figure 12.

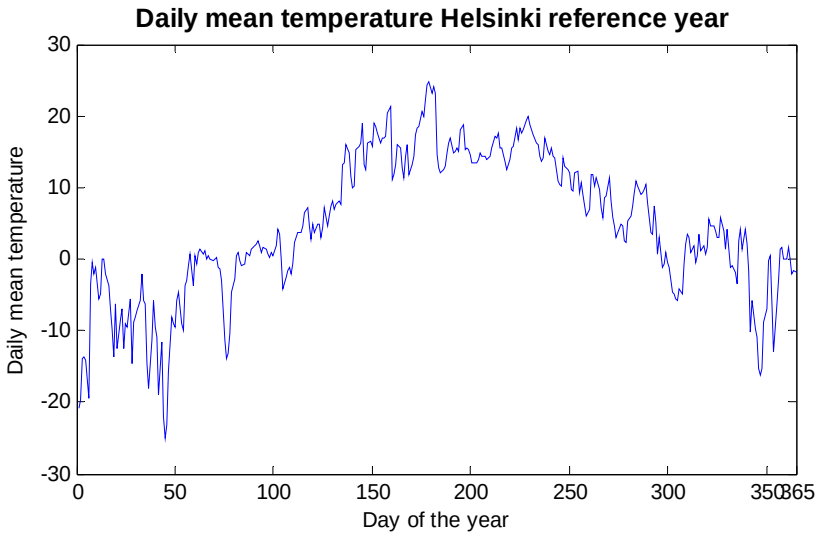

Figure 12: Daily mean temperatures for a reference year located in Helsinki, Finland.

Solution procedure

The solution procedure for load aggregation has been presented in Figure 11, but a short overview will be presented here. When the specified planning area is identified with all the required input parameters for the buildings within the system boundaries, the generalized load profiles are applied. The specific load indicators for all archetypes or building categories are used to restore the design load profile for each building, as well as each buildings available area [8].

The yearly load profiles, and consequently load duration profiles, divided into heat and electricity are calculated based on the generalized load profiles. The HCIs and ELCIs are applied to restore the generalized yearly load profiles for each building within the system boundaries, as well as available area.

The maximum load is estimated using the 95% t-quantile with n-1=729 degrees of freedom, based on the number of buildings within the system boundary. The expected yearly load profiles for heat and electricity are estimated based on a reference year for Helsinki as well as degree days. The distribution losses for maximum load and annual energy consumption are included for both energy carriers; district heating and electricity.

Results

Design or maximum estimated load for heat and electricity demand occurred during weekdays, and the design load profiles for both purposes including standard deviations, 95% quantile intervals and distribution losses are shown in Figure 13. The design heat load is estimated based on the design temperature and the generalized heat load profiles for weekdays during the temperature-dependent season. The design heat load occurred at 8 a.m. during weekdays and is estimated to 10.9 MW. The distribution loss at heat load design conditions is set to 2% of maximum estimated heat load, i.e. at the 95% quantile.

The design electricity load is estimated based on the generalized electricity load profiles for weekdays during the winter season. The design electricity load occurred at 11 a.m., also during weekdays. The estimated design electricity load is 3.8 MW. The distribution loss at electricity load design conditions is set to 8%.

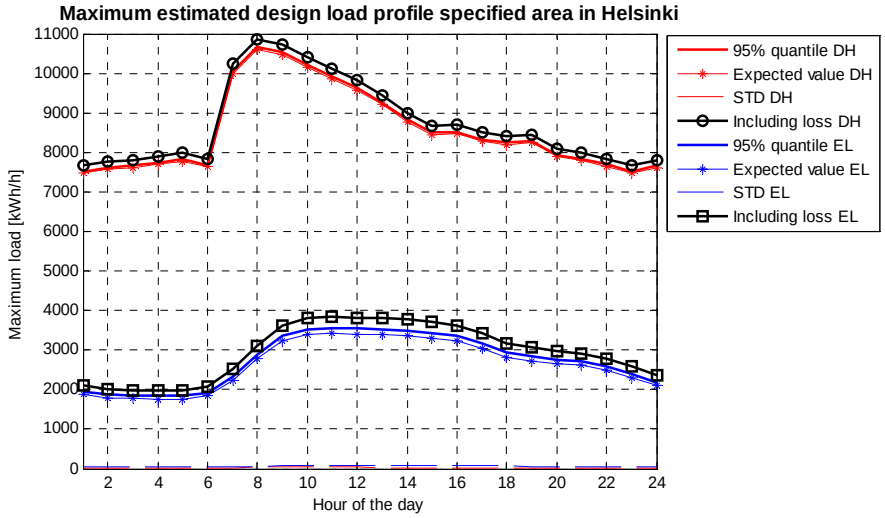

Figure 13: Design load profiles for heat and electricity for specified planning area in Helsinki.

Yearly load profiles and load duration profiles for heat and electricity are estimated for the purpose of this case study, and the results are shown in Figure 14. The annual distribution heat loss is set to 10% for a new district heating system with twin pipes. The annual heat demand is estimated to 25.6 GWh/yr and a utilization time of 2349 h/yr. The annual distribution loss in the electricity grid is calculated based on the k-value to 7%. The annual electricity demand is then estimated to 22.5 GWh/yr with a utilization time of 5921 h/yr.

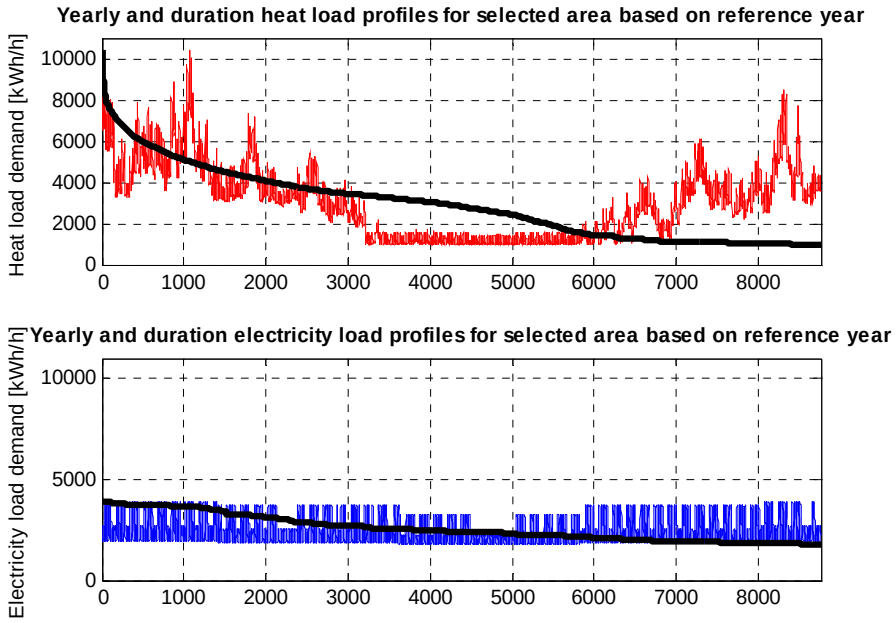

Figure 14: Yearly and duration load profiles for heat and electricity for a specified planning area in Helsinki. The profiles are based on a reference year.

The load duration profiles for heat and electricity are emphasized in Figure 15 for the specified planning area in Helsinki. The maximum heat load from the heat duration profile is slightly lower than the estimated design load profile. This is due to the use of two different indicators, specific heat load and specific heat consumption, as well as the maximum temperature in the reference year being lower than the design temperature for Helsinki.

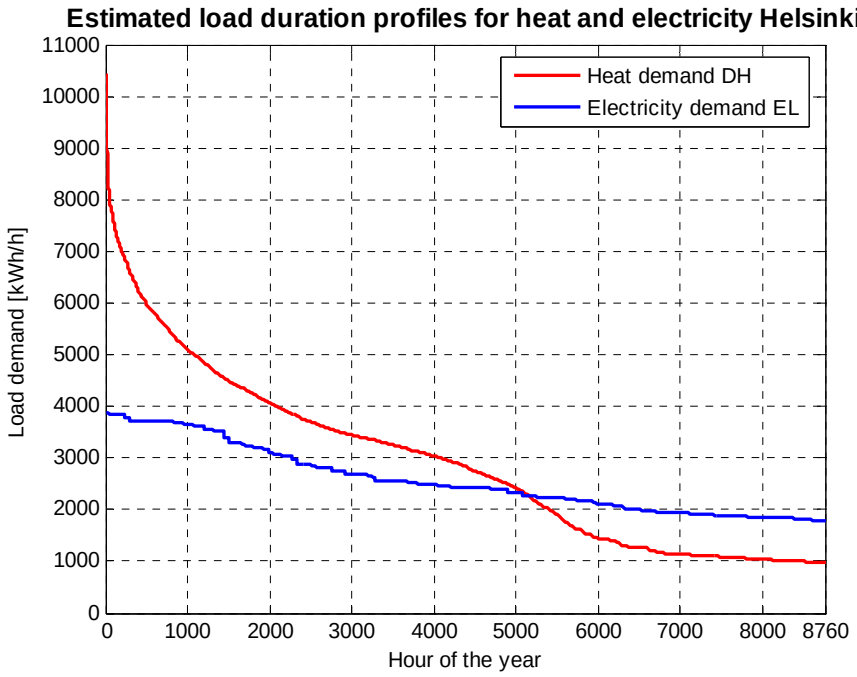

Figure 15: Estimated duration load profiles for heat and electricity load demand for the specified planning area in Helsink.

3 Improving CHP systems with long-term thermal storages

Parts of this section is based on the work presented in the work by Tveit et al. [39].

3.1 Analysis of the long-term storage technologies

There are mainly three different technologies seen from the heat storage aspect and these are: storage in water, storage in the ground and rock and finally storage in form of chemical compound. At current technology level only water or ground/rock can be considered when it comes to storing of large quantity of heat. Chemical heat storages are still under development [14] and they do not offer economically viable solution for large systems.

3.1.1 Water storage

Steel accumulator tanks

Steel tanks are very common components in CHP systems. The largest steel tanks that exist in Sweden have a size of about 50 000 m^3. These storages are used within district heating (DH) systems to balance operation. The DH water is stored directly in the tank.

There are two types of accumulator tanks, pressurized and non-pressurized. These are constructed for over pressure and atmospheric pressure respectively. In Sweden, the non-pressurized tanks are common mainly because it is possible to get a reasonable cost for storage volume (larger than 10 000 m^3). Charging of the tank is done with water at a temperature of 98°C (this is the highest charging temperature for a non-pressurized accumulator tanks). Charging is done in such a way that the hot water is led to the tank through a pipeline at the top while at the same time colder water from the bottom layer is being fed to hot water boiler. The water level in the tank varies all the time and this is because of the water temperature and the difficulty to regulate charging and discharging at constant level.

To protect the tank from corrosion, the space in the upper part of the tank is filled with saturated steam (at low temperature applications as in the case of solar heat system nitrogen gas is used instead of steam).

In all heat storages, bedding is done depending on how warm the water is. Bedding is based on density differences due to different water temperature. Due to the fact that cold water has higher density it will take the space in the lower part of the tank while warm water will take the upper part. To get a good bedding between cold and warm water the accumulator should be high. The system for feeding in and out is designed to support bedding. Bedding enables that water with a temperature of prime quality is available when it is needed (seeFigure 16).

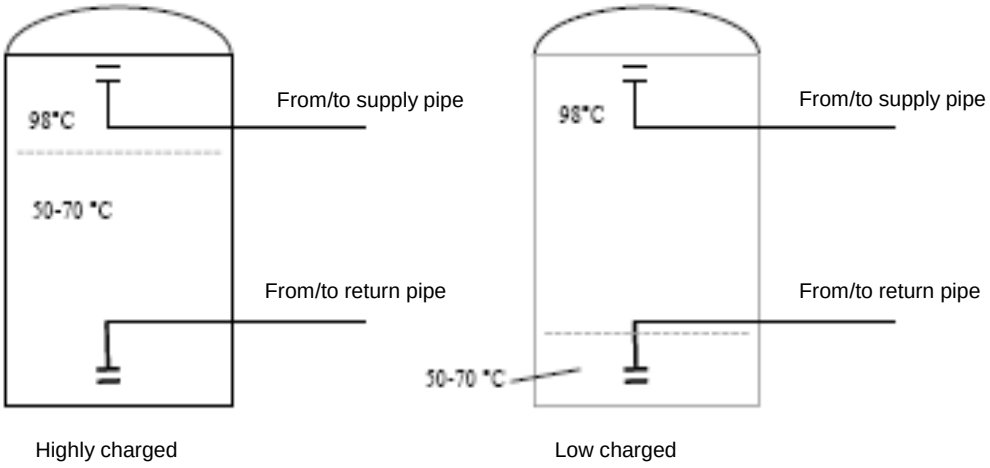

Figure 16: Principle of bedding DH tanks [15].

Rock cavern

The technology to store warm medium in rock cavern has been in application for long time, for instance in Sweden since 1950. In those days the technology has been used to store oil and other petroleum products. There are about 200 such oil storage facilities in Scandinavian and in Sweden alone there are 140 of them. In about 80 of these facilities, petroleum products are stored directly on the surface of ground water in rock cavern with coarse sides. Traditional oil storages are designed as long tunnels and they are 15-20 meters wide and up to 30 meter high. The storage is situated with the top of the head about 20-30 m under ground level. The length of the rock cavern is usually 50-200 meter and it is adjusted based on the geological situation and production method. It is common that several storages are built next to each other and they are connected by a distribution tunnel. The roof structure and the walls are often reinforced. In Sweden the sizes of rock caverns are between 50 000 till 2 000 000 m^3 single or interconnected [16].

The oil rock caverns in Sweden are owned by the state, county council and municipal and private energy companies. Some of the rock caverns are also owned by private industry and oil companies. These storages were built primarily for strategic purposes during cold war period between the end of 1950 and the end of 1970. Many of these facilities are today under a process to be phased out. In many studies it has been investigated how these storages can be used for heat storage application [17] and in some places there is a CHP plant close to the oil storages (e.g. in Norrköping, Nynäshamn).

The construction of big rock cavern is a known technology but the problem is however only few such projects are under way and it seems that this technology is on the way to be forgotten. As a result of this it is difficult to get up-to-date information concerning the cost of rock cavern.

When construction rock cavern, a leading channel has to be prepared through blasting. This channel will be then used to transport mass of rock during construction period. Since the cost for the channel is high compared to costs of rock blasting, it is important to maintain an optimal length of the channel. When the channel has reached the designed ceiling height, the blasting process to get the roof arch will begin. The work continues with stepwise blasting until the bottom limit is reached. The bench height varies between 8 and 14 meter. Since the rock has a relative high thermal conductivity and the rock is built without insulation, the size of the heat storage in rock cavern should be big to keep the energy loss low. Open rock cavern with water has high storage capacity because water has high heat capacity.

One known example of heat storage in rock cavern is the solar heat storage in Lyckebo outside Uppsala (Sweden). The storage was built 1982 as a toroid with rock pillar in the centre.

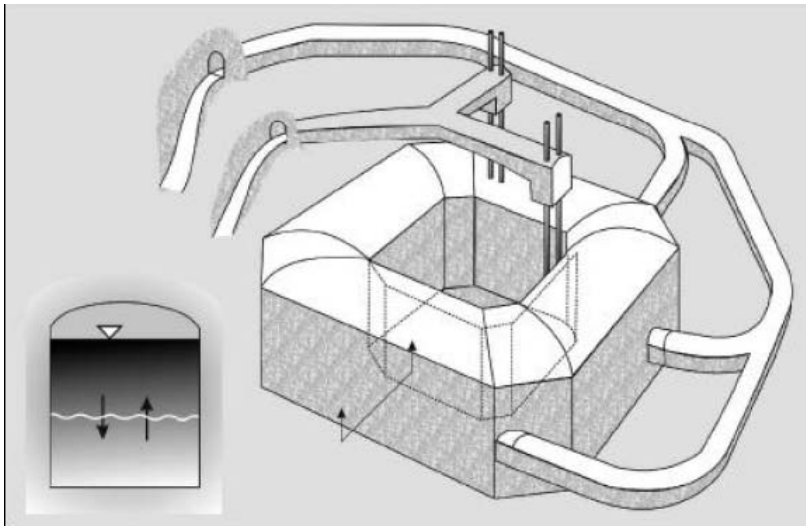

Figure 17: The lay-out of rock cavern heat storage, Lyckebo.

The storage is still in operation but the heat comes today from a biofuel boiler. At the beginning, measuring showed high heat losses but this has gone down to the normal level since 1993. There are many theories concerning the rather high loss at the beginning but the main reason could probably be self-circulation processes caused by fractures.

The heat conductivity for non-insulated rock cavern from granite has been investigated for Lyckebo. Figure 18 illustrates the fact that heat losses are high at the beginning and it will decrease with time since the surrounding rock in the mean time will be heated up then. After about 5 years the heat losses reach steady state condition.

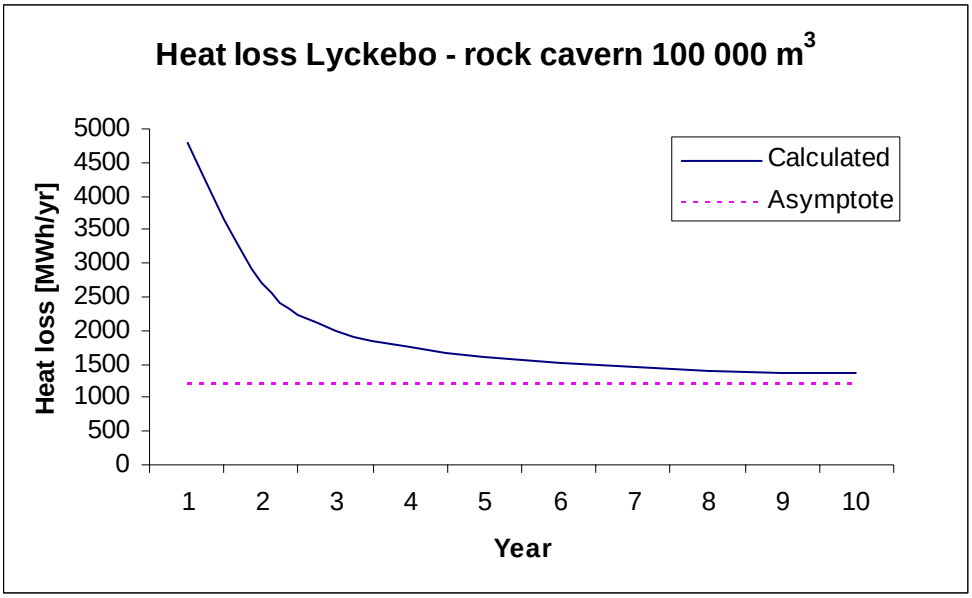

Figure 18: Calculated heat loses for the rock cavern in Lyckebo [17].

Heat losses during the first years should be seen as part of the investment while losses thereafter can be considered as operation costs. Rock cavern bigger than 300 000 m^3 can be designed as traditional oil storages with oblong headings, where heat losses between the spaces are insignificant, ca 10 % per year. It is therefore possible to recover primary energy from rock cavern heat storage.

Pit storage

Pit storage consists of an excavated pool where the heated water is stored. The surrounding ground absorbs the water pressure. The tightening layer can be made of thin material like rubber, plastic or metal foil. On the top there is a closing that function as vapour barrier and insulation.

Heat storage in insulated water-filled pit is an interesting method for smaller DH system. This storage technology can be used for long and short-term storage and it is advantageous compared with accumulator tank. The ground is utilized as insulation and as part of the structure. Originally, pit storage has been used in solar heat system applications with limited temperature up to 70°C. However, new materials have been tasted since 1980 indicating that pit storage can be used for applications with temperatures above 90°C [16].

Construction details

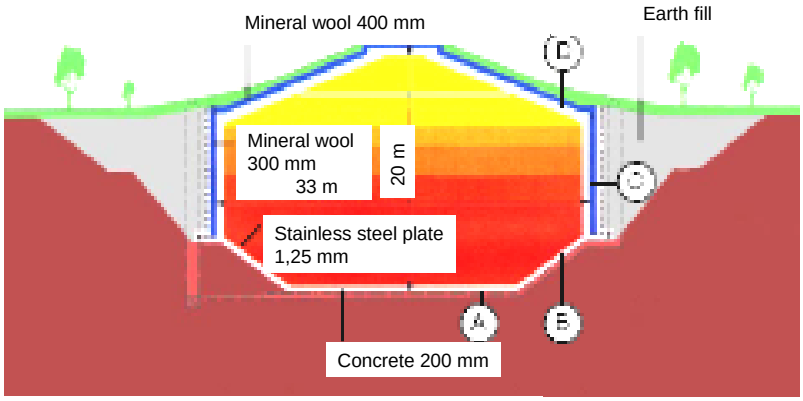

Figure 19: construction details of successful pit storage in Fridriechshafen, Germany.

Figure 19 shows the construction principle of storage designed as excavated concrete tank. This construction can handle to store water at 90ºC. A disadvantage of pit storage is that they are relatively shallow (10 – 12 m) and this makes the area very big for large volumes. Thus, pit storage is most suitable when the size is less than 50 000 m^3, i.e. the same size as steel tanks. A large number of pit storages with different constructions and sizes up to 10 000 m^3 have been built in Germany since 1995 and it has been achieved a notable cost reduction.

3.1.2 Ground storage

Ground heat storage belongs to the group of heat storages where the ground is used as a storage medium and the water as heat transport medium.

Borehole storage

In borehole storage, heat is exchanged between the water and the rock or ground. Holes with diameter of 100-150 mm and depths in the range of 50-100 meter are drilled in to the ground. The distance between the holes has often been 3 – 4 meter. The heat exchange system can be open or closed with a pipe or tube system. Figure 20 shows the construction of borehole storage in Luleå (Sweden).

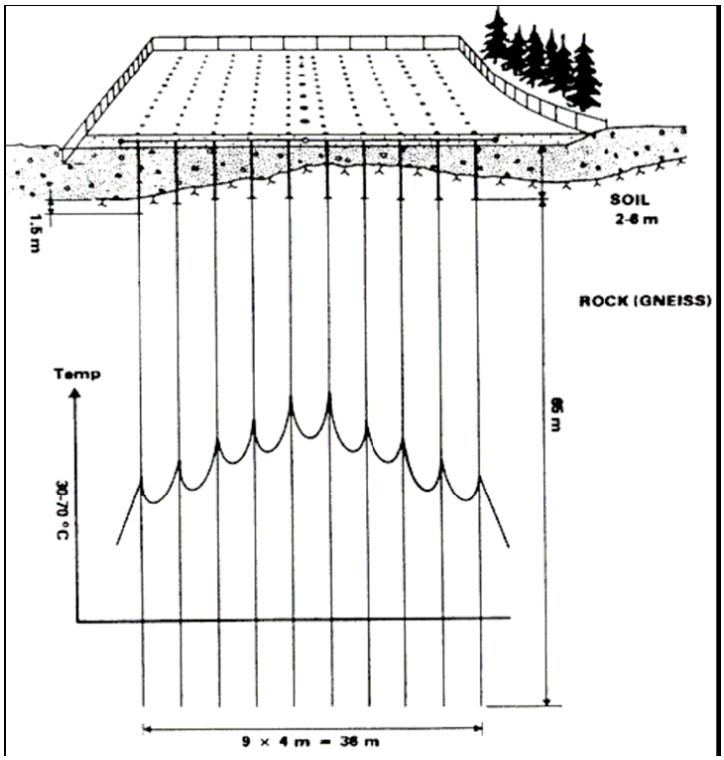

Figure 20: Principle picture of borehole construction. The temperature is high in the middle [18].

Heat distribution in the storage with the highest temperature in the middle and around the holes is shown in the picture. The storage is charged in such a way that warm water circulates through the pipes and drill holes and thereby emits the heat to the rock. During discharging, the circulating water take back the heat from surrounding rock [19].

There are two different operational strategies that can be used during charging and discharging. In the simplest case, all holes are connected in parallel and charging and discharging take place simultaneously in the entire rock volume. In this arrangement, a high charging output will be achieved. In the other case, the holes are connected in serious in radial direction and the storage is charged from the centre and in radial direction outward. Discharging will take place in the opposite direction. In this case, the temperature is the highest in the centre. Though using the second arrangement, higher energy and temperature efficiency can be obtained but this has a higher cost compared with the first case.

The relative heat loss decreases with increasing storage volume also for this type of storage. In most cases, the geometrical form (seen from above) of the storage is rectangle or circle. In order to get equal temperature distribution in the ground, the boreholes are placed in such a way that they are uniformly distributed across the storage area. The depth of the boreholes depends among other things on the type and quality of the rock.

The depth of the boreholes and the space between them has to be optimised for each specific

borehole storage. The geological condition has to be investigated; for instance, the soil layer should not be too deep. Borehole storages are always built on a plain ground surface.

The boreholes can be designed as open or closed system. In the open system, the water is in direct contact with the rock and this system has therefore a better heat transfer. The closed system allows that the design of the ground heat exchanger can be varied easily. However, the heat transfer is poorer in this system. If the ground is argillaceous or sandy, the design of boreholes must be of a closed system [19].

Ground storage of this type is slow compared with water storage system. Technically, it is possible to construct the storage in such a way that high heat transfer can be achieved. This would demand big heat exchanger area meaning more boreholes with shorter mutual space.

Aquifer

An aquifer or a natural ground water reservoir consists of earth or porous rock where the hollow space is filled with water. The water in the ground has to be in motion for heat storage application. Aquifer storage is characterised by the property of the water and it has many similarities with water storage. One big difference is that the storage space is already available and it does not have to be built. The cost of the storage will therefore include basic investigation of the ground and installation of ground water circulation [20].

In order to limit the influence of heat losses, storage in aquifer assumes normally a large-scale application with a magnitude of 1 million m^3. Artificial demarcations are not common both from technical and economical point of view. Small-scale storage in artificial aquifer with tight layer has been studied. The application of this technology has been limited because of difficulties to find suitable tightening method, but this problem was solved during 1990.

For storages in superficial ground water reservoirs, low temperatures in the interval of 20-50°C has been studied. On the other hand, deep reservoirs are necessary for storages at higher temperatures around 60-90°C [21]. The hydraulic capacity of the well system and the way in which heat exchanging takes place determines the momentary capacity of the aquifer.

There is always a risk for chemical precipitations in aquifer storage. For example, an iron containing water can prevent the oxygen feed to the pumped water. Stowing of filter well is common and pumping to get rid of this is a normal maintenance measure. Aquifer storage is most suitable as low temperature storage. There are limited experiences from high temperature aquifer in Germany. These are artificial aquifers with limited water volume. It is therefore uncertain

whether high temperature aquifer can be used as a storage that returns heat with prime quality (as an alternative a rock cavern filled with blast stone should be considered).

3.1.3 Storage costs

The best way to compare storage costs in fair way is to compare the same quality, for instance, available energy for different storages. This quality varies because of different storage medium (water, ground) on the one hand and because of heat losses on the other hand. From Table 4, it can be seen the necessary storage volume to store 1 MWh heat in different types of storages.

Storage type	Volume m^3	Reference	Reference year
Accumulator Tank	17	A. Hedbäck	2006
Pit storage	17	A. Gabrielsson	1991
Rock cavern	20	H. Pilebro	1981
Borehole	60	B. Nordell	1983

Table 4: storage size to store 1 MWh heat at temperature difference 50 °C.

Costs for heat storage have been taken from different references and they are valid for different time period. In order to estimate current costs, the referred costs are adjusted using building cost index (see Figure 1.6). With the exception of pit storage, all costs are verified and discussed with experts. It should be noticed that costs can vary quite a lot depending on different circumstances as trade outlook, location, orders, applied technique etc. Figure 21shows storage costs as a function of equivalent volume for different types of heat storage.

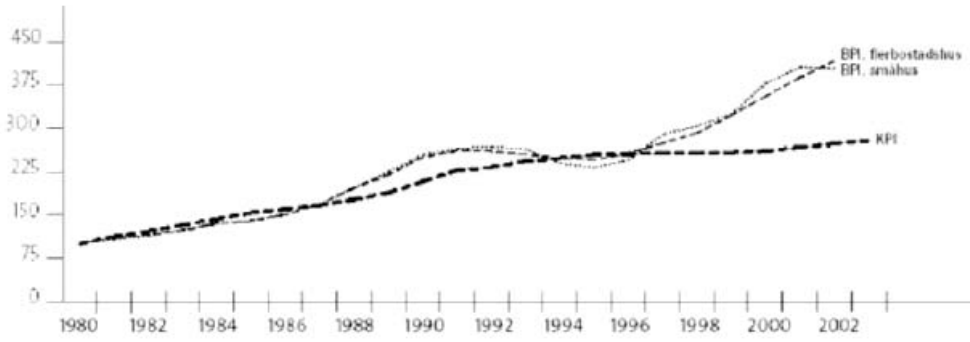

Figure 21: Development of building costs. Bulding price index PBI compared with consumer price index KPI (according to Swedish competition authority).

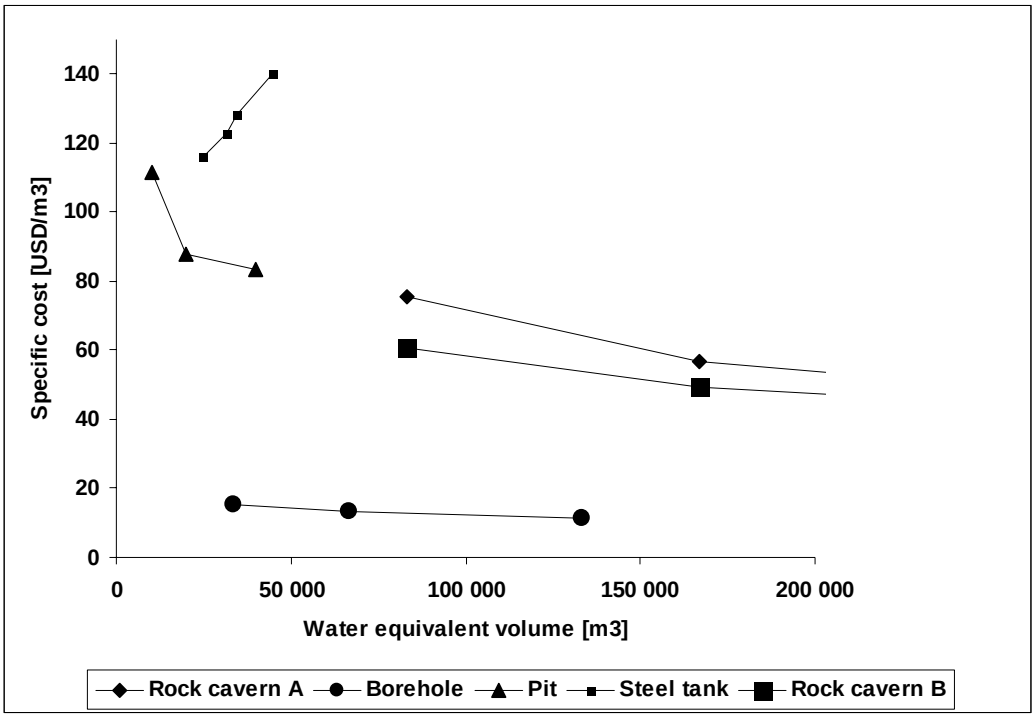

Figure 22: Specific costs for different storages as a function of water equivalent volume

As it can be seen from Figure 22, rock cavern and pit lie approximately on the same cost level. Two levels of cost are used for rock cavern. As far as it known, no pit storages that is larger than 12.000 m^3 has been built. Steel tanks are more expensive than pit storage.

Borehole storages are the cheapest. Large borehole storages are under construction in Germany. In order to use borehole storages in CHP systems where high heat transfer rate is expected, more densely placed boreholes than it is the case in existing borehole storages, which mostly are used in solar heat applications, are necessary. However, the price difference is so high that a thorough investigation on how borehole storage can be used in CHP systems should be conducted.

It should be mentioned that studies on artificial aquifer where the price is about 60 USD/m^3 water equivalent (50 000 m^3) have been carried out in Germany. According to Figure 22, this price lies in the region between pit and rock cavern and this confirm the price situation for such a technology where earth excavating exists.

3.1.4 Costs for large rock cavern

For further analysis of heat storage in CHP systems, it is assumed that only rock cavern will be used. The cost of rock cavern is assumed to be regressive, i.e. the specific investment cost decreases with increasing volume according to the following relation:

$$K_{storage} = K_{storage(V_0)} * \left(\frac{V}{V_0} \right)^{eb} \quad [\text{USD/m}^3].$$

Based on previous estimation [9] and using the figures from Figure 21 a cost/volume relation is obtained as it can be seen in Figure 23.

The following cost parameter count:

V_0: 100 000 m^3

$K_{storage\ (V0)}$: 50 USD/m^3

eb: -0,3.

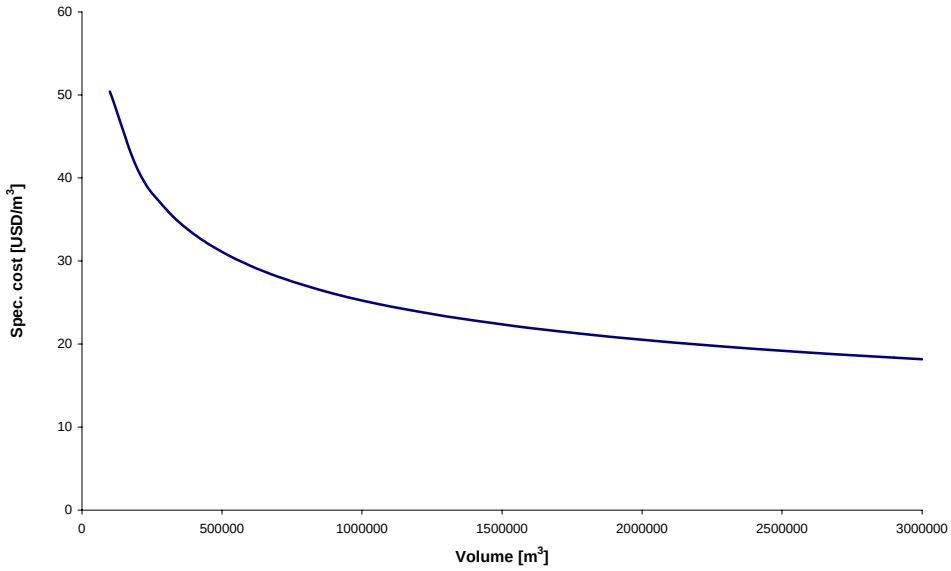

Figure 23: Specific investment costs for large rock cavern according to reference [9].

3.2 Economic simulation model study for a system with CHP plants, heat storage and DH network

One application for seasonal heat storage is to supply heat from an existing district heating system to an area outside of the reach of the existing net. For this purpose the area has to be connected by a transmission line. If the system of the new area incorporates a seasonal heat storage (SHS), it is possible that the transmission pipe feeding the SHS can be made smaller than in the case that the area is connected directly. The saving in pipe costs can outweigh the costs of the SHS.

3.2.1 The case of Linghem

In a practical application, the goal of this study is to analyze if it is possible to connect a local district heating net for the village of Linghem to the district heating system of Linköping by means

of a relative small district heating transmission pipe in combination with seasonal heat storage. In that way, excess heat from summer CHP operation could be used to provide heat to Linghem.

Figure 24: Map of the area of Linköping and Linghem.

Heat supply to Linghem

Linghem village is located approximately 5 km towards east from Linköping's district heating net, which is operated by the Tekniska Verken i Linköping (TVL). A DH - transmission pipeline can stretch for example along Norrköping's road or along the railroad in order to connect to a heating central at the western road entrance to Linghem. Figure 24 shows a view of the pipeline along the railroad. The DH transmission pipe can offer heating of Linghem by using the summer heat from Gärstad municipality waste incineration plant. No other energy supply system is needed; the objective is instead that all heat supply to Linghem comes from the TVL net and is locally distributed via seasonal heat storage.

The heating system

We suppose that the Linghem area should be provided with district heating from TVL by a transmission pipe, which connects at a suitable site to the district heating net of Linköping. Heating is distributed to a heat storage installed at the outskirts of Linghem and further from there it is distributed to the local network. We suppose for this analysis that heat distribution to Linghem

is operated the whole year with a temperature difference (supply – return) of 40°C. The non-pressurised heat storage separates the two networks in Linköping and Linghem (see Figure 25).

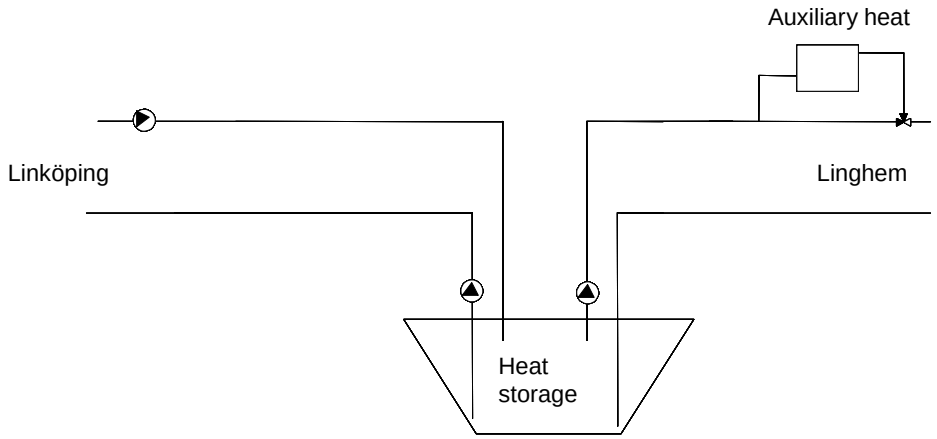

Figure 25: Schematic connection diagram between Linghem and Linköpings DH network.

For the analysis we suppose that the heat load in Linghem is 20GWh/year and that 80% of the load will be covered by district heating (following assumptions given by the Swedish district heating Association, [23]). This results in an annual heat load of 16 GWh and in a maximum heating capacity of 5,4 MW for the total heat supply in Linghem (the full capacity operation time is assumed to be 2900 h in accordance with [23]). The heat delivery is distributed over the whole year according to the duration-diagram shown in Figure 26.

Different operational cases

We can now analyze 4 different operational cases for the heat delivery to Linghem, which consequently involves different sizes of the heat storage and different dimensions of the transmission pipes:

a) Heat delivery from TVL takes place only during three summer months (2200h).
b) Heat delivery from TVL takes place during seven summer months corresponding to 5100 heating hours.
c) Heat delivery to and from the heat storage takes place all year at a constant capacity.
d) Heat delivery takes place all year without heat storage.

a) Heat delivery takes place only during three summer months

In this case the whole heat delivery stems from the Gärstad waste incineration plant. The heat delivery supposes to sum up to the annual load of 16000 MWh plus heating losses from the storage, which were calculated by means of the seasonal heat storage program MINSUN [24], being 2000 MWh for a rock cavern of 400000 m3 in operation a couple of years. The transmission

pipe line must be dimensioned that way that the whole necessary energy is delivered and charged to the storage in 2200 h, i.e. for 8,1 MW.

The heat storage must take up the necessary energy for a whole year except the summer months during which the energy is delivered directly to the load. Hence the supplied energy is 18000 MWh and the energy to be stored is 16272 MWh.

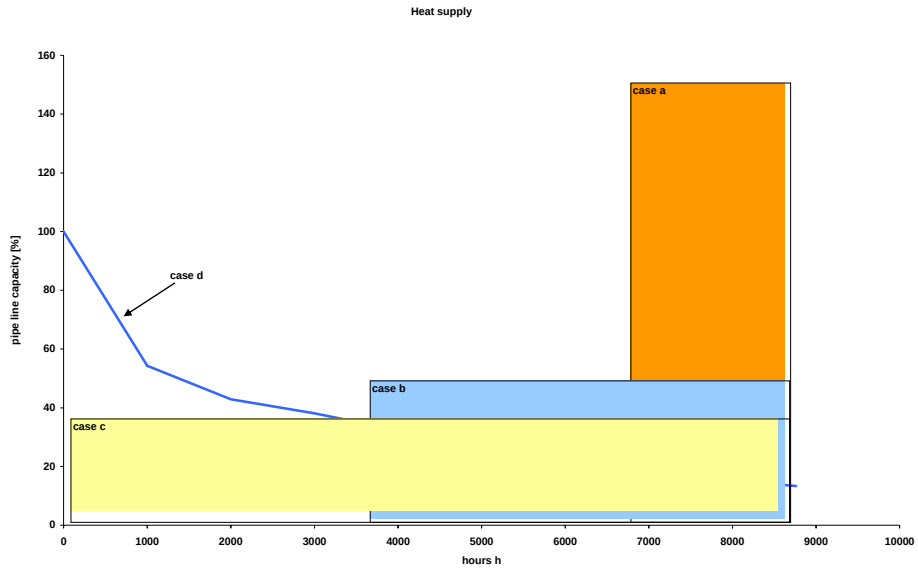

Figure 26: Duration diagram for assumed heat load in Linghem.

b) Heat delivery takes place during 7 summer months (5100 hours)

The heat delivery is arranged so that the Gärstad plant of TVL delivers all the necessary heat during a period of seven months (summer period), but no heat during the winter period November to March. The total energy consumption is calculated to 18053 MWh and the storage capacity (inclusively heating loss) will be 12817 MWh. The transmission pipe should be dimensioned for 3,4 MW heat supply.

c) Heat delivery to and from the heat storage takes place all year.

Additionally an alternative is that heat from TVL-net is delivered at a constant load during the whole year. In that case the charging power will be 1,9 MW and the necessary heat storage capacity is 4200 MWh inclusively heat losses. The total energy demand is 16700 MWh/year.

d) Reference case (no heat storage)

In the reference case of none heat storage and a pipe line design according to the maximum load, a heat load of 16000 kWh must be supplied and the dimensioned pipeline capacity is 5,4 MW.

Cost calculations

In order to compare the different cases, a simple calculations model of the total annual costs for those four different cases is established. Cost calculations include transmission pipe cost, storage cost and cost for delivered heat. An income can also be accounted for due to sales of heat and electricity to the people of Linghem.

Cost of heat production

In order to simplify the calculation we can assume different production costs over the year in the TVL-net. One important point is that heat production from the Gärstad waste incineration plant has negative marginal costs due to the fact that people has to pay for the rubbish to be incinerated. For our calculation we set the marginal costs for heat delivery to Linghem to 0 USD/MWh for the month June, July and August. This assumes that the operating costs for the heat distribution are outweight by the negative fuel costs. Anyhow there will be an income for TVL by selling electricity.

For the month April, May, September and October we set an intermediate marginal heat cost to 25 USD/MWh, indicating, that besides municipality waste some other fuels are used, especially biomass and an electrical heat pump.

During wintertime, oil might be used at top load production and the amount of biomass and other fuels is higher in the total mix. For this reason we set the costs of delivered heat to 44 USD/MWh.

Income from heat and electricity sale

Income from heat delivery is based on a heat sale price to customers of 44 USD/MWh all year. That means that the profit from heat selling is largest, when the heat is delivered to the storage summer time and less in spring and autumn and none in wintertime.

Additional income stems from sales of electric power. We assume here that half of the heat amount is the corresponding electricity production in the cogeneration plant. That means that for every MWh delivered to the Linghem system, 0,5 MWh electricity can be sold to the grid at a production price of 50 USD/MWh. The value of the income can be converted to the present value factors 7,36 respectively 11,47 for periods of 10 and 20 years, respectively. These present value factors are based on an interest rate of 6%.

.

Heat delivery	Net income	Income	Present value	Present value
summer/spring-aut/ winter	heat	electricity	10 year	20 year
	USD	USD	USD	USD
180000/0/0	705 555	396 875	8 113 885	12 644 872
7753/10300/0	446 012	398 043	6 212 245	9 681 311
4209/5582/6909	260 230	368 212	4 625 332	7 208 227
1975/3873/10152	160 287	352 778	3 776 156	5 884 851

Table 5: Net income from heat and electricity supplied from Linghem for above four operational cases.

Expenses for heat storage

Heat storage costs for large thermal heat storages have been investigated carefully in the 1980s. The last reported costs originate from a handbook published by the Council of Building Research (BFR) 1996 [16]. In that BFR energy review the costs for large seasonal storage systems for solar heating are given with 0.37 – 0.56 USD per kWh stored heat capacity (price depends on the size of the storage, but since we only have to do with large storages above 12 GWh, the size variation is not an important factor).

For large storages we recommend and prefer rock cavern storages which can be blasted into rock formations and have been demonstrated at Lyckebo [25]. Alternatively, earth pits could be used at slightly higher costs than rock caverns. This techniques have been extensively studied in Denmark, Sweden and recently in Germany [26].

A third technique is drilled boreholes in rock, which is judged to be essentially cheaper than the rock cavern, i.e. 0.06 – 0.25 USD/kWh. However, the charging and discharge of large amount of heating power needs to be investigated in more detail. Probably the borehole storage must be combined with short-term buffer storage in this case.

The study from [16] is now more than 10 years old and therefore costs should be recalculated. For the purpose of this study we assume a heat storage cost of 0.5[2] USD/kWh, which is assumed to be an achievable cost for any type of large heat storage. The Heat storage is dimensioned for a ΔT of 40°C. Resulting heat storage costs are shown in Table 6: Heat storage costTable 6.

[2] This price is however significantly lower than the prices used rock cavern in the next sections where the cost close to 0.9 USD/kWh.

	Storage capacity	Storage size	Storage cost
	MWh/year	m³	USD
Case a	16 272	350 690	8 200 567
Case b	12 817	276 228	6 459 358
Case c	4 209	90 711	2 121 201
Case d	0	0	0

Table 6: Heat storage cost

Expenses for transmission pipe

Current costs for district heating pipes can be found in [23]. Such costs depend evidently on how and who we ask, but for this analysis we choose the middle line of Figure 27, representing practical results of the year 2000. The diagram refers to the completely installed transmission pipe per trench meter. In order to get the right price, the dimension has to be translated into heat capacity (heating power). The relation can be found in Table 7:Relation between Cost and Power for different pipelines. We presume that the dimensioning temperature difference is 40°C.

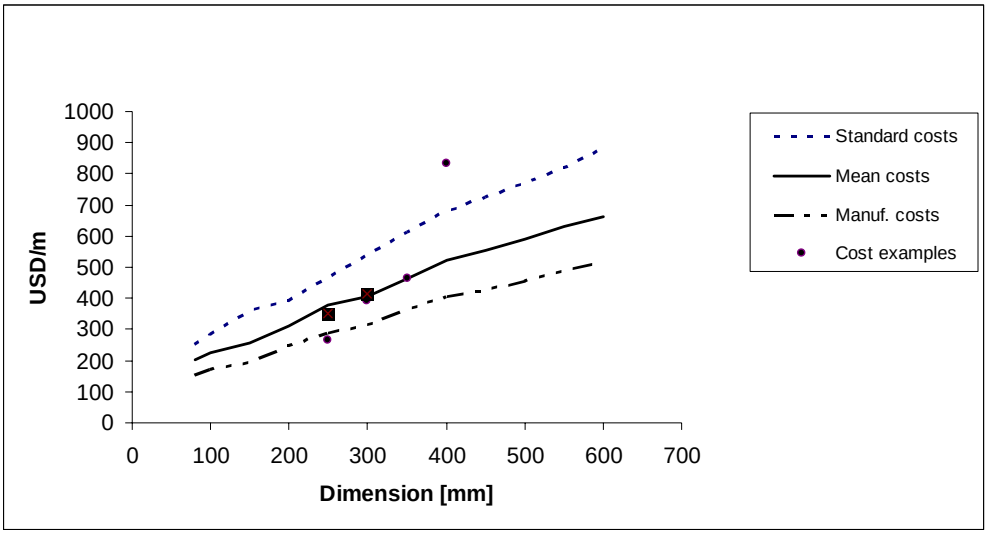

Figure 27: Costs of transition pipes [23]. The dots refers to field experiences and the middle curve is according to a standard calculation for smaller pipes.

	Transport power	Pipe dimension	Cost	Cost for 5 km
	MW	DN	USD/m	USD
Case a	8.1	200	307	1 537 102
Case b	3.5	150	239	1 196 924
Case c	1.9	125	227	1 133 928
Case d	5.4	180	277	1 385 912

Table 7:Relation between Cost and Power for different pipelines

Cost comparison

The total system costs can be calculated as the difference between income and expenses, integrated over the assumed life time. The net income is shown in Table 5 and the costs of the heat storages and of the transmission pipe is according to Table 6 and Table 7, respectively. Positive values indicate that the income exceeds expenses and that the system alternative is profitable. Results for the 4 different operation cases are shown in Table 8.

	Present value	Present value
	10 year	20 year
	USD	USD
Case a	-1 623 785	2 907 202
Case b	-1 444 037	2 025 030
Case c	1 370 202	3 953 098
Case d	2 390 244	4 498 939

Table 8: Total system income for four system alternatives with 10 and 20 years depreciation time.

As it gets evident from of Table 8 so are today's costs not directly motivating the investment for heat storage connected to a transmission pipe between the TVL-net and Linghem. The most profitable alternative is to directly distribute the heat through a pipeline.

However the difference between the case c) (continuous storage charging) and case d) (no storage) is small in the case of 20 year depreciation time. Therefore, a sensitivity study is made in which the four operation cases are varied with reduced storage costs.

Reduced storage costs can be particularly the case for borehole storages, because our costs were taken much higher than the costs indicated in [16] for this technology. In a recent study [27] the investment costs for borehole storages were estimated to 0.25 USD/kWh. Hence in Table 9, the results are shown for a varied storage cost of 0.37 and 0.25 USD/kWh, respectively.

	Present value 10 years		Present value 20 years	
	Storage cost		Storage cost	
	0.38 USD/kWh	0.25 USD/kWh	0.38 USD/kWh	0.25 USD/kWh
Case a	1 109 738	2 476 499	5 640 725	7 007 486
Case b	709 083	1 785 642	4 178 149	5 254 709
Case c	2 077 269	2 430 803	4 660 165	5 013 699
Case d	2 390 244	2 390 244	4 498 939	4 498 939

Table 9: Total system income for two alternate storage costs

Table 8 shows that already at 10 years depreciation time and at a storage cost of 0.25 USD/kWh, seasonal heat storage which is charged during three summer months (case a) shows the highest

income. It is therefore of interest to study in depth the application of borehole storage together with buffer tanks. If the cost of storage is 0.38 USD/kWh, a higher depreciation time is needed. It is however important to utilize surplus heat instead of just wasting it. Case c) would be of interest if the surplus heat has to be utilized in anyway.

3.2.2 Simulations

In the previous chapter, a case study of a possible application of heat storage as a means to supply the heat demand in Linghem, Linköping is presented. A similar study can be carried out for small areas in Norway and Finland. In order to perform the simulation, the load profile for the area that can be connected to an existing main network has to be defined. Load profiles models for heat and electricity have been developed by SINTEF. For this purpose, a case study for a fictious area in Helsinki, Finland has been made. As a reference load profile, heat load duration as studied by SINTEF is used in this study (see Figure 14).

When a new area is supposed to be connected to an existing DH network, the pipeline is dimensioned for the maximum load. Since the cost for the pipeline is proportional to the dimension, it should be of interest to reduce the dimension when the distance is long between the networks. Seasonal heat storage can give smaller pipe dimension and thereby decrease the cost in the long-term. The purpose of this section of the study is to build a simulation model and evaluate the profitability of heat storage from different boundary values.

Method

The model contains different terms as storage volume, storage cost, pipeline cost and present value factor. The formula to calculate the different terms are given below:

$$V_{storage} = \left(\frac{Q}{Cp_v X \Delta T} \right) \text{ [m}^3\text{]}.$$

Q is the heat demand, ΔT is temperature difference and Cp is assumed to be one. The formula for storage cost is given in section 1.1.4. The pipeline dimension is given only for ΔT = 55 in the pipeline catalogue. Since in this study is assumed ΔT = 40, a formula which considers this is taken from the catalogue:

$$P_{\dim} = \left(\frac{Q}{\Delta T.55} \right) \text{ [MW]}.$$

Present value factor, PVF

$$PVF = \frac{1-(1+r)^{-a}}{r}$$

Where r is interest rate a is number of years.

Different operation cases

Three different operational cases have been chosen to make comparison:

a) Heat delivery takes place all year without heat storage.

b) Heat delivery takes place during seven summer months corresponding to 5100 heating hours.

c) Heat delivery to and from the heat storage takes place all year at a constant capacity.

Input parameters that are used in the simulation

To evaluate the benefit of heat storage for such application, some key parameters have been chosen. These are: distance to main network, power price, heat price to customer, heat production cost at different season (see Table 10).

Parameters	Variation
Distance, m	2/5/10/20
Power price, USD/MWh	37.8/63/94.5/126
Heat price to customer, USD/MWh	37.8/50.4/63
Heat production cost at different season, USD/MWh	-12.6/0/12.6 summer 12.6/25.2/37.8 autumn and spring 44/56.7/75.6 winter
Heat demand, GWh/year	20/60/200

Table 10: Parameter interval chosen in the simulation

Simulation results and sensitivity analysis

Since the model is not optimising and the variables give many combinations, it would simplify the analysis to focus on the indications the simulations give. This will give an indication when seasonal heat storage can be more beneficial than a direct connection. The analysis is done in such a way that one parameter is varied while others are kept constant. Thereafter, some parameters have been varied simultaneously to see if there is more or less profitability. As reference values, averages of the figures as given in the above table are used.

The impact of variation of heat production cost

In this case only the production cost is varied while the other parameters were kept constant. The variation of the cost is as follow: expensive the whole year, cheap the whole year, expensive/cheap during summer/winter and cheap the whole year except winter. The simulation shows that the case without heat storage (case a) is profitable. There is however an indication that the difference in profitability between the cases decreases when the cost of heat production is cheap the whole year except wintertime.

The impact of the length of pipeline

When only the length of the pipeline is varied, the simulation shows that case c more economical than the other two cases. However, this holds true only when the distance is longer than 40 km

(when the heat demand is 60 GWh and the depreciation time is 20 years). The reason for this is that the pipeline cost will be much higher as the distance increases. In Figure 28, the relationship between the pipeline length and the income is presented.

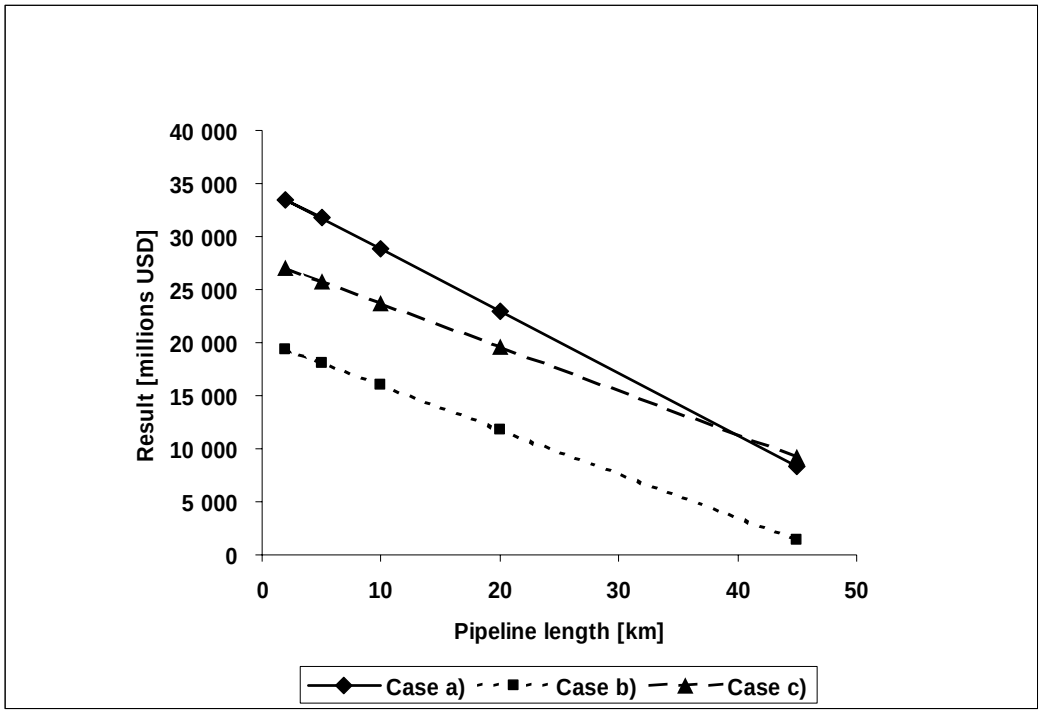

Figure 28: Pipeline length verses income.

The impact of heat delivery cost to customers

Variation of consumer heat and electricity prices does not give any indication concerning the economical benefit of heat storage.

The impact of variation of heat demand

Changing the heat demand of the local area does not bring a new solution. The income increases in all cases but it is still the case without storage that is economical. Figure 28 shows the result when the demand is varied.

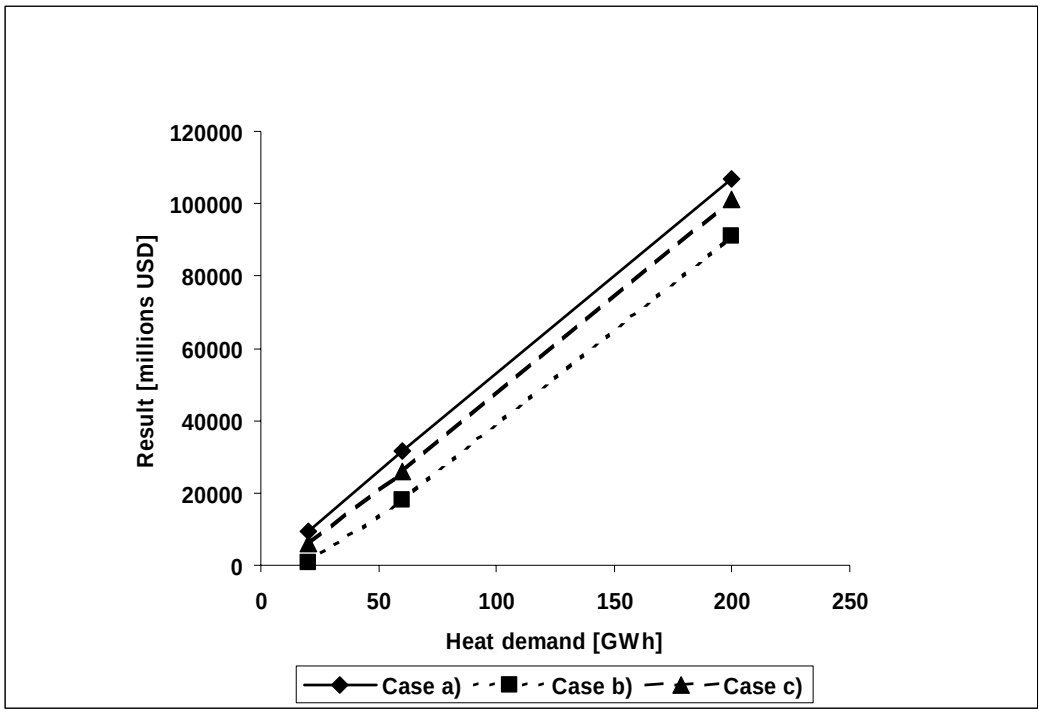

Figure 29: Heat demand verses income

The impact of variation of more than one parameter

Several simulation have been carried out to find out if there are combinations of parameter that can lead to a better economy situation for heat storage application. The simulation shows that there is an indication on cost benefit (provided the depreciation time is 20 years) of heat storage when the heat demand is high and the production cost is high/low during winter/the rest of the year. This situation occurs because the storage stores the heat from cheap periods and this heat can then be used during winter. Figure 30 shows this result

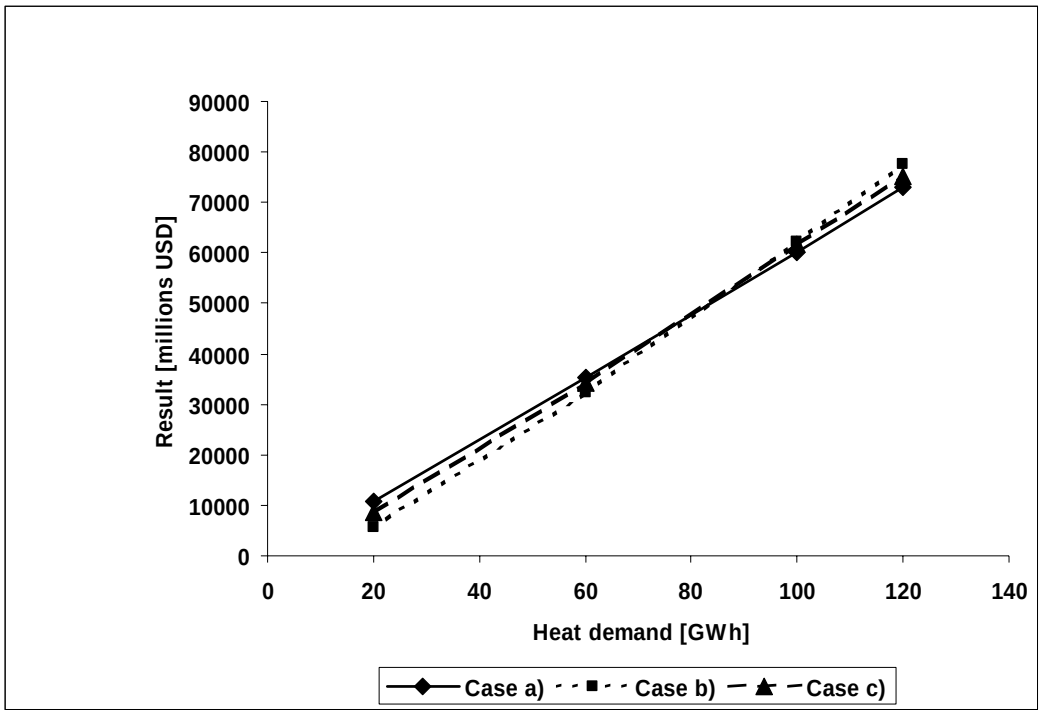

Figure 30: Heat demand verses income, high/low production cost winter/the rest of the year

3.3 Case evaluations of the economics of the DH systems with thermal storages

In the following analysis, a description on how heat storages can be used in CHP systems and the economic aspect of the use of heat is given. It is desirable to use the heat from the CHP instead of wasting it. For instance, the power price in 2006 was so high in Sweden that it was profitable to run CHP during summertime. However, the situation was different the year before where it was not profitable to run CHP summertime due to the rather lower power prices. However, it should in both cases under certain conditions be profitable to utilise the heat and use it another time.

Analysis of three different CHP systems with different conditions for the application of heat storage is presented in this section. To illustrate different application cases, real operational cases from DH systems from Linköping and Enköping are investigated [28]. In the case of Linköping, a fictious case where combined cycle plant assumed to generate heat and power is analysed.

3.3.1 Production and production cost for Linköping

The company, TekniskaVerken in Linköping, has a number of CHP plants and heat-only boilers with a total capacity of 350 MW heat and 105 MW electricity, see Table 11.

Plant	Heat output	Power output	Production cost
	MW	MW	USD/MWh
Gärstad P1-P3 (waste)	66,3	16,1	-41
Gärstad P4 (waste)	57,3	19,8	-41
CHP Tornby Biofuel	105,6	33,1	-13
CHP Tornby Oil	105,7	34,9	45
Mjölby wood chips	24,3		28
Ljungsbro wood chips	3,9		21
Boiler, oil	100		51

Table 11: CHP and heat boilers in Linköpings DH system.

There are different ways to calculate the production costs. In the case of CHP, the cost is calculated as a difference between fuel cost and the income from power generation. The heat production cost for CHP can be negative depending on the fuel cost and power prices. The municipal waste used in Gärstad has negative cost because customers have to pay 17.9 USD/MWh to get rid of their waste. In the above table, it is assumed that the generated power can be sold for 56.7 USD/MWh and if biofuel is used an additional income of 26.9 USD/MWh can be obtained from green certificate.

Figure 31 shows the projected production for the year 2007. To maximize the profit, the municipal waste fuelled plants in Gärstad cover the base load. Afterwards, biofuel fired plants stands for most of the production while the rest is covered by other plants. Some of the assumption to construct this production pattern are: a total of 5 weeks production break for maintenance purposes, operation with maximum output to enable high output from exhaust gas condensing and the company has sufficient cooling capacity. In the diagram, the output is sorted within each month.

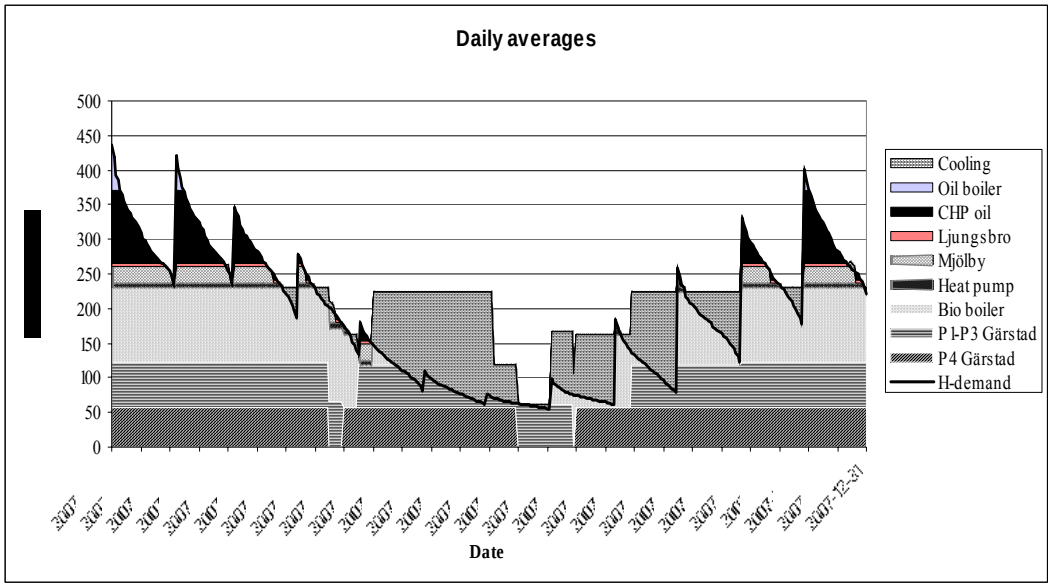

Figure 31: Load curve based on daily production data for the base case in Linköping 2007.

The heat demand for Linköping is 1 670 GWh in 2007. Table 12 shows in figures how the demand is covered for the reference case and two other cases with different sizes of heat storages.

Plant	**Produced heat [GWh]**	**Produced heat 200 000 m^3**	***Produced heat 3 000 000 m^3***
P4 Gärstad	454	454	*454*
P1-P3 Gärstad	504	504	*504*
Biofuel boiler	836	836	*836*
Heat from storage		47	*164*
Heat pump	31	35	*24*
Mjölby	74	73	*46*
Ljungsbro	12	10	*7*
CHP oil	118	96	*7*
Boiler Oil	7	0	*0*
Cooling	*-366*	*-341*	*-210*

Table 12: Produced heat for the reference case and for two different heat storage sizes

The rather high cooling in the reference case is obtained when maximized power production is desired in summertime where the heat demand is not high. Since the cooling capacity is assumed to be sufficient, the steam generating boilers can be run with maximum output even during summertime. The total production cost for the reference case will be – 32.7 millions USD.

Use of heat storage

In the case of Linköping, storage sizes between 100 000 m^3 and 5 000 000 m^3 have been studied. It is therefore interesting to see how the use of oil decreases and consequently reduction of CO2 emission by using different storages. It is assumed that the CO2 emission when oil is used is

280 kg/MWh.

Storage size m^3	Heat quantity MWh	Storage cycle per year	Oil reduction MWh	*CO_2 reduction ton*
100 000	5 000	4.1	20 000	*5 600*
200 000	10 000	4.7	30 000	*8 300*
300 000	15 000	3.0	35 000	*9 700*
500 000	25 000	2.1	44 500	*12 500*
1 000 000	50 000	1.6	68 500	*19 200*
2 000 000	100 000	1.3	93 500	*26 200*
3 000 000	150 000	1.1	118 500	*33 200*
4 000 000	*200 000*	*0.9*	*125 400*	*35 000*

Table 13: Storage cycle, oil reduction and CO2 -reduction for TVL's system with heat storage

As it can be seen in the above table, a 200 000 m^3 storage can store 10 000 MWh heat and reduce the use of oil by 30 000 MWh per year (this corresponds 8 300 ton CO2). In Figure 32, it is shown how heat production will look like when a storage with a size of 200 000 m^3 is used. The investment space for this size of the storage will be 1.4 millions USD.

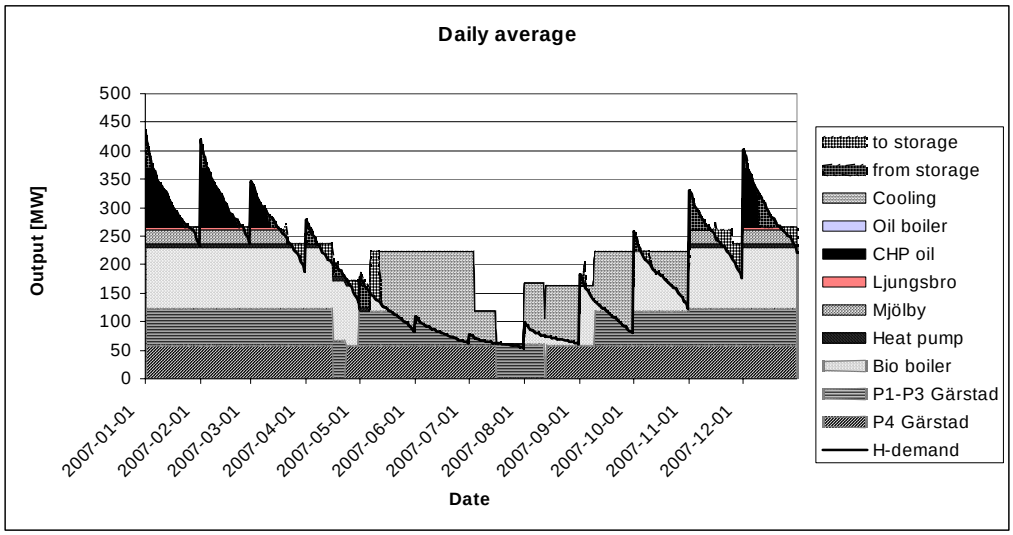

Figure 32: Load curve when storage with a size of 200 000 m3 is used

As can be seen from Figure 32, a 200 000 m^3 storage can replace all heat which otherwise has to be produced by oil-fired heat-only boilers in the reference case. A heat storage with the size of 3 000 000 m³ would replace almost all oil. An economic analysis has to be done to decide which storage should be chosen. The investment cost for heat storages larger than 300 000 m^3 exceed 12.6 millions USD.

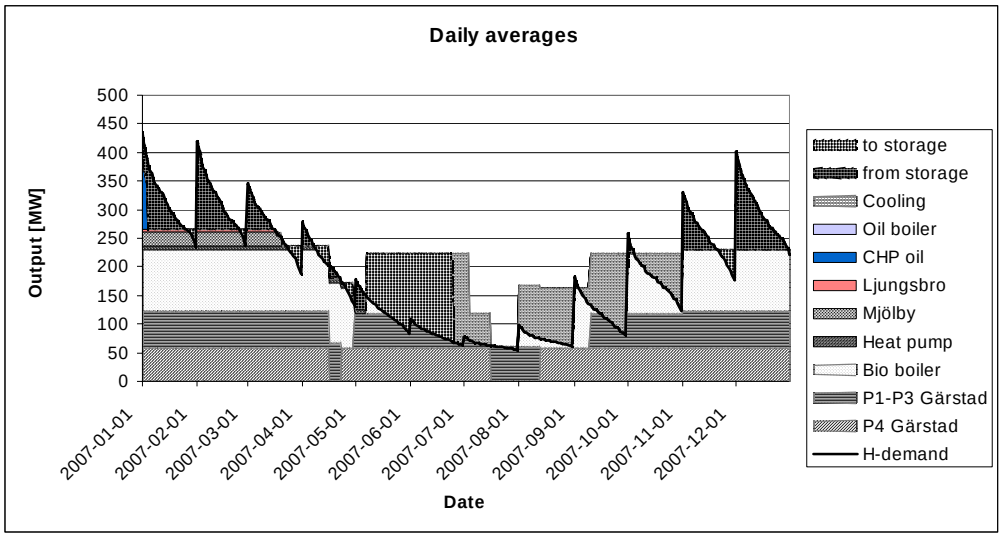

Figure 33: Load curve based on daily data and with 3 000 000 m3 heat storage.

Economic analysis of heat storage

The analysis is based on the investment space (cost reduction compared with the reference case) and the cost of the storage the annuity for storage investment. Since the annuity is dependent of depreciation time, there are different possibilities to calculate the cost benefit of heat storage.

A simple way to do so is to analyse the reimbursement time, i.e. to compare the investment space with the cost and calculate payoff time. The result is summarised in Table 14. As it can be seen in the table, the payoff time is between 5 and 10 years and this indicates that this figures are not unreasonable for investment within energy sector.

Storage size	Investment	Investment space	Payoff time
m^3	USD	USD	year
100 000	5 039 680	1 011 022	4,98
200 000	8 186 984	1 397 080	5,86
300 000	10 873 963	1 614 535	6,74
500 000	15 548 266	2 054 791	7,57
1 000 000	25 258 233	3 133 724	8,06
2 000 000	41 032 120	4 700 074	8,73
3 000 000	54 498 913	5 989 852	9,1
4 000 000	66 656 876	6 722 251	9,92

Table 14: Payoff time for heat storages at current production system Linköping

A fair way to do the analysis is to consider the interest charge during the loan period. The annuity (mortgage plus interest charge for certain loan period) is calculated and a constant amount is paid annually until the dept is paid.

Table 15 shows the annuity for 10 and 20 years and it indicates whether the investment is profitable or not. To better describe the profitability of an investment, the ratio between investment space and annuity is used. An investment can be considered profitable if the ratio is greater than one. It is also shown in the table the difference between investment space and annuity. Investment in a storage up to a size of 300 000 m^3 is profitable at a depreciation time of 10 years. On the other hand, all sizes of storages give investment spaces higher than the annuity if 20 years of depreciation time is considered.

Storage size	Annuity		Investment/ Annuity Ratio		Investment - Annuity Difference	
m^3	USD	USD			USD	USD
	10 year	20 year	10 year	20 year	10 year	20 year
100 000	684 731	439 382	1.477	2.301	326 291	571 640
200 000	1 112 349	713 779	1.256	1.957	284 731	683 301
300 000	1 477 423	948 042	1.093	1.703	137 112	666 493
500 000	2 112 511	1 355 569	0.973	1.516	-57 720	699 223
1 000 000	3 431 784	2 202 128	0.913	1.423	-298 061	931 596
2 000 000	5 574 950	3 577 367	0.843	1.314	-874 876	1 122 707
3 000 000	7 404 656	4 751 464	0.809	1.261	-1 414 804	1 238 388
4 000 000	9 056 534	5 811 450	0.742	1.157	-2 334 283	910 801

Table 15: Economical comparison of different storage sizes

A storage with a size of 3 000 000 m^3 is a suitable size if the desire is to replace all use of oil. The surplus after 20 years depreciation is about 1.2 millions USD. A 200 000 m^3 storage is a sufficient size if only the production from oil-fired heat-only boilers needs to be replaced. This storage gives a surplus of 126 000 USD already after 10 years of depreciation.

Using sensitivity analysis one can examine what will happen when the power and oil prices change. It is obvious that increased oil prices make the investment even more profitable. A price increase of oil with 30 % would mean that all investment for heat storage sizes up to 3 000 000 m^3 can be written off within 10 years. Even an oil price increase with 10 % gives profitability at a depreciation time of 10 years but the size is limited to 1 000 000 m^3.

3.3.2 Heat storage for a system with gas-fired combined cycle plant in Linköping

As alternative to the existing system in Linköping, the system in this case is assumed to consist of a gas-fired combined cycle plant which covers the base load and heat-only oil boiler. Furthermore, it assumed that the combined cycle plant will be run att maximum output of 179,6 MW throughout the year except 5 weeks of brake for maintenance. There is also sufficient capacity to get rid of the heat when the heat demand is less than 179,6 MW.

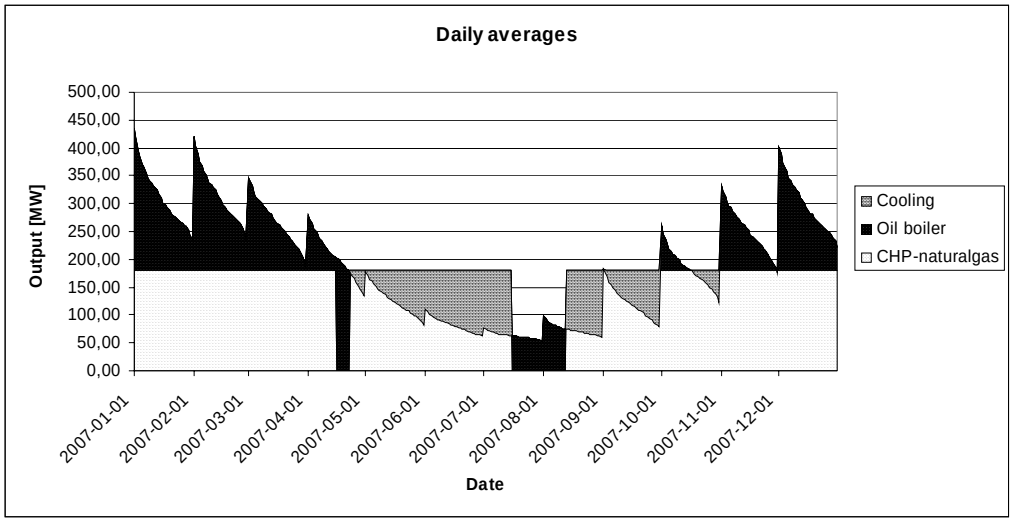

Figure 34: Daily data for the reference production with a fictitious combined cycle plant

The production for the reference case is shown in Figure 34 Since the share of oil in this system is larger than the previous case, the potential of oil saving through the use of storages is higher. Table 16 shows oil saving potential and CO2 emission reduction as a function of storage size.

Storage size m^3	Heat quantity MWh	Storage cycle per year	Oil reduction MWh	*CO_2 reduction ton*
100 000	5 000	3	15 200	*4 200*
200 000	10 000	2,9	29 000	*8 100*
300 000	15 000	2,7	40 400	*11 300*
500 000	25 000	2,4	59 000	*16 500*
1 000 000	50 000	2,1	105 600	*29 600*
2 000 000	100 000	1,6	155 500	*43 500*
3 000 000	150 000	1,4	205 600	*57 600*
4 000 000	*200 000*	*1,3*	*255 600*	*71 600*

Table 16: Storage cycle, oil reduction and CO2 -reduction for the fictious system with combined cycle plant in the TVL system

The storage sizes that are of interest to study are 200 000 m^3 and 4 000 000 m^3. A storage with the size of 200 000 m^3 reduce the use of oil with 29 000 MWh per year. This implies that the CO2 emission decreases with 8 100 ton per year. Figure 35 shows how the production looks like and how the storage is used.

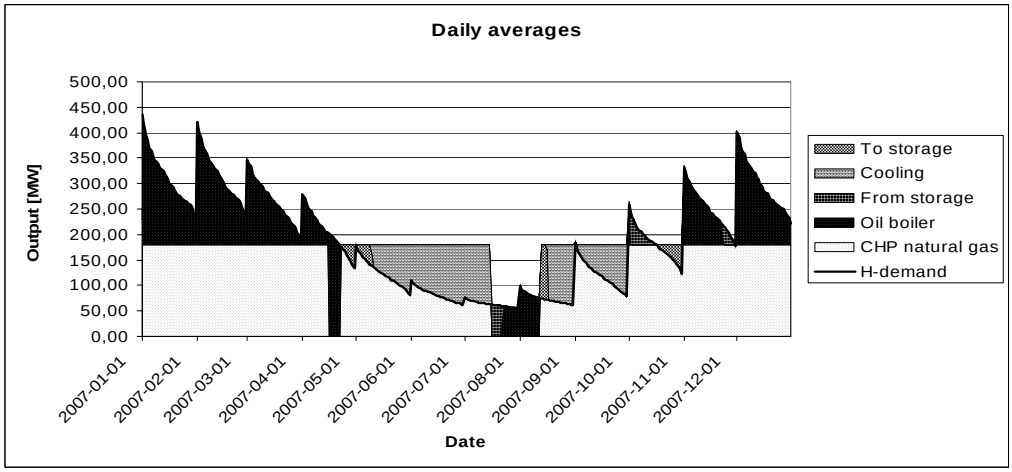

Figure 35: Load curve based on sorted daily data with 200 000 m3 stoarge

A storage of 200 000 m^3 gives an investment space of 1.7 millions USD per year. If the storage is emptied one time 10 GWh heat can be drawn. However, this storage can be used 2.9 times per year.

A storage of 4 000 000 m^3 will reduce the use of oil with 255 600 MWh per year. The corresponding reduction of CO2 emission will be 71 600 ton per year. Figure 1.22 shows how the different units are run and how the storage is used. All generated heat will be utilized and no cooling is necessary.

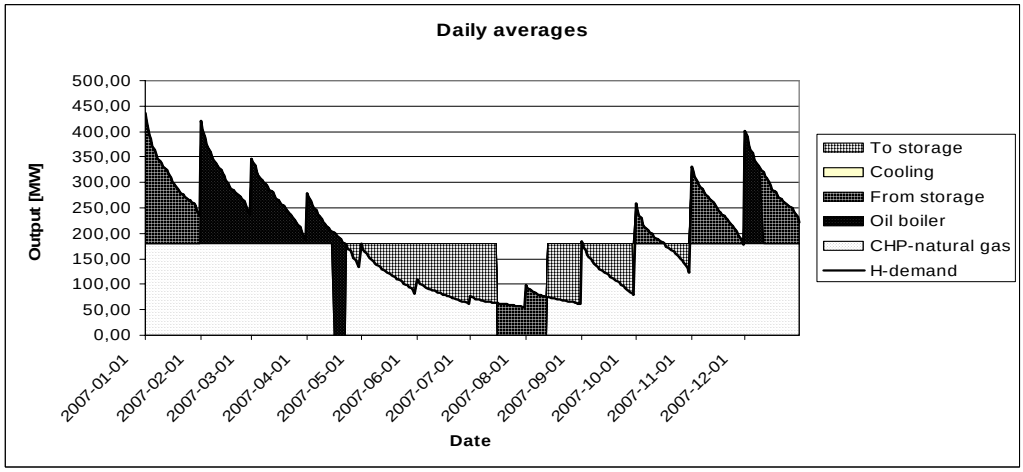

Figure 3.22: Load curve based on sorted daily data with a 4 000 000 m^3 storage

A storage with this size gives an investment space of 13 millions USD per year. If the storage is discharged fully, a total of 200 GWh heat can be obtained. As a whole, the storage is used 1.3 times per year. Table 1.14 shows the investment cost, investment space and payoff time for this case.

Table 3.14: Payoff time for heat storages for a system with combined cycle plant in Linköping

Storage size	Investment	Investment space	Payoff time
m^3	USD	USD	year
100 000	5 039 680	770 364	6,5
200 000	8 186 984	1 472 649	5,6
300 000	10 873 963	2 053 713	5,3
500 000	15 548 266	2 999 624	5,2
1 000 000	25 258 233	5 373 463	4,7
2 000 000	41 032 120	7 913 811	5,2
3 000 000	54 498 913	10 463 269	5,2
4 000 000	66 656 876	13 008 302	5,1

The maximum attainable investment space with storage is 13 millions USD. This can be possible because the combined cycle is operated with maximum output and the storage with the size 4 000 000 m^3 enables that no heat has to be wasted through cooling.

Table 1.15 shows some key figures such as the ratio between investment space and annuity and the difference between them. All of the investments are economical even with short depreciation time of 10 years. The storage that gives the highest return per invested USD is the storage with the size of 1 000 000 m^3. This size of the storage gives the best economy even if the oil price would fall by 30 % and this indicates that this storage can be considered as an optimal solution.

Table 3.15: Economical comparison of different storage sizes in TVL's system with combined cycle plant

Storage size	Annuity		Investment/ Annuity		Investment - Annuity	
			Ratio		Difference	
m^3	USD	USD			USD	USD
	10 year	20 year	10 year	20 year	10 year	20 year
100 000	684 731	439 382	1,125	1,753	85 633	330 981
200 000	1 112 349	713 779	1,324	2,063	360 301	758 871
300 000	1 477 423	948 042	1,39	2,166	576 290	1 105 671
500 000	2 112 511	1 355 569	1,42	2,213	887 113	1 644 055
1 000 000	3 431 784	2 202 128	1,566	2,44	1 941 678	3 171 335
2 000 000	5 574 950	3 577 367	1,42	2,212	2 338 861	4 336 444
3 000 000	7 404 656	4 751 464	1,413	2,202	3 058 613	5 711 806
4 000 000	9 056 534	5 811 450	1,436	2,238	3 951 768	7 196 852

3.3.3 Biofuel fired CHP

Production and production costs for ENA AB in Enköping

As a case study for biofuel based CHP, the DH system from ENA Energi AB in Enköping is used. The company delivers DH to almost all residence within the municipality of Enköping. The

production for the year 2005 was 230 GWh heat and 95 GWh electricity. The heat is mainly produced by woodchip fired CHP but during summer when the demand is low and during peakload times a boiler fired with wood-powder is used. There are several production units with a total capacity of more than 200 MW heat but the demand is only 65 MW. The CHP generates 55 MW heat and the capacity from the exhaust gas condenser is 20 MW heat. The CHP cannot be run during summer so a wood-powder fired boiler with a capacity of 22 MW heat is used. This unit is used even during times of peakload where the CHP is not sufficient.

Table 3.16: Production units at ENA Energi AB.

Plant	Heat output MW	Power MW
CHP (wood chip)	55	24
Boiler (wood-powder)	22	
Boiler (oli/gas)	50	
Boiler (oil)	25	
Electric boiler	36	
Accumulator	25 (325 MWh)	

The production capacities that are available and a short-term accumulator are shown in Table 1.16 and Figure 1.23 shows the current production pattern at ENA Energi AB. The black line shows the heat demand over the year and the other lines show how the demand is supplied.

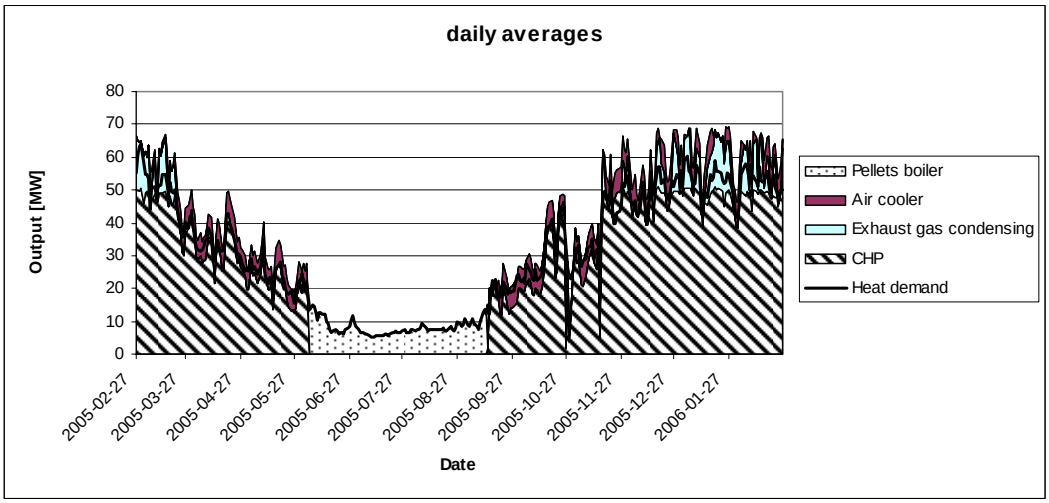

Figure 3.23: Heat demand and production based on daily data

The production cost is calculated in a different way compared to the case with Linköping. The net income is the sum of revenues that come from the sale of heat and electricity minus the sum of fuel costs. The considered time period in this case study was 27 February 2005 until 26 February 2006. The power price for this period is taken from NordPool while the price for green certificate (an average value of 26 USD/MWh) is from Svenska Kraftnät. The average sale price for the heat was 61 USD/MWh in 2005. The revenues from power sale follows the NordPool power market, where the price was below 37.8 USD/MWh most of the year 2005. A price corresponding to 56

USD/MWh was noticed at the end of 2005 and the first two months of 2006. During the considered period, the net income for the company was 15.2 millions USD.

The use of heat storage

To simplify the analysis some assumption have been made. The maximum heat output from the CHP is assumed to be 50 MW and the minimum load limit for the CHP is 30 MW. Table 1.17 shows the energy production ratios that are used in the calculations.

Table 3.17: Ratios between DH, power and fuel in ENA system.

Ratios	
Generated power/generated DH	0,420
Generated DH from CHP/fuel	0,645
Generated power from CHP/fuel	0,275
Sold power /generated power	0,905

With a heat storage in the system it is possible to reduce the use of wood-powder fired boiler which does not produce electricity. The utilisation time of the CHP increases and it can be operated at higher output level. To compare the different alternatives it is assumed that all storages are half filled the 26 February and they start to be emptied the 1 June every year. Storage sizes between 100 000 m^3 and 800 000 m^3 are studied.

In Table 1.18 it is presented the number of days the storage would supply the network and the number of days the CHP run at certain output level. It can be clearly seen how the utilization time of the CHP at 50 MW output increases with increased size of the storage.

Table 3.18: Utilisation time of CHP and storage

Storage size m^3	Supply the network days	CHP operation, days		
		50 MW	40 MW	30 MW
100 000	85	127	15	138
200 000	92	136	24	113
300 000	82	132	2	149
400 000	98	156	1	110
500 000	112	178	0	75
600 000	122	192	2	49
700 000	129	203	1	32
800 000	132	208	0	25

The quantity of heat that can be stored, the corresponding replaceable heat by each storage and the storage cycle is shown in Table 1.19.

Table 3.19: Storage size and annual storage cycle

Storage size m^3	Heat quantity GWh	Replaceable heat [GWh]	Storage cycle/year
100 000	5	33,9	6,8
200 000	10	36,0	3,6
300 000	15	34,5	2,3
400 000	20	40,6	2,03
500 000	25	41,7	1,67
600 000	30	46,7	1,56
700 000	35	49,2	1,41
800 000	40	50,0	1,25

The reason why the use of the 300 000 m^3 storage decreases compared to the two smaller storage is because this storage is not filled up some times in summer. The following two figures show examples of load profile where 100 000 m^3 and 300 000 m^3 are used.

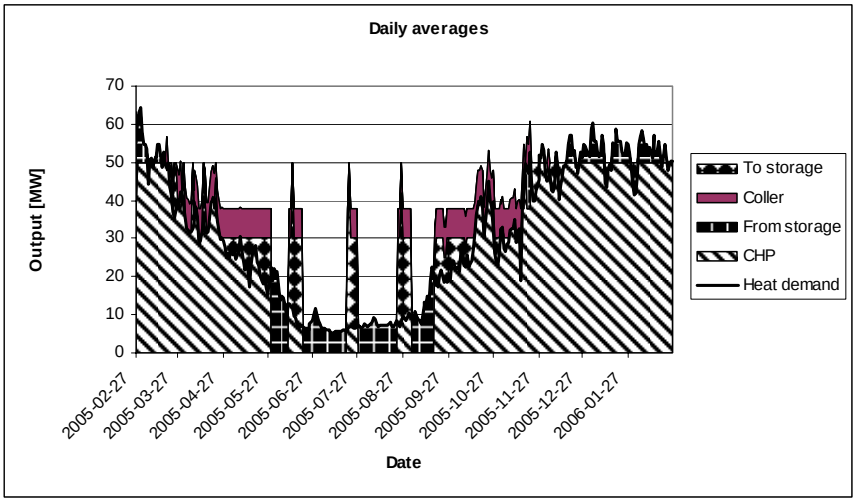

Figure 1.24: Duration curve with a 100 000 m^3 storage

Figure 1.24 illustrate clearly that the storage is charged three times during summer while no charging takes place during summer in Figure 1.25. All storages larger than 300 000 m^3 are filled up only before and after summer. It is also shown in the figures that the demand during peakload times in winter is supplied by the storage.

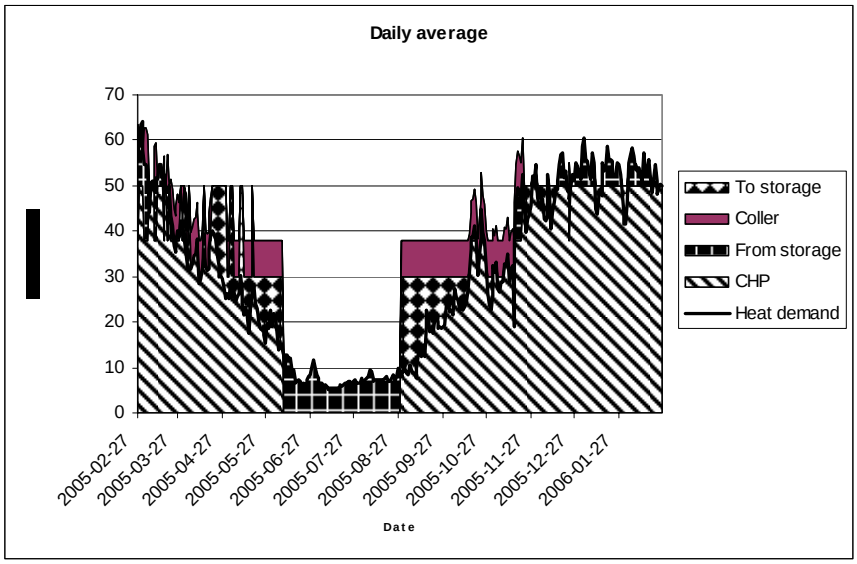

Figure 1.25: Duration curve with a 300 000 m^3 storage

Table 1.20 presents investment cost, investment space and payoff time for the studied storage sizes. It is also shown clearly that the storage with the size 100 000 m^3 is the most profitable with the shortest payoff time.

Table 1.20: Payoff time for heat storages at current production system Enköping

Storage size	Investment	Investment space	Payoff time
m^3	USD	USD	Year
100 000	5 039 680	405 022	12.4
200 000	8 186 984	423 115	19.3
300 000	10 873 963	417 042	26.1
400 000	13 299 800	441 841	30.1
500 000	15 548 266	449 811	34.6
600 000	17 664 805	452 618	39
700 000	19 677 576	447 663	44
800 000	21 605 581	447 867	48.2

Table 1.21 shows the ratio of annuity and investment space the difference between them.

Table 1.21: Economical comparison of different storage sizes in ENA Energi ABs system, 2005

Storage size	Annuity		Investment/ Annuity Ratio		Investment - Annuity Difference	
m^3	USD	USD			USD	USD
	10 year	20 year	10 year	20 year	10 year	20 year
100 000	684 731	439 382	0,592	0,922	-28 690	-38 895
200 000	1 112 349	713 779	0,38	0,593	-290 663	-171 660
300 000	1 477 423	948 042	0,282	0,44	-530 999	-372 939
400 000	1 807 016	1 159 537	0,245	0,381	-717 696	-524 375
500 000	2 112 511	1 355 569	0,213	0,332	-905 758	-679 754
600 000	2 400 081	1 540 098	0,189	0,294	-1 087 481	-830 711
700 000	2 673 552	1 715 581	0,167	0,261	-1 267 918	-981 891
800 000	2 935 506	1 883 673	0,153	0,238	-1 435 806	-1 121 755

As can be seen in Table 1.21, none of the storages generate any surplus in this example. The storage with a size of 100 000 m^3 is close to profitability if 20 years of depreciation time is used. Thus, it can be concluded that based on power prices from 2005 only a storage with a size of 100 000 m^3 might be of interest for the system in Enköping.

If however power prices from 2006 are used in the analysis, the result will be quite different as it is shown in Table 1.22. It can be mentioned that peak prices as high as 85.7 USD/MWh was noticed during 2006.

Table 1.22: Economical comparison of different storage sizes in ENA Energi AB's system, 2006

Storage size	Investment/ Annuity Ratio		Investment - Annuity Difference	
m^3			USD	USD
	10 year	20 year	10 year	20 year
100 000	1,182	2,849	567 155	885 759
200 000	1,112	1,733	124 744	642 317
300 000	0,86	1,341	-206 518	480 924
400 000	0,649	1,011	-634 831	205 969

So it is obvious from Table 1.23 that the electricity price has a significant role in determing the right size of the storage. Power prices in Sweden may go up and this can make the storage of 200 000 m^3 even more attractive.

3.4 Conclusion

Technology of heat storage

The only proven technology of heat storage in CHP application is steel tanks. The volume of these tanks can be as high as 60000 m³ and is well enough to meet the need for short-term storage.

Regarding long-term storage with sizes above 100 000 m³ water equivalent, there are two technologies that are of interest for CHP system: rock cavern and borehole storage. With these technologies it is possible to attain high heat storage volumes.

Non-insulated rock cavern has high initial heat losses and these losses should be included as part of the investment. After 5 years of operation, the heat balance of the rock cavern reaches steady of state condition with a moderate heat loss of about 10 % annually. Rock cavern with dynamic heat inflow and outflow can generate heat of prime quality most of the year.

Today's borehole storages are dimensioned for solar heat system application therefore they have limited charging and discharging capacity. A CHP demands higher heat transfer capacity and because of this the borehole storage should be equipped with buffer tanks or more borehole (with tighter distance) are necessary. Since the cost of borehole storages is low compared to the other technology, it might be of interest to improve the technology for CHP application.

The costs of heat storage are uncertain. The cost of a rock cavern was given to be 0.5 USD/kWh in 1996 and this will correspond to 0.8 USD/kWh being adjusted to today's cost using building cost index. For large rock cavern, the cost is expected to fall to lower level. The cost of borehole storage for large system application can be as low as 0.25 USD/kWh and this may stimulate to further develop the technology for CHP application

Concerning pit heat storage, there is, in the near future, nothing that indicate that this technology might be of interest for long-term storage in CHP application.

Heat storage in CHP system

The function of long-term heat storage in CHP system should primarily be seen as a way to take care of the surplus heat which otherwise will be wasted through cooling. The main reason of using the storage is to increase power production summertime and to decrease the use of fossil fuel during peakload time.

The study shows that the best economy is found in a system where peakload demand is supplied

by oil boilers. To replace oil-based peakload of 60 MW wintertime is the most economical solution in the case of Linköping. For this case 200 000 m³ rock cavern would be enough. Replacing oil-based CHP-heat with summer heat from incineration plant could be also interesting. A rock cavern with a size of 3 000 000 m³ manages summer operation of Gärstadverket (100 MW) without a need for cooling and without a use of oil. This system would give a surplus at depreciation time of 20 years.

For a system with a gas-fired combined cycle plant (178 MW) and oil-fired peakload boiler, it is economical to reduce the share of oil as much as possible. The economy is independent of the size of the storage where the limit line is 1 000 000 m³.

If the heat storage can only replace heat from biofuel-fired peakload boilers, the profitability is not certain. The case of Enköping shows that power price has a decisive role. Power prices from 2005 do not stimulate investment on heat storage while the price from 2006 does. This implies that heat storage can be considered as a possible part of the syetm in the long-term perspective.

Heat storage in a local DH network

When a new area is to be connected to existing network, it can be imagined that the heat comes from cheap summer production where the only option was wasting the surplus heat. The storage and the transmission pipeline should be dimensioned to utilize this surplus heat.

In the example of Linghem, the use of heat storage is interesting when the price is 0.5 USD/kWh or lower. This would make the use of rock cavern uncertain while the use of borehole storage might be interesting.

The result from the simulations with sensitivity analysis give similar indication. Rock cavern is quite expensive and the profitability of seasonal storage in this application is highly dependent on the type storage and its costs. The cost of generated energy has also a certain impact whether a seasonal storage application in this area is economical or not.

However, since the application of storage in this area replaces heat from existing plants, which uses electricity and oil, a system solution, which utilise surplus heat, should be of high priority.

4 Increasing the power production of CHP plants integrated in DH networks

The cogeneration plants connected to a small-scale DH network are usually operated according to the heat load in the network. The district heating network properties affecting most the CHP plant performance are the thermal load changes, the durations of the different loads, and the forward temperature of the district heating water exiting the district heat exchanger. These factors become especially apparent in single units or in low heat density district heating networks, where there may be long periods when the cogeneration plant has to operate at partial heat loads and where the differences between the load levels may be significant. In networks, where there exists several CHP plants, the properties and the thermal loads of the network may have an effect also on the joint operation of the units connected to the network.

4.1 Standard CHP production process

Figure 36 shows the flow sheet of a standart process for CHP production from biomass. The process is based on an existing 6 MWe plant. The plant has a BFB boiler and uses wood as fuel. The district heat production is 16 MW. The process is presented in more detail in the article by Savola and Keppo [37].

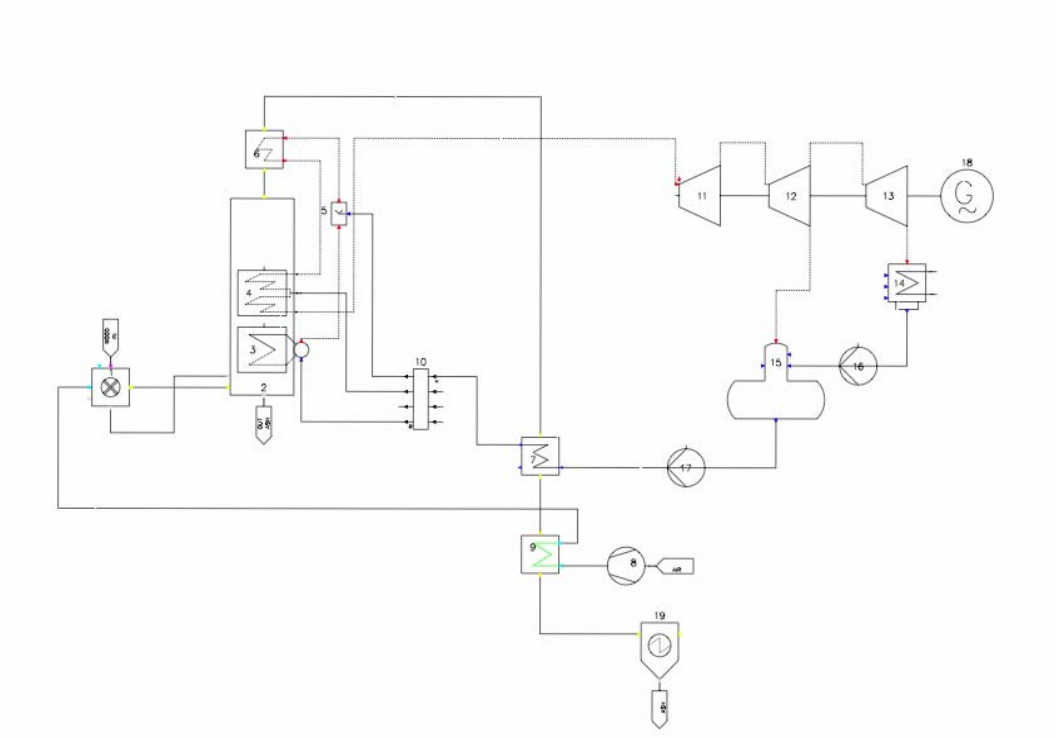

Figure 36: Standard small-scale CHP plant process..

For the small scale plants, the economic constraints make the introduction of new and advanced technolgy available to large plants infeasible. However, many smaller changes to the process can give an increased efficiency, and still be economically viable. This is discussed further in the article by Savola and Fogelholm [38]. Two of the most promising process changes are presented in the following sections.

4.2 Two stage DH heat exchanger

In a standard CHP plant, the exit pressure of the steam leaving the DH heat exchanger is defined by the DH water forward temperature. The advantage of a two stage DH heat exchanger is that the exit pressure of the steam can be significantly lower than the pressure defined by the forward temperature of the DH water. This will increase the power production and the overall efficiency of the CHP plant. Figure 37 shows the flowsheet of the a modified version of the small-scale CHP plant process shown in Figure 36, where a two stage DH heat exchanger has been added to the process.

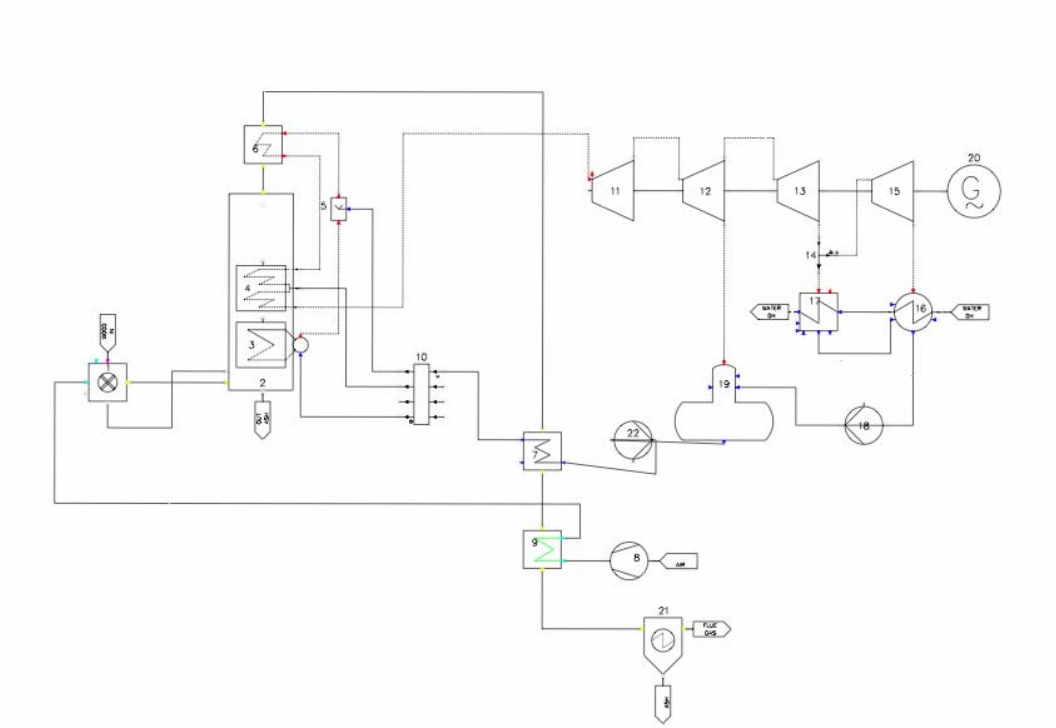

Figure 37 Small-scale CHP plant with two stage DH heat exchanger

A more detailed description of two stage DH heat exchangers and their advantages can be found in the doctoral dissertation by Savola [29]. The two-stage DH exchangers have already been used in the CHP plants producing from 15 to 20 MWe, but their economical feasibility in smaller plant sizes has not yet been demonstrated.

4.3 Steam reheat and feedwater preheater

Reheating and feedwater preheating is common in larger plant. For small-scale power generation the relatively low return of the additional investments so far means that the technology has not been widely utilised for small-scale generation. Figure 38 shows how a standard CHP production process can be modified by adding steam reheating and feedwater preheating.

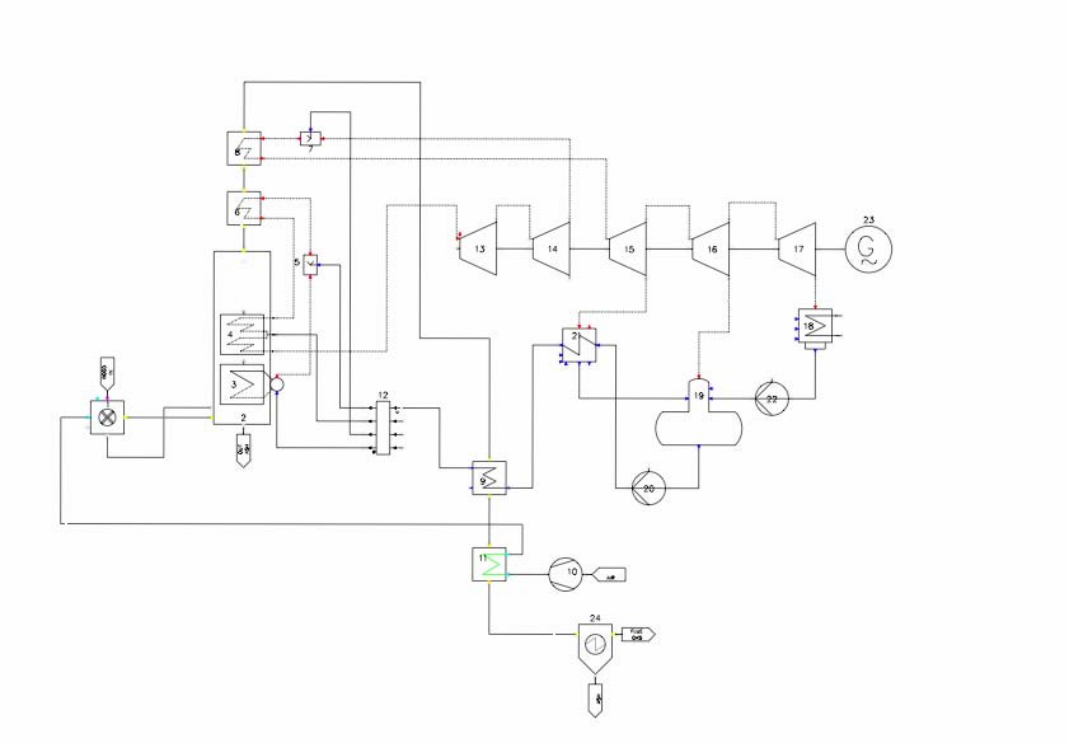

Figure 38: Small-scale CHP plant with steam reheat and feedwater preheater.

A discussion about the advantages of steam reheat and feedwater preheater for CHP plants can be found in the dissertation by Savola [29].

5 Improving the DH network with efficient combination of CHP plants and thermal storages

Most of this section is based on the work presented in the work by Tveit et al. [39].

This section presents an optimisation model for increasing the cogeneration plant power production taking into account the possibility to use long-term thermal storages in the network for reducing the part load operation time of the plant. The main input to the model is the part load performances of the process modules and the conditions for the use of thermal storages. The model can take into account the operation of several CHP plants together with the utilisation of a thermal storage in a small network. With the resulting CHP process improvements the overall power production of the cogeneration plants connected to small DH networks should be increased in an economically feasible way. Prices are converted from EUR to USD, and the conversion rate used is 1.47 USD/EUR.

5.1 Multi-period MINLP model

The optimisation model is a multi-period mixed integer nonlinear programming model. The mathematical model is presented in detail in Appendix A. The model consists of an objective function and constraints. The objective function to be maximised is the sum of the incomes from the power generation and the district heating with the subtraction of the fuel costs and any investment costs for modifications to the plants. The constraints consists mainly of energy- and mass balances, and equations related to these. The model uses regression models to calculate the power generation and the forward temperature for the plants. The methodology used is similar to the methodologies presented in the doctoral dissertation theses by Savola [29] and by Tveit [30]. The model is implemented in a high-level modelling system for mathematical programming and optimisation, the *General Algebraic Modeling System* (GAMS) by GAMS Development Corporation. The model is solved using the MINLP solver *SBB* with *CONOPT* as the NLP solver [31, 32, 33].

5.2 Demonstration of the model for improving a DH network with long-term storage

Figure 39 shows the topology of the district heating system, with all the units and streams. The streams are labeled in italic. The main components in the system are the DH network, the thermal storage and the two CHP plants labeled *PlantA* and *PlantB*. The remaining components comprising the system are splitters and mixers. The modelling of the thermal storage and the DH network is explained in detail in Appendix A.

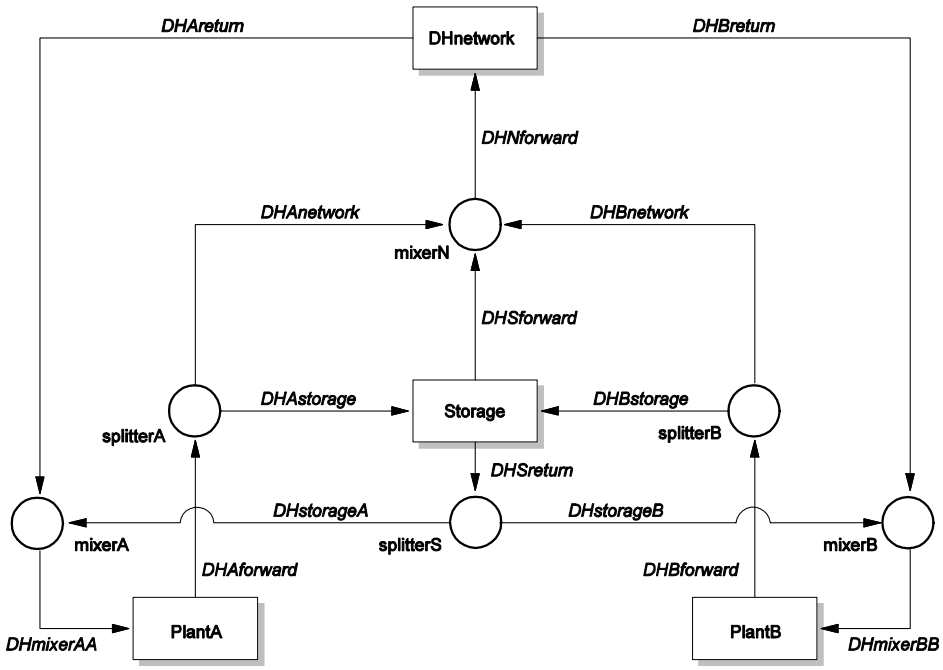

Figure 39: District heating system model topology.

The district heating network, the storage and *PlantB* have a fixed design, while design changes to *PlantA* is under consideration (depending on the economical feasibility). Figure 40 shows the simulation model of *PlantB*. The fuel for the plant is light fuel oil, and at the design point the power generated is 20.5 MWe, and the generated heat is 55 MWth.

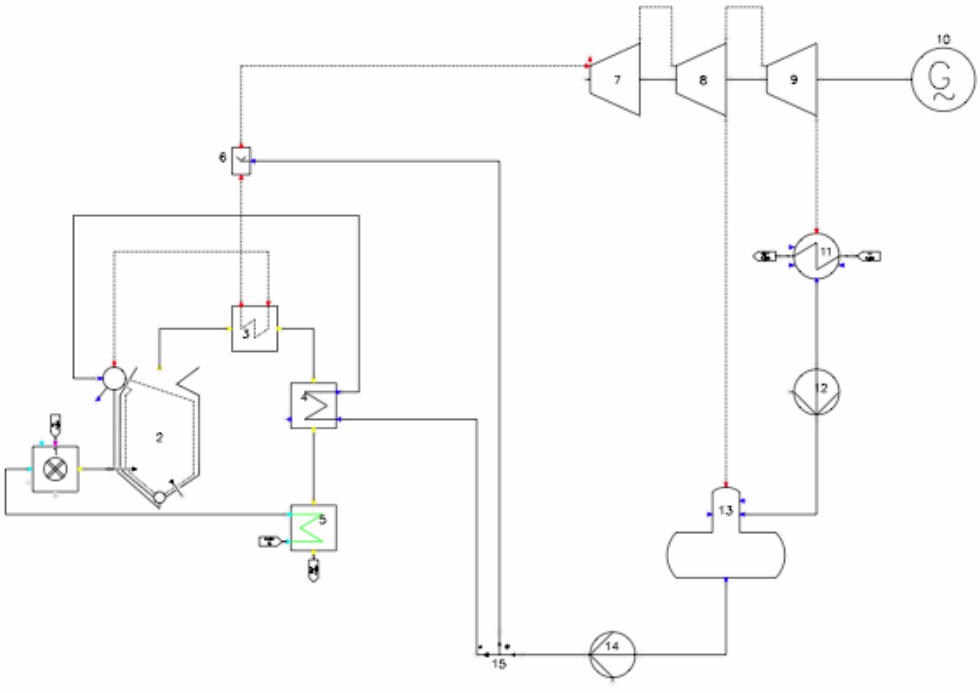

Figure 40: Flowsheet of PlantB

5.2.1 Process modifications taken into account for PlantA

There are two options for *PlantA*, the basecase and addition of a feedwater preheater and a reheater. The simulation models for the options are shown in Figure 36 and Figure 38 in Section 0.

The investement costs of the heat exchangers, C_{hex}, are calculated according to the following linear formula:

$$C_{hex} = a + b \cdot A$$

where A is the heat exchanger surface area, which is calculated as follows:

$$A = \frac{Q}{LMTD \cdot U}$$

where Q is the heat load, $LMTD$ is the logarithmic temperature difference and U is the overall heat transfer coefficient. For both the reheater and feedwater preheater, a is equal to 11800 USD/unit and b is equal to 150 USD/m^2. The overall heat transfer coefficient is set to 4 kW/m^{2}K for the feedwater preheater and to 0.1 kW/m^{2}K for the reheater. These values are taken from the doctoral dissertation by Savola [29]. The values for Q are taken from the simulation model shown in Figure 40, and are approximately 800 kW and 1650 kW for the feedwater preheater and the reheater respectively. Based on these parameters, the investment costs for the design changes are 46300 USD. These costs are annualised in the optimisation model, where the annual costs will vary with the stated interest rate and investment periods. Note that the investment periods are not the same as the periods for the discretisation of the time series. The size of the storage is approximately 300 000 m^3 (= $3 \cdot 10^8$ kg water).

5.2.2 Additional input to the model

The most important inputs to the model are the heat load of the DH network together with requirements for the minimum forward temperatures, prices and investment data (*e.g.* interest rates, investment periods etc.). All data must be discretised into periods. Figure 41 shows the discretised prices for power, fuel and district heating for the Finnish market in 2006 [34, 35, 36]. The prices for a year have been divided into 13 periods.

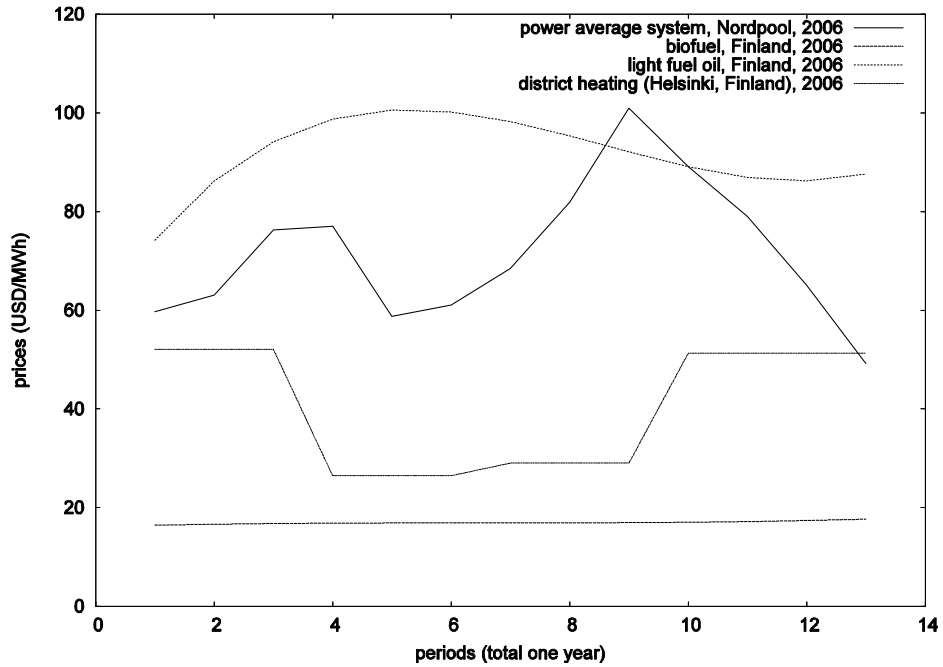

Figure 41: Discretisised price data for the Finnish market in 2006

In the results presented in the following sections, the ratio between the electricity price and the fuel price is varied. This is done by scaling the fuel price by a factor. It it is the ratio of the one year average that is reported.

The heat load of the DH network is taken from the district heating network of *Keravan Energia* in Finland. Keravan Energia delivered 378 GWh district heating to 1137 customers in 2006. The heat load has been scaled to fit the capacities of PlantA and PlantB presented earlier. Figure 42 shows the scaled district heating load for on year used in the model.

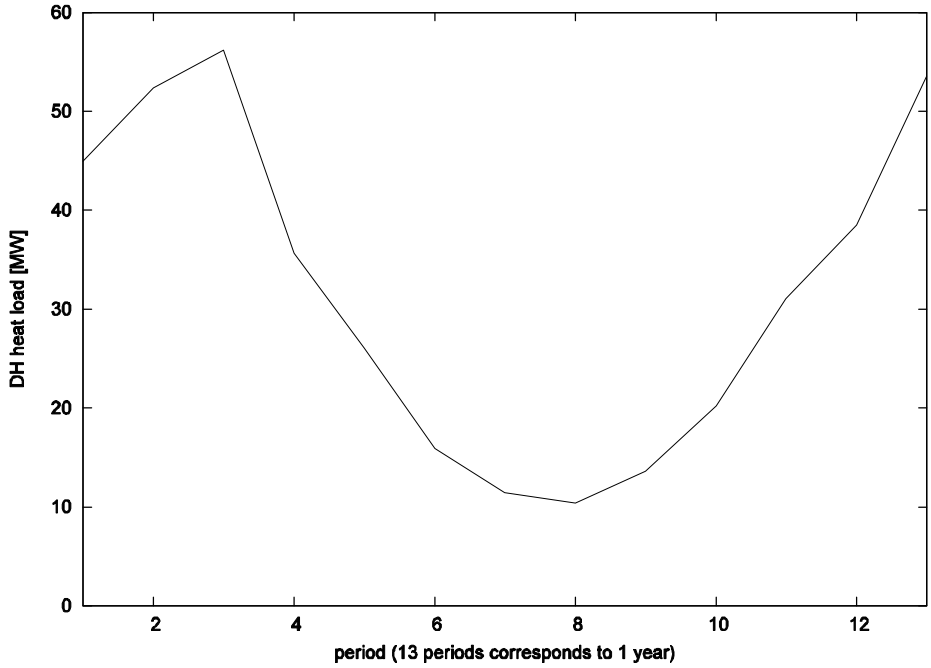

Figure 42 : Heat load for 1 year, based on the actual heat load in 2006 for Keravan Energia, Finland

The profile of the requirement for the forward temperature is based on the heat load, and varies from 80 to 110 °C, where 80 °C corresponds to the minimum heat load and 110 °C corresponds to the maximum heat load.

5.3 Model analysis

The size of the model is dependent on the number of periods included in the data-set. For a data-set with 78 periods (corresponding to 6 years), the model consists of approximately 5900 equations and 8200 variables. Correspondingly, for a data-set with 26 periods (2 years), the model consists of roughly 2000 equations and 2700 variables.

The model is non-convex, and subsequently global optimality cannot be guaranteed with the local solvers used. Due to the size of the model the use of global solvers are not possible. The main source of the non-convexities comes from the bilinear energy balances and the regression models. The non-convexities mean that the model is sensitive to the initial values. To test the sensivity to the initial values the model with a 26 periods data-set was solved 100 times with the initial values varying randomly between their lower and upper bound. Figure 43 shows the result of the analysis.

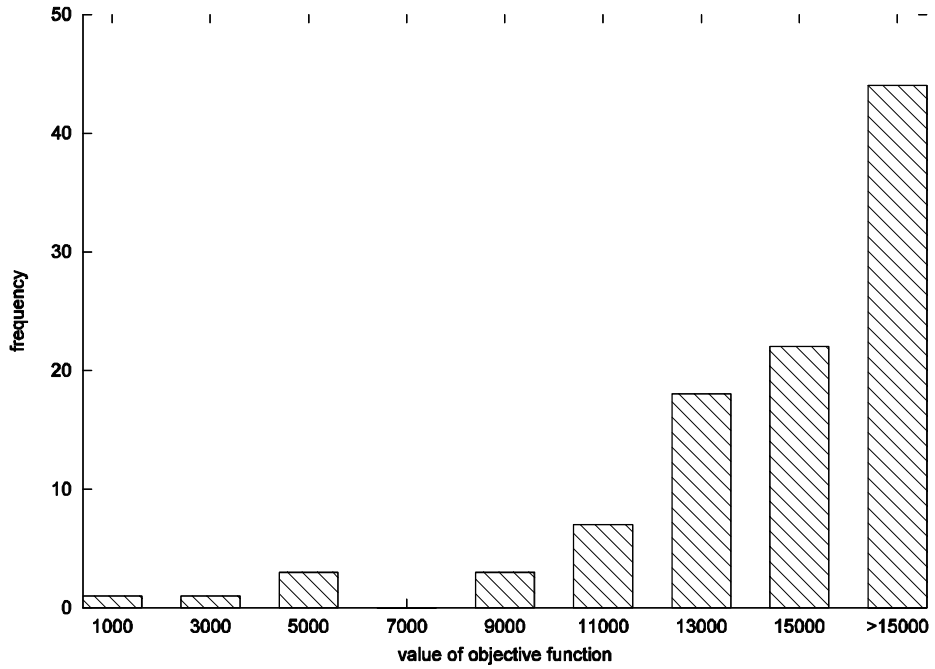

Figure 43: Sensitivity of the MINLP model to the initial values.The model is solved 100 times.

The figure contains 99 values, as one of the simulation run returned an infeasible solution.

As can be seen from the figure, the model contains many local optima, thus it is recommended that the model should be run several times with different initial points to ensure that a good solution is found. In the results presented here, the optimisation model is run 20 times with the initial values varying randomly with a uniform distribution between the lower and upper bounds. The lower and upper bounds are chosen as tight as possible, with the addition of slack variables to the nonlinear equations to improve the possibilities of the NLP solver to find a good solution.

5.4 Results

The MINLP model is capable of returning a variety of results of interest with respect to investments aswell as operation of the network. In this section the results of changing the ratio between the electricity and the fuel prices for different investment periods is presented. In addition the optimal operation of the heat storage for a fixed fuel/electricity price ratio is presented.

Figure 44 shows how the best found objective value varies with the ratio of the annual average electricity and fuel prices for 3 different investment periods. To obtain the results, the optimisation model is run for different values of the fuel price, which is scaled relatively to the electricity price. All the other parameters are kept constant.

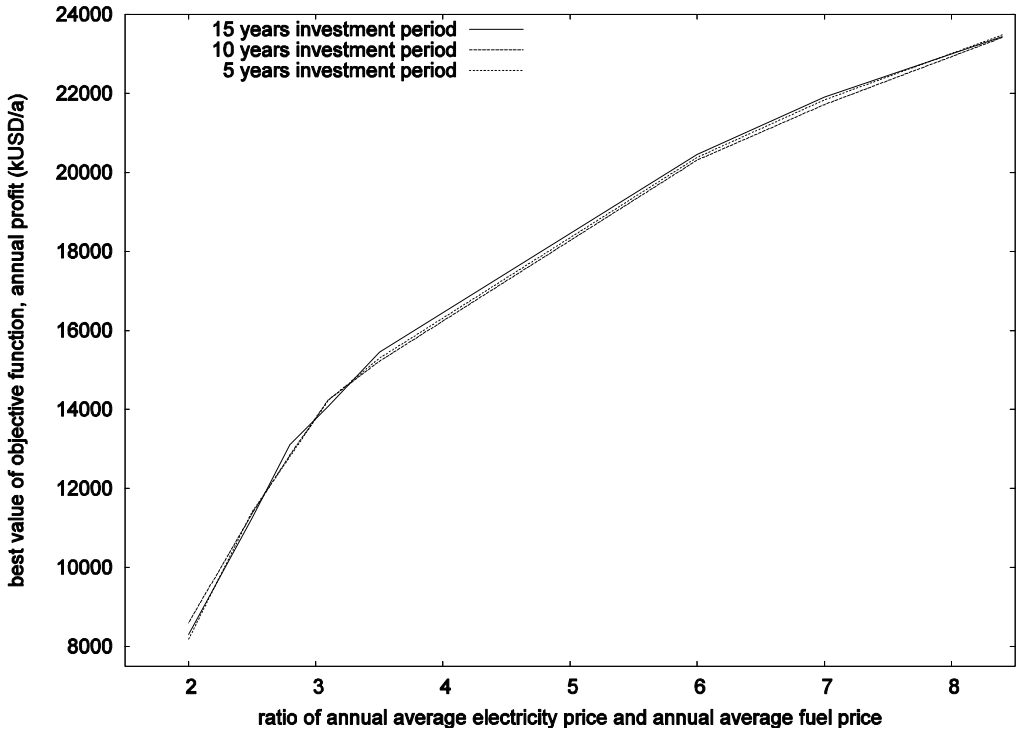

Figure 44: The best objective function after 20 optimisation model runs for different ratios of electricity/fuel prices for 3 different investment periods.

Table 17 shows which configuration for PlantA had the best value of the objective function for the different runs.

investment years/ price ratio	*8.4*	*7.0*	*6.0*	*3.5*	*3.1*	*2.8*	*2.5*	*2.0*
15	RPH	RPH	RPH	RPH	RPH	RPH	RPH	RPH
10	RPH	RPH	RPH	BaC	RPH	BaC	BaC	BaC
5	RPH	RPH	RPH	BaC	BaC	BaC	BaC	BaC

Table 17: Configuration of PlantA for the best objective function for the different investment periods and electricity/fuel price ratio. 'BaC' is the base case and 'RPH' is the configuration with steam reheat and feedwater preheating.

PlantA will be able to generate more heat per unit fuel for the base case than for the configuration with steam preheat and feedwater preheating. This is due to the higher power to heat ratio for the configuration with reheat and preheat, thus more fuel will be used per generated heat unit, but this will also generate more electricity. For a 15 years investment period the annualised costs for the steam reheat and feedwater preheat heat exchangers are always lower than the income from the additional generated power, which makes this option the optimal for all the electricity/fuel ratios. For the 10 and 5 years investment periods, for the lowest electricity to fuel price ratios, the relative higher costs of the fuel make the base case the optimal option.

5.5 Optimal usage of the long-term thermal storage

The optimal usage of the storage is an important result from the optimisation model. Figure 45 shows the amount of heat being removed or added to the thermal storage for a data set with 78 periods corresponding to 6 years. The input data do not vary from year to year, *i.e*. the input data is repeated 6 times.

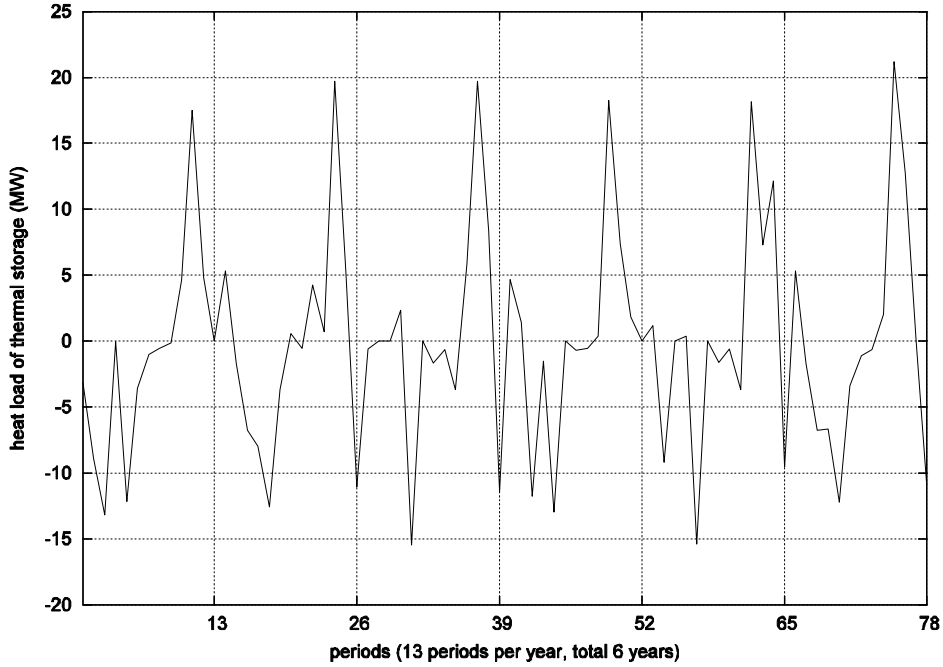

Figure 45: Optimal usage of the long-term thermal storage for a 6 years period.Positive values of the heat load mean that heat is added to the storage,subsequently negative values mean that heat is taken from the storage.

The variation in the usage of the storage from year to year is due to the conditions at the end and the start periods. There is no previous period for the first period, and no next period for the last period. This means that even if all the data is similar for each year, the starting point will be different resulting in a different optimal usage.

Figure 46 show the corresponding temperature for the thermal storage. The lower and upper bounds for the thermal storage temperature are set to 40 and 140 °C respectively.

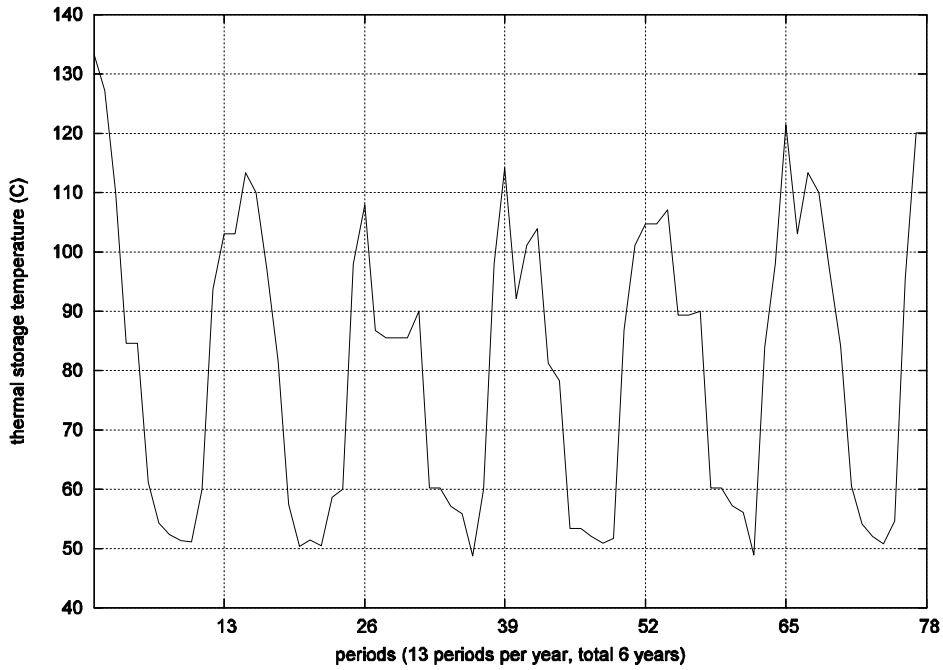

Figure 46: Temperature of the thermal storage for the optimal use.

As can be seen from the two previous figures, the thermal storage usage in the first and the last years are noticably different from the other years. Since from the model point of view there are no costs or penalties connected with setting the temperature of the storage to the maximum in the first period (corresponding to a fully charged storage), or emptying the thermal storage in the last period, this usage is obviously optimal.

5.6 Discussion and results

The optimisation model is capable of returning a variety of results of interest with respect to investments aswell as operation of the network, which makes it a powerful tool for improving district heating networks. The nonconvexities make the model very sensitive to the initial values, which increases the chance of finding a suboptimal local solution. The probablility of finding good local solutions is increased by running the model repeatedly with different initial values.

5.6.1 Further work

Further work could be to make the model more convex, to reduce the sensitivity to initial values. This will be a trade-off, since convexifying the model would most likely increase the size of the model and/or make the model less accurate.

With the respect to improvements related to the modelling of the district heating network system, there are several modifications that would improve the model. The thermal storage is at present modelled as a fixed unit. An obvious improvement would be to let the storage size be a variable, and let the optimisation model search for the optimal size, depending on the usage of the thermal storage and the costs. The possibility of shutting down plants with associated shutdown, startup and stand-by costs would also improve the model. Finally, in the current model only annualised costs are implemented. However, different companies uses different investment criteria to evaluate investments. To accommodate this other investment criteria (*e.g.* NPV), should be implemented.

6 Increasing the CHP production and combining long-term thermal storages – Transferring the methods into existing DH network

Most of this section is based on the work presented in the work by Tveit et al. [40].

In this section the model developed in Section 5 is applied to an existing district heating network. The network in question is the DH network in the Suwon area in Korea, owned by the Korea District Heating Corporation (KDHC). In addition a brief analysis of the benefit of thermal storage in the future Suwon network is presented. All data for the network in this section, including prices, of which the source is not specified, is supplied directly by KDHC.

6.1 Description of the district heating network in the Suwon area

In 2006 the district heating network in the Suwon area supplied heat to 99 000 households, 140 commercial and public buildings. In 1997 a CHP plant was built in the network, with a capacity of 82 MW_t and 43 MW_e. Figure 47 shows the duration curves for the heat supplied in the Suwon area from the CHP plant and the heat only boilers in 2005.

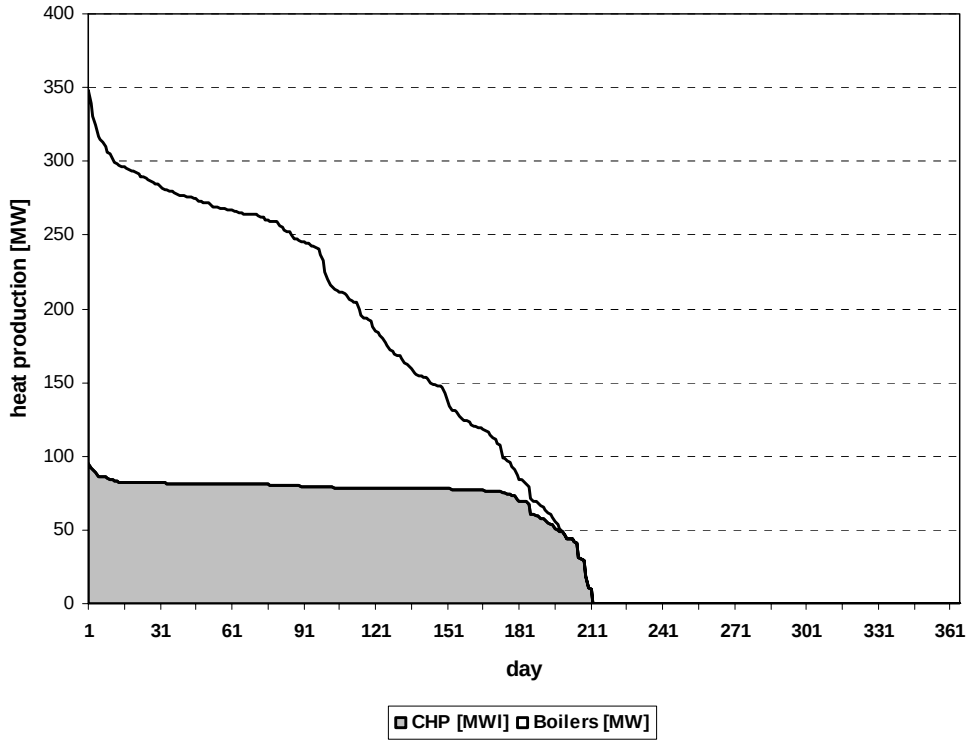

Figure 47: Duration curve for the heat supply in the Suwon area for 2005.

Figure 48 shows the daily average heat load curve for the Suwon area in 2005. This is the data used for the optimisation model, where the daily average curve is discretised into 13 periods of equal length. The discretised heat load curve is also shown in the figure.

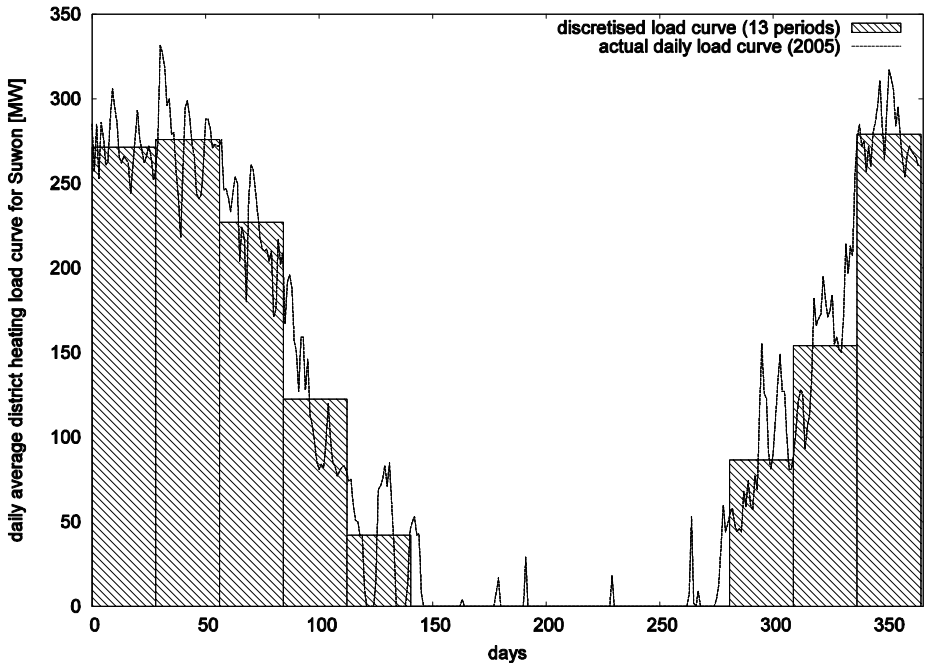

Figure 48: Daily average district heating load curves for the Suwon area, the actual daily load curve from 2005 and the 13 periods discretised load curve used in the optimisation model.

6.1.1 Brief analysis of future demand and thermal storage utilisation

The heat load demand for the Suwon area for 2008 until 2025 is predicted based on estimations of the regional development in the region. A detailed table of the heat load predictions is given in Appendix B.

A simple analysis of the use of an additional thermal storage and the increase of district cooling, shows that the operating hours for a CHP plant can be increased by almost 3600 hours, with an average load of 93 MW_t. Based on data from 2005, the payback time for the investment in the thermal storage would be approximately 12 years.

6.2 Optimisation model for analysing the CHP production and long-term thermal storage

The optimisation model used for analysing the CHP production and the long-term thermal storage for the district heating network in the Suwon area, is for most part similar to the model presented in Section 5.2 and Appendix A. The main differences are that there are no new investements in the network, apart from the long-term thermal storage, that is taken into account, and the model includes the possibility of turning the plants on and off in each period. This means that the operation of the network is the only part that will effect the CHP production and the long-term storage usage.

The generation units in the network are modelled as two plants, one CHP plant and one heat only boiler (that represents the 5 boilers available in the network). The prices for the heat and the power are given in Figure 49.

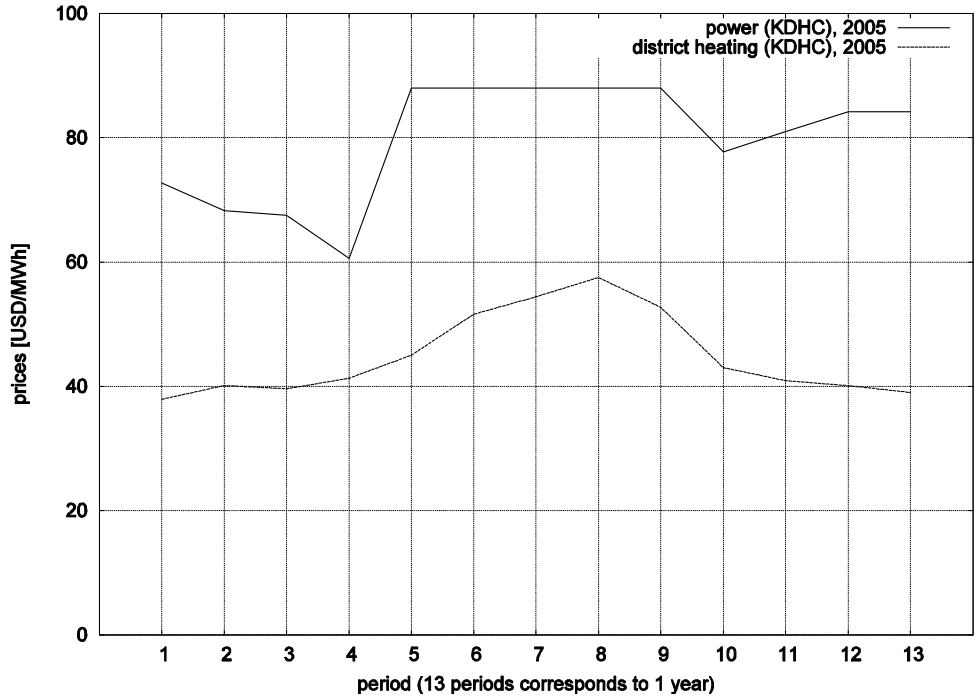

Figure 49: Discretisied price data for power and district heating for 2005 from the Suwon area.

Both the CHP plant and the boilers use oil as fuel. The prices for the fuel for 2005 is shown in Figure 50.

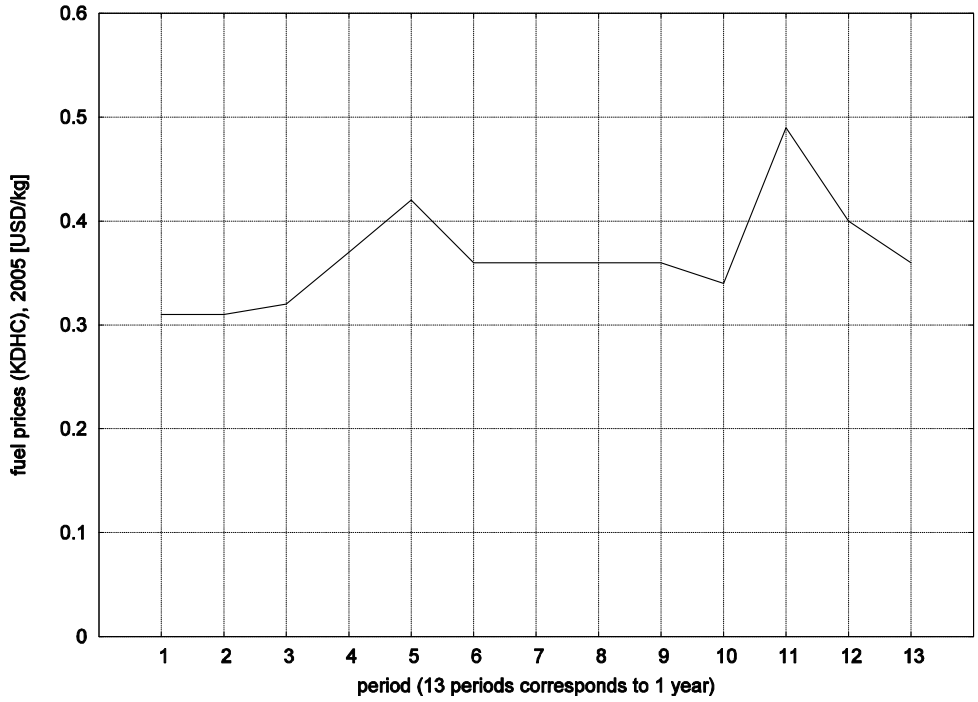

Figure 50: Discretisied price data fuel for 2005 from the Suwon area.

The other parameters, including the size of the thermal storage of 300 000 m^3 (= $3 \cdot 10^8$ kg water), are the same as for the model described in Section 5.2. An additional constraint added to the model is that the thermal storage cannot be pressurised, which means that the temperature of the

storage should be below 100 °C.

6.2.1 Model analysis

Due to the modifications the size of the model and the degrees of freedom is smaller than for the model(s) presented in Section 5.2. However, the implemenation of the possibility of turning a plant on and off for a period increases the number of binary variables and make the model harder to solve. For a data set with 13 periods the model has 1144 equations and 1080 variables, where 26 of the variables are binary.

6.3 Results and conclusions of the optimisation

For each result the optimisation model is run 20 times with the initial values of the variables varying with a uniform random distribution, due to the non-convexities of the model. The best result found shows an annual profit of approximately 22.9 million USD. The temperature and heat load profiles of the thermal storage for a year are shown in Figure 51 and Figure 52, respectively.

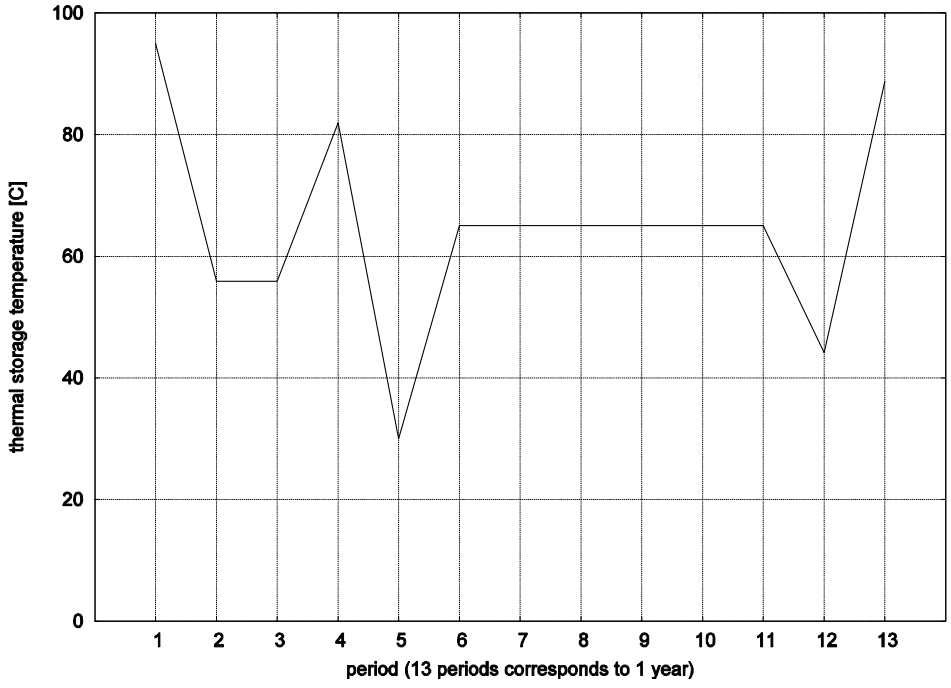

Figure 51: Annual temperature profile for the long-term thermal storage for Suwon for the best solution found .

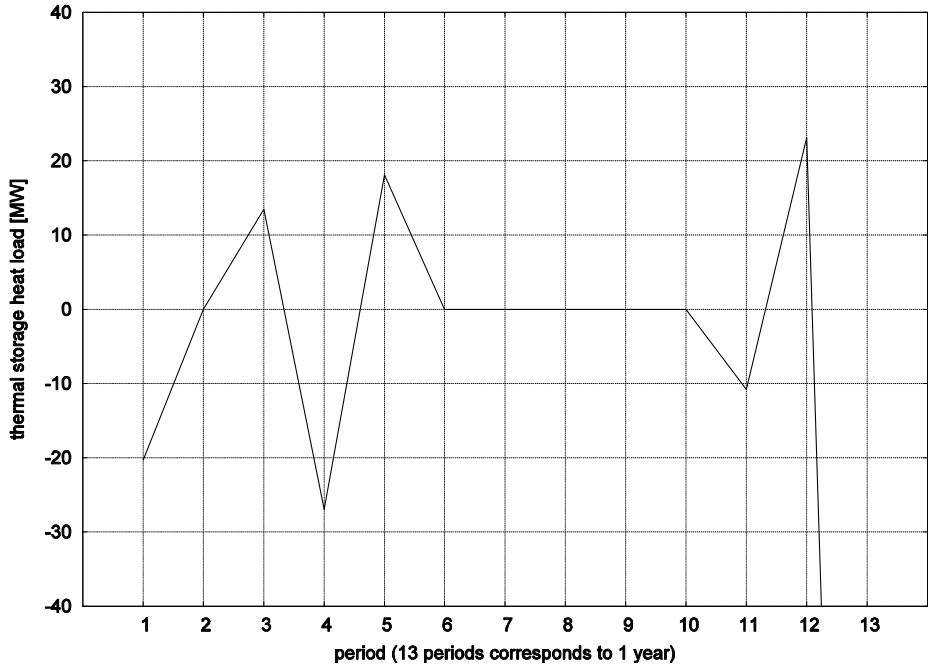

Figure 52: Annual heat load profile for the long-term thermal storage for Suwon for the best solution found..

6.3.1 Estimating the value of the long-term thermal storage

In order to get a value for the long-term thermal storage, the optimisation model described in Section 6.2 is run without the implementation of a long term thermal storage. The best solution found without the thermal storage shows an annual profit of 18.1 million USD. This gives an estimate of the value of the long-term thermal storage of 4.8 million USD/a. Comparing this to the possible types of thermal storages and the estimated prices given in Section 3.1.4, Figure 22 and Figure 23, means that the storage would be a rock cavern type storage with an estimated price of about 20 USD/m^3 or about 6.0 million USD in total.

7 Conclusions

As stated in the introduction, the objective of this project has been to "*evaluate and develop approaches that will improve the economic feasibility and the thermal efficiency of cogeneration through better utilisation of the produced heat and higher power generation in the CHP plant*". There are three main results of this project, in addition to the evaluation of long-term storage technology and applications, two approaches (or tools) have been developed, namely a load model for estimation of simultaneous heat and electricity demand in buildings for a specified planning area and a multi-period MINLP model for optimising structural changes and the operation of CHP plants in DH network with long-term storages.

With respect to further use of the MINLP model developed in this project, the model is capable of returning a variety of results of interest with respect to investments aswell as operation of the network, which makes it a powerful tool for improving district heating networks. It is important to note, however, that the nonconvexities make the model very sensitive to the initial values, which increases the chance of finding a suboptimal local solution. The probablility of finding good local solutions is increased by running the model repeatedly with different initial values.

According to the results presented in Section 3, the only proven technology of heat storage in CHP application is steel tanks. The volume of these tanks can be as high as 60 000 m³ and is well enough to meet the need for short-term storage. Regarding long-term storage with sizes above 100 000 m³ water equivalent, there are two technologies that are of interest for CHP system: rock cavern and borehole storage. With these technologies it is possible to attain high heat storage volumes. Both the study presented in Section 3 and the results of the MINLP model presented in Sections 5 and 6 indicate that the economic feasibility and the thermal efficiency of cogeneration can be improved by introducing long-term storages in the DH network. The study presented in Section 3 shows that the best economy is found in a system where peakload demand is supplied by oil boilers. Replacing oil-based CHP-heat with summer heat from incineration plant could be also interesting. With network and price data from 2005, the multi-period MINLP model applied to the DH network in the Suwon area in Korea, gives an estimate of the value of the long-term thermal storage of 4.8 million USD/a, where the costs of the rock cavern storage would be about 6.0 million USD in total.

References

[1] EPBD (2002); "Directive 2002/91/EC of the European Parliament and of the Council of 16 December 2002 on the energy performance of buildings"

[2] Feilberg, N. (2002); "USELOAD Version 6.5.2 – User manual", Technical report TR F5131, Project number 11x063.00, ISBN 82-594-1737-2

[3] Fredriksen, S. and Werner, S. (1993); "Fjärvärme – Teori, teknik och function (District heating – Theory, technique and function", Studentlitteratur, Lund, ISBN 91-44-38011-9

[4] Hoftvedt, K. (2004); "Analysis of heat loss from district heating pipe systems in areas with low heat density", Project report EPT-P-2004-23, Norwegian University of Science and Technology, in Norwegian

[5] Jardini, J. A., Tahan, C. M. V., Gouvea, M. R., Ahn, S. E. and Figueiredo, F. M. (2000); "Daily Load Profiles for Residential, Commercial and Industrial Low Voltage Consumers", IEEE Transactions on Power Delivery, Vol. 15, No. 1, January, pp. 375-380

[6] Løvås, G. (2004); " Statistikk for universiteter og høgskoler (Statistics for universities and colleges)", 2nd edition, Universitetsforlaget, ISBN 82-15-00224-2, in Norwegian

[7] Moeller Jensen, J. and Lund, H. (1995); "Design Reference Year, DRY. A New Danish reference year", Technical report no. DTU-LV-MEDD—281, CNN: Contract ENS-1213/92-0023, Technical University of Denmark

[8] Pedersen, L. (2007); "Load Modelling of Buildings in Mixed Energy Distribution Systems", Doctoral thesis, Norwegian University of Science and Technology, ISBN 978-82-471-1710-1 (printed ver.), ISBN 978-82-471-1724-8 (electronic ver.)

[9] Sylte, A. (2007), TEV Nett, Grid company in Trondheim, Norway

[10] TEK (1997); "FOR-1997-01-11 nr 33: Forskrift om krav til byggverk og produkter til byggverk (TEK)", http://www.lovdata.no/for/sf/kr/kr-19970122-0033.html

[11] Ulseth, R. (2006); "TEP24 Energy Supply of Buildings: District Heating – Systems and Properties", Lecture compendium, Norwegian University of Science and Technology, in Norwegian

[12] Wachenfeldt, B. J. and Satori, I. (2005); "ePlan – Evaluation of energy intensities in buildings and experiences from modeling", Project memo Sintef Building and Infrastructure, File code AN no. 2, Project no. 22414410

[13] Walpole, R. E., Myers, R. H. and Myers, S. L. (1998); "Probability and Statistics for Engineers and Scientists", 6th edition, Prentence Hall International Inc., ISBN 0-13-095246-X

[14] Climatewell., http://www.climatewell.com/, visited August 2007

[15] Stenlund Johan, Dimensionering av en accumulator för Umeå Energis fjärrvärmesystem, 2005.

[16] Calorstock Proceedings: Thermal energy storage, 1994.

[17] C. Brunström, B. Eftring, J. Claesson: The Lyckebo-project – Heat Losses from the rock cavern storage. Report RUL-FUD-B 87:13. Vattenfall, 1987.

[18] Bo Nordell: Bergvärme och bergkyla., 2004.
http://www.siki.se/sownloads/solvarme.pdf.

[19] U. Edstedt, B. Nordell: Borrhålslager, 1994.

[20] Council of Building Research: The Energy book – Status and research front. (Byggforskningsrådet: Energiboken. Kunskapsläge och forskningsfront). T6:1996.

[21] B. Svedinger: Värme i jord, berg och vatten 1981.

[22] C.-G. Hillström, L. Åstrand: Solvärme med säsongvärmelagring i berg för 550 lägenheter i Lyckebo, Uppsala. Från idé till idrifttagning. R 43:1985. Byggforskningsrådet, Stockholm.

[23] Swedish District Heating Association (Svenska Fjärrvärmeföreningens Service AB): Svenska Värmenät (Swedish District Heating Nets). FVF 03 12 12, 2003.

[24] Livio Mazzarella, Central solar heating plants with seasonal storage: The MINSUN simulation program. IEA-R&D report 1989.

[25] Solar thermal energy storage, Lyckebo project on rock cavern, report
UL-FUD-B 86:15

[26] Volkmar Lottner, Dirk Mangold: Status of Seasonal thermal energy storage in Germany. Proc. of Terrastock 2000, Stuttgart.

[27] Daniel Sandborg: Inventering av värmelager för kraftvärmesystem (Analysis of heat storages for cogeneration systems). Examensarbete. LITH-IKP-ING-EX--06/043-SE, 2006.

[28] Johan Andersson, Stefan Nilsson: Simulering av långtidsvärmelager för drift i kraftvärmesystem. Examensarbete. LITH-IKP-ING-EX-06/042-SE, 2006.

[29] Tuula Savola. *Modelling Biomass-Fuelled Small-Scale CHP Plants for Process Synthesis Optimisation.* Doctoral dissertation. TKK Dissertations 75. Espoo 2007.

[30] Tor-Martin Tveit. *A Systematic Procedure for Analysis and Design of Energy Systems*. TKK Dissertations 27. Espoo 2006.

[31] Anthony Brooke, David Kendrick, Alexander Meeraus and Ramesh Raman. *GAMS – A User's Guide*. GAMS Development Corporation, 2004.

[32] GAMS Development Corporation. *Solver Manual – SBB*, 2002, `http://www.gams.com/solvers/sbb.pdf`

[33] Arne Drud. *Solver Manual – CONOPT*, GAMS Development Corporation 2006, `http://www.gams.com/solvers/conopt.pdf`

[34] Nordpool ASA. *Market Data*, Nordpool corporate web-page, 2007 `http://www.nordpool.com/`

[35] Statistics Finland. *Statistics concerning the production, consumption, imports, exports and prices of energy, and investments in energy 2006*, 2007 `http://www.stat.fi`

[36] Helsinki Energy. *District heating prices 2006*, Helsinki Energy corporate web-page, 2007, `http://www.helsinginenergia.fi/`

[37] Tuula Savola and Ilkka Keppo. *Off-design simulation and mathematical modeling of small-scale CHP plants at part loads*. Applied Thermal Engineering, 25(8-9):1219-1232, 2005.

[38] Tuula Savola and Carl-Johan Fogelholm. *Increased power to heat ratio of small scale CHP plants using biomass fuels and natural gas.* Energy Conversion and Management 47:3105-3118, 2006

[39] Tor-Martin Tveit, Tuula Savola, Alemayehu Gebremedhin and Carl-Johan Fogelholm. *Multi-period MINLP model for optimising operation and structural changes to CHP plants in district heating networks with long-term thermal storage,* Energy Conversion and Management, In review.

[40] Tor-Martin Tveit, Sangsu Kim and Carl-Johan Fogelholm. *Multi-period MINLP model for investigating long-time thermal storages in DH network applied to Suwon, Korea.* In Proceedings of the 11th International Symposium on District Heating and Cooling, August/Sepember 2008

Appendix A

Multi-period MINLP model for optimising structural changes to CHP plants in district heating networks with long term thermal storage.

Tor-Martin Tveit
Helsinki University of Technology
Energy Engineering and Environmental Protection
P.O.Box 4400, FIN-02015 TKK, Finland

December 19, 2007

1 Introduction

This paper presents a multi-period MINLP model for optimising structural changes and the operation of CHP plants in district heating networks with long term thermal storage. The model was developed as a part of the project "Improved cogeneration and heat utilization in DH networks" within Annex VIII of the Implementing Agreement DHC-CHP within a framework created by the International Energy Agency (IEA).

2 Equations

The model consists of an objective function and constraints, which are presented in Sections 2.1 and 2.2 respectively.

The general formulation of the model is given in the following equation.

$$\max f(\mathbf{x},\mathbf{y}) \quad \text{subject to} \begin{cases} h_i(\mathbf{x},\mathbf{y}) = 0 & i \in \{1,2,\ldots,k\} \\ g_i(\mathbf{x},\mathbf{y}) \leq 0 & i \in \{1,2,\ldots,l\} \\ \mathbf{x} \in X \subseteq \mathcal{R}^n, \mathbf{y} \in Y \subset \mathcal{Z}^m \end{cases} \tag{1}$$

where $\mathcal{R}^n$ is the n-dimensional Euclidian space and $\mathcal{Z}^m$ is the m-dimensional set of integers. The function $f(\mathbf{x},\mathbf{y})$ is the objective function, while the equations $h_i(\mathbf{x},\mathbf{y}) = 0$ and $g_i(\mathbf{x},\mathbf{y}) \leq 0$ are the constraints that define the feasible region. The indices, sets, variables, and parameters used are described in Appendix A.

2.1 Objective function

The objective function to be maximised is the sum of the incomes from the power generation and the district heating with the subtraction of the fuel costs and any investment costs for modifications to the plants.

$$z = \sum_{p \in plants} \sum_{i \in periods} \left(I^{PG}_{(p,i)} + I^{DH}_{(p,i)} - C^{F}_{(p,i)} \right) + \sum_{p \in options} \left(C^{I}_{(p)} \right) \tag{2}$$

The evaluation of the different incomes and costs are given in Equations 19, 18, 17 and 16.

2.2 Constraints

The constraints consists mainly of energy- and mass balances, and equations related to these.

The model uses regression models to calculate the power generation and the forward temperature for the plants. Both the power production and the forward temperature are

functions of the mass flow of district heating water, the return temperature of the district heating water and the mass flow of fuel. In the cases presented here, all the regression models are third order polynomials. If desired, these can be replaced by other expressions.

Equations related to the CHP plants

For the plants in the network that are not being considered for design changes (*i.e.* the members of the set *nooptions*), the expressions for the power generation and forward temperature are given in Equations 3 and 4, respectively.

$$\begin{aligned} P_{(p,i)} = a_{0,p} &+ \sum_{j=1}^{3}\big(a_{(j,p)} \cdot (m^{F}_{(p,i)})^{j}\big) + \sum_{j=1}^{3}\big(b_{(j,p)} \cdot (T^{IN}_{(p,i)})^{j}\big) \\ &+ \sum_{j=1}^{3}\big(c_{(j,p)} \cdot (m^{DH}_{(p,i)})^{j}\big) + d_{ab}\big(m^{F}_{(p,i)} \cdot T^{IN}_{(p,i)}\big) + d_{ac}\big(m^{F}_{(p,i)} \cdot m^{DH}_{(p,i)}\big) \\ &+ d_{bc}\big(T^{IN}_{(p,i)} \cdot m^{DH}_{(p,i)}\big), \qquad \forall (p,i) \in (nooptions, periods) \end{aligned} \tag{3}$$

$$\begin{aligned} T^{Fwd}_{(p,i)} = \alpha_{0,p} &+ \sum_{j=1}^{3}\big(\alpha_{(j,p)} \cdot (m^{F}_{(p,i)})^{j}\big) + \sum_{j=1}^{3}\big(\beta_{(j,p)} \cdot (T^{IN}_{(p,i)})^{j}\big) \\ &+ \sum_{j=1}^{3}\big(\gamma_{(j,p)} \cdot (m^{DH}_{(p,i)})^{j}\big) + \delta_{ab}\big(m^{F}_{(p,i)} \cdot T^{IN}_{(p,i)}\big) + \delta_{ac}\big(m^{F}_{(p,i)} \cdot m^{DH}_{(p,i)}\big) \\ &+ \delta_{bc}\big(T^{IN}_{(p,i)} \cdot m^{DH}_{(p,i)}\big), \qquad \forall (p,i) \in (nooptions, periods) \end{aligned} \tag{4}$$

For the plants where there are possibilities of design changes, there are some additional equations needed. For each design change that is taken into account, there are separate regression models for calculating the power generation and the forward temperature. The additional equations are needed to activate the correct equations, depending on which design change is selected.

The following equation sets the logical requirement that only one of the design case can be active.

$$\sum_{p \in options} y_p = 1 \tag{5}$$

The binary variables y_p function as Boolean variables, with 0 corresponding to *true* and 1 corresponding to *false*.

Equation 6 sums the dummy variables $\widehat{P}$. Equations 7 through 9 make sure that $\widehat{P}$ only differs from zero in the case that the corresponding design change is active. These equations are traditional *Big-M* formulations of the disjunctions.

$$P_{(p,i)} = \sum_{p \in options} \widehat{P}_{(p,i)}, \qquad \forall i \in periods \tag{6}$$

$$\widehat{P}_{(p,i)} \leq \widetilde{P}_{(p,i)} + M_p\,(1 - y_p), \qquad \forall (p,i) \in (options, periods) \tag{7}$$

$$\widehat{P}_{(p,i)} \geq \widetilde{P}_{(p,i)} - M_p\,(1 - y_p), \qquad \forall (p,i) \in (options, periods) \tag{8}$$

$$\widehat{P}_{(p,i)} \leq M_p\,y_p, \qquad \forall (p,i) \in (options, periods) \tag{9}$$

Equations 7 and 8 also connect the expression for power generation in Equation 6 with the regression models for the different design changes, given in Equation 10.

$$\begin{aligned} \widetilde{P}_{(p,i)} = a_{0,p} &+ \sum_{j=1}^{3}\big(a_{(j,p)} \cdot (m^{F}_{(p,i)})^{j}\big) + \sum_{j=1}^{3}\big(b_{(j,p)} \cdot (T^{IN}_{(p,i)})^{j}\big) \\ &+ \sum_{j=1}^{3}\big(c_{(j,p)} \cdot (m^{DH}_{(p,i)})^{j}\big) + d_{ab}\big(m^{F}_{(p,i)} \cdot T^{IN}_{(p,i)}\big) + d_{ac}\big(m^{F}_{(p,i)} \cdot m^{DH}_{(p,i)}\big) \\ &+ d_{bc}\big(T^{IN}_{(p,i)} \cdot m^{DH}_{(p,i)}\big), \qquad \forall (p,i) \in (options, periods) \end{aligned} \tag{10}$$

The forward temperatures for the plants with possibilities of design changes are calculated in the similar way as the power generation explained previously. Equations 11 through 11 activates the correct regression model given in Equation 15, depending on the value of the corresponding binary variable, y_p.

$$T^{Fwd}_{(p,i)} = \sum_{p \in options} \widehat{T}^{Fwd}_{(p,i)}, \qquad \forall i \in periods \tag{11}$$

$$\widehat{T}^{Fwd}_{(p,i)} \leq \widetilde{T}^{Fwd}_{(p,i)} + M_T\,(1 - y_p), \qquad \forall (p,i) \in (options, periods) \tag{12}$$

$$\widehat{T}^{Fwd}_{(p,i)} \geq \widetilde{T}^{Fwd}_{(p,i)} - M_T\,(1 - y_p), \qquad \forall (p,i) \in (options, periods) \tag{13}$$

$$\widehat{T}^{Fwd}_{(p,i)} \leq M_T\,y_p, \qquad \forall (p,i) \in (options, periods) \tag{14}$$

$$\begin{aligned}\widetilde{T}^{Fwd}_{(p,i)} = \alpha_{0,p} &+ \sum_{j=1}^{3}\big(\alpha_{(j,p)} \cdot (m^{F}_{(p,i)})^j\big) + \sum_{j=1}^{3}\big(\beta_{(j,p)} \cdot (T^{IN}_{(p,i)})^j\big) \\ &+ \sum_{j=1}^{3}\big(\gamma_{(j,p)} \cdot (m^{DH}_{(p,i)})^j\big) + \delta_{ab}\big(m^{F}_{(p,i)} \cdot T^{IN}_{(p,i)}\big) + \delta_{ac}\big(m^{F}_{(p,i)} \cdot m^{DH}_{(p,i)}\big) \\ &+ \delta_{bc}\big(T^{IN}_{(p,i)} \cdot m^{DH}_{(p,i)}\big), \qquad \forall (p,i) \in (options, periods)\end{aligned} \tag{15}$$

The income from the power generation from each plant is given in Equation 16.

$$I^{PG}_{(p,i)} = P_{(p,i)} \cdot R^{P}_{i} \cdot t^{TOTAL}, \qquad \forall (p,i) \in (plants, periods) \tag{16}$$

Where $P_{(p,i)}$ is the power generated from each plant in each period, R^P_i is the price of power in each period, and t^{TOTAL} is the total time in each period. If the units for the power generation and price are MW and EUR/MWh respectively, the unit of the total time would be h.

Equation 17 shows the expression for the income from the district heating generated in the plants. The calculation is equivalent to the income from the power generation shown in Equation 16.

$$I^{DH}_{(p,i)} = Q_{(p,i)} \cdot R^{DH}_{i} \cdot t^{TOTAL}, \qquad \forall (p,i) \in (plants, periods) \tag{17}$$

The amount of district heating generated for the plants, $Q_{(p,i)}$, is calculated according to Equation 22.

The cost of the fuel for each plant in each period is given in Equation 18.

$$C^{F}_{(p,i)} = m^{F}_{(p,i)} \cdot R^{F}_{i} \cdot t^{TOTAL}, \qquad \forall (p,i) \in (plants, periods) \tag{18}$$

In contrast to the cost of fuel, the investment costs are not calculated for each period. Instead, the costs are annualised (AI_p) and multiplied with to total number of years for the period, n^I.

$$C^{I}_{(\hat{p})} = n^{I} \sum_{p \in options} (y_p \cdot AI_p), \qquad \forall \hat{p} \in (plants) \tag{19}$$

Since only the investment costs for the design change that is active should be included, AI_p is multiplied with the binary variable y_p.

Equations related to the DH network and long-term thermal storage

The mass balance for all the units for all the periods are calculated according to Equation 20.

$$\sum_{s \in in(p,s)} m^{DH}_{(s,i)} = \sum_{s \in out(p,s)} m^{DH}_{(s,i)}, \qquad \forall (p,i) \in (units, periods) \tag{20}$$

The equation simply states that the sum of all streams in to a unit must equal the sum of all streams out of the unit in each period.

The energy balance for units without heat consumption or generation is given in Equation 21.

$$\sum_{s \in in(p,s)} m^{DH}_{(s,i)} h_{(s,i)} = \sum_{s \in out(p,s)} m^{DH}_{(s,i)} h_{(s,i)}, \quad \forall (p,i) \in (mixers \cup splitters, periods) \quad (21)$$

The equation is similar to the calculation of the mass balance. The energy balance for units with heat consumption and generation is given in Equation 22.

$$\sum_{s \in in(p,s)} m^{DH}_{(s,i)} h_{(s,i)} = \sum_{s \in out(p,s)} m^{DH}_{(s,i)} h_{(s,i)} + Q_{(p,i)}, \quad \forall (p,i) \in (storage \cup DHconsumer \cup plants, periods) \quad (22)$$

The calculation of the enthalpy for all streams necessary for the energy balance, is given in Equation 23.

$$h_{(s,i)} = T_{(s,i)} \cdot cp_s, \qquad \forall (p,i) \in (units, periods) \quad (23)$$

The energy balance equation does not take into account that the temperatures of the streams going out from a splitter should be equal to the temperature of the stream going in. The additional constraints needed for this are given in Equations 24 and 25.

$$T^{SP}_{(p,i)} = T_{(s,i)}, \quad \forall (p,s,i) \in \big((splitters, streams) \cap in, periods\big) \quad (24)$$

$$T^{SP}_{(p,i)} = T_{(s,i)}, \quad \forall (p,s,i) \in \big((splitters, streams) \cap out, periods\big) \quad (25)$$

The temperature in a storage is a function of the temperature and the amount of heat put into or removed from the storage in the previous period. The expression for the calculation of the storage temperatures is shown in Equation 26.

$$T^{ST}_{(p,i+1)} = T^{ST}_{(p,i)} + \frac{Q_{(p,i)}}{cpmt_p}, \qquad \forall (p,i) \in (storage, periods) \quad (26)$$

where the parameter $cpmt_p$ contains the mass, heat capacity for the storages, in addition to the length of the periods.

The temperatures of the streams leaving a storage is set equal to the temperature of the storage in the current period.

$$T^{ST}_{(p,i)} = T_{(s,i)}, \quad \forall (p,s,i) \in \big((storage, streams) \cap out, periods\big) \quad (27)$$

Equations 28 and 29 are the constraints for, respectively, the heat and temperature demands for the district heating network.

$$Q^{DH}_i = Q^{Demand}_i, \qquad \forall i \in periods \quad (28)$$

$$T^{Fwd,DH}_i \geq T^{Demand}_i, \qquad \forall i \in periods \quad (29)$$

A Indices, sets, variables and paremeters

The following indices, sets, variables, and parameters are used in the model.

Indices

p	units
i	periods
s	streams

Sets

$units$	$= \{p \mid p \text{ is a unit}\}$
$plants$	$= \{p \mid p \text{ is a power plant}\} \subset units$
$nooptions$	$= \{p \mid p \text{ is a power plant without design changes}\} \subset plants \subset units$
$options$	$= \{p \mid p \text{ is a power plant with design changes}\} \subset plants \subset units$
$mixers$	$= \{p \mid p \text{ is a mixer}\} \subset units$
$splitters$	$= \{p \mid p \text{ is a splitter}\} \subset units$
$storage$	$= \{p \mid p \text{ is a storage}\} \subset units$
$DHconsumer$	$= \{p \mid p \text{ is a DH consumer}\} \subset units$
$periods$	$= \{i \mid i \text{ is a period}\}$
$streams$	$= \{s \mid s \text{ is a district heating stream}\}$
in	$= \{(p,s) \mid s \text{ is a stream entering unit } p, p \in units, s \in streams\}$
out	$= \{(p,s) \mid s \text{ is a stream leaving unit } p, p \in units, s \in streams\}$

Variables

z	objective
I	income
C	costs
$P_{(p,i)}$	generated power in plant p in period i
$m^{F}_{(p,i)}$	fuel flow to plant p in period i
$T_{(s,i)}$	temperature of DH stream s in period i
$T^{SP}_{(p,i)}$	inlet temperature of splitter p in period i
$T^{ST}_{(p,i)}$	temperature of storage p in period i
$T^{IN}_{(p,i)}$	return temperature of DH to plant p in period i
$m^{DH}_{(p,i)}$	mass flow of DH from plant p in period i
$\widetilde{P}$	dummy variable
$\widehat{P}$	dummy variable
$\widetilde{T}$	dummy variable
$\widehat{T}$	dummy variable
$h_{(s,i)}$	enthalpy of stream s in period i
$Q_{(p,i)}$	heat load of unit p in period i
y_p	binary variable for selection of process options.

Parameters

a	coefficient for regression model for estimating the generated power
b	coefficient for regression model for estimating the generated power
c	coefficient for regression model for estimating the generated power
d	coefficient for regression model for estimating the generated power
α	coefficient for regression model for estimating the forward temperature
β	coefficient for regression model for estimating the forward temperature
γ	coefficient for regression model for estimating the forward temperature
δ	coefficient for regression model for estimating the forward temperature
cp_s	heat capacity of stream s
$cpmt_p$	$\frac{cp_p \cdot m_p}{t_i}$ (time dependent heat capacity for storages, t_i equals period length)
M_p	big-M for logical constraints
M_T	big-M for logical constraints
n^I	number of investment years (for annuity)
AI_p	annualised investment costs for process options

Superscripts

PG	generated power
DH	district heating
F	fuel
I	investment

Appendix B – Detailed description of the Suwon area heat load

ITEM			unit	2004	2005	2006	2007	2008	2009	2010	2011	2012	2013	2014	
SUWON	HOUSING	District Heating	Area	m2	4 504 162	4 761 861	4 800 469	5 089 216	5 226 316	5 753 438	5 768 672	5 768 672	5 768 672	5 768 672	5 768 672	
			Heat Load	Mcal/h	312 483	330 129	332 716	352 489	361 950	397 810	398 861	398 861	398 861	398 861	398 861	
			Households	No	55 497	58 524	59 118	62 044	63 756	69 091	69 282	69 282	69 282	69 282	69 282	
		District Cooling	Area	m2	0	0	0	0	0	0	0	0	0	0	0	
			Heat Load	Mcal/h	0	0	0	0	0	0	0	0	0	0	0	
	BUSINESS	District Heating	Area	m2	382 077	382 077	403 131	418 251	433 372	448 492	463 612	478 732	493 853	508 973	524 093	
			Heat Load	Mcal/h	37 296	37 296	39 254	40 759	42 265	43 770	45 276	46 781	48 286	49 792	51 297	
		District Cooling	Area	m2	71 720	71 720	71 720	76 256	80 792	85 328	89 864	94 400	98 936	103 472	108 008	
			Heat Load	Mcal/h	13 377	13 377	13 377	14 211	15 045	15 878	16 712	17 546	18 380	19 213	20 047	
	PUBLIC	District Heating	Area	m2	293 360	293 360	293 360	315 620	344 855	347 328	349 802	349 802	349 802	349 802	349 802	
			Heat Load	Mcal/h	27 584	27 584	27 584	29 677	32 441	32 674	32 906	32 906	32 906	32 906	32 906	
		District Cooling	Area	m2	93 639	93 639	93 639	96 978	100 317	100 688	101 059	101 059	101 059	101 059	101 059	
			Heat Load	Mcal/h	13 031	13 031	13 031	13 534	14 037	14 093	14 149	14 149	14 149	14 149	14 149	
	SUM	District Heating	Area	m2	5 179 599	5 437 298	5 496 959	5 823 088	6 004 543	6 549 259	6 582 085	6 597 206	6 612 326	6 627 446	6 642 566	
			Heat Load	Mcal/h	377 362	395 008	399 554	422 926	436 656	474 254	477 043	478 548	480 053	481 559	483 064	
			Households	No	55 497	58 524	59 118	62 044	63 756	69 091	69 282	69 282	69 282	69 282	69 282	
		District Cooling	Area	m2	165 359	165 359	165 359	173 234	181 109	186 016	190 924	195 460	199 996	204 532	209 068	
			Heat Load	Mcal/h	26 408	26 408	26 408	27 745	29 082	29 971	30 861	31 695	32 529	33 362	34 196	

ITEM				unit	2015	2016	2017	2018	2019	2020	2021	2022	2023	2024	2025	
SUWON	HOUSING	District Heating	Area	m2	5 768 672	5 768 672	5 768 672	5 768 672	5 768 672	5 768 672	5 768 672	5 768 672	5 768 672	5 768 672	5 768 672	
			Heat Load	Mcal/h	398 861	398 861	398 861	398 861	398 861	398 861	398 861	398 861	398 861	398 861	398 861	
			Households	No	69 282	69 282	69 282	69 282	69 282	69 282	69 282	69 282	69 282	69 282	69 282	
		District Cooling	Area	m2	0	0	0	0	0	0	0	0	0	0	0	
			Heat Load	Mcal/h	0	0	0	0	0	0	0	0	0	0	0	
	BUSINESS	District Heating	Area	m2	524 093	524 093	524 093	524 093	524 093	524 093	524 093	524 093	524 093	524 093	524 093	
			Heat Load	Mcal/h	51 297	51 297	51 297	51 297	51 297	51 297	51 297	51 297	51 297	51 297	51 297	
		District Cooling	Area	m2	108 008	108 008	108 008	108 008	108 008	108 008	108 008	108 008	108 008	108 008	108 008	
			Heat Load	Mcal/h	20 047	20 047	20 047	20 047	20 047	20 047	20 047	20 047	20 047	20 047	20 047	
	PUBLIC	District Heating	Area	m2	349 802	349 802	349 802	349 802	349 802	349 802	349 802	349 802	349 802	349 802	349 802	
			Heat Load	Mcal/h	32 906	32 906	32 906	32 906	32 906	32 906	32 906	32 906	32 906	32 906	32 906	
		District Cooling	Area	m2	101 059	101 059	101 059	101 059	101 059	101 059	101 059	101 059	101 059	101 059	101 059	
			Heat Load	Mcal/h	14 149	14 149	14 149	14 149	14 149	14 149	14 149	14 149	14 149	14 149	14 149	
	SUM	District Heating	Area	m2	6 642 566	6 642 566	6 642 566	6 642 566	6 642 566	6 642 566	6 642 566	6 642 566	6 642 566	6 642 566	6 642 566	
			Heat Load	Mcal/h	483 064	483 064	483 064	483 064	483 064	483 064	483 064	483 064	483 064	483 064	483 064	
			Households	No	69 282	69 282	69 282	69 282	69 282	69 282	69 282	69 282	69 282	69 282	69 282	
		District Cooling	Area	m2	209 068	209 068	209 068	209 068	209 068	209 068	209 068	209 068	209 068	209 068	209 068	
			Heat Load	Mcal/h	34 196	34 196	34 196	34 196	34 196	34 196	34 196	34 196	34 196	34 196	34 196	




IEA DHC|CHP

International Energy Agency
IEA Implementing Agreement on District Heating and Cooling, including the integration of CHP

Published by: SenterNovem
PO Box 17, 6130 AA Sittard, The Netherlands
Telephone: + 31 46 4202202
Fax: + 31 46 4528260
E-mail: iea-dhc@senternovem.nl
www.iea-dhc.org
www.senternovem.nl

SenterNovem